INVESTIGATING THE ROLE OF THE SHEDDASE BACE2 IN VERTEBRATE PIGMENTATION AND MELANOMA PROGRESSION

A Dissertation

Presented to the Faculty of the Weill Cornell Graduate School

of Medical Sciences

in Partial Fulfillment of the Requirements for the Degree of

Doctor of Philosophy

by

Yan Zhang

August 2018

INVESTIGATING THE ROLE OF THE SHEDDASE BACE2 IN VERTEBRATE PIGMENTATION AND MELANOMA PROGRESSION

Yan Zhang, Ph. D.

Cornell University 2018

Patterning of vertebrate melanophores is essential for mate selection and protection from UV-induced damage. Patterning can be influenced by circulating long-range factors, such as hormones, but it is unclear how their activity is controlled in recipient cells to prevent excesses in cell number and migration. The zebrafish *wanderlust* mutant harbors a mutation in the sheddase bace2 and exhibits hyperdendritic and hyperproliferative melanophores that localize to aberrant sites. We performed a chemical screen to identify suppressors of the *wanderlust* phenotype and found that inhibition of insulin/PI3Kg/mTOR signaling rescues the defect. In normal physiology, Bace2 cleaves the insulin receptor, whereas its loss results in hyperactive insulin/PI3K/mTOR signaling. Insulin B, an isoform enriched in the head, drives the melanophore defect.

Melanoma is malignant skin cancer derived from transformed melanocytes. Bace2 also negatively regulates melanoma cell proliferation and affects morphology. Loss of Bace2 leads to early onset tumors with migratory and invasive phenotype. These results suggest that signaling from a long-distance

factor, insulin, can be negatively regulated by a melanophore-specific expression of a sheddase and melanoma cells utilize this mechanism to regulate tumor cell progression.

BIOGRAPHICAL SKETCH

Yan Zhang was born in Zhuzhou, a small city in the Central South of China. Yan completed her college at Sichuan University, where she majored in Biology. She went to the University of Washington in her junior year as an exchange student. In 2012, she started her doctoral study in the Cell and Developmental Biology Program at Weill Cornell Graduate School of Medical Sciences in New York City. During her graduate study, Yan investigated the role of the sheddase BACE2 in vertebrate pigmentation and melanoma progression with her mentor Dr. Richard White at Memorial Sloan Kettering Cancer Center.

DEDICATION

This dissertation is dedicated to my loving family

本论文献给我亲爱的家人

ACKNOWLEDGEMENTS

At the end of my Ph.D. study at Weill Cornell Graduate School of Medical Sciences, I would like to express my deepest gratitude to those who are important along the way.

First of all, I want to thank my mentor Dr. Richard White, who is the first PI I rotated with 6 years ago. Very early on I already saw the chemistry between us and decided to work with this young, unique and energetic fish PI. Dr. White has guided me through the entire Ph.D. research, no matter we were towards a uphill or in the difficulty. He was always willing to listen, good at mentoring and respected every aspect of me. He not only trained me into a developmental biologist and cancer biologist, but also he showed me how much positive impact a PI can have on a student. Without his constant support, encouragement and care, this work would not be possible.

Secondly, I am very grateful for having exceptional doctoral committees. I sincerely appreciate Dr. Carl Blobel for his assistance and supervision during my Ph.D. study, as well as Dr. Todd Evans, Dr. Yueming Li and Dr. Andrea Ventura for their guidance on my thesis work. All of them gave me tremendous help when I was looking for a postdoc lab.

Next, I would like to thank all the labmates and friends in my daily work: Scott Callahan, Maomao Zhang, Kelsey Temprine, Milena Zimmer, Isabella Kim, Theresa Simon-Vermot, Mohita Tagore, Nathaniel Campbell, Joshua Weiss, Richard Huang, Thijs VanBoxtel, Emily Johnson, Grant Robinson, Emily

Kansler, Liz Perry, Kajan Ratnakumar and Sara Fischer. All of them made lab feel like home and became my motivation to come to lab when experiments did not work well. It has been a wonderful experience to work with a group of talented people who gave me great support.

In the end, I would like to present my special thanks to my husband Songan Mao. His role transited from my best friend, boy friend, fiancé and now become my husband within this six years. Without his accompany, I would not have accomplished all this work. My beloved parents have been supporting me with the best of they can in China. Without their love and encouragement, this six-year journey would not have come to a successful completion.

TABLE OF CONTENTS

LIST OF FIGURES

LIST OF TABLES

CHAPTER 1: INTRODUCTION

1.1 Vertebrate pigmentation development

1.1.1 Background

Pigment patterning has been a long-term attraction for both non-scientists and scientists. The complex combination of melanin in the butterfly, versatile fish stripe in the aquarium and beautiful fur colors in a running leopard have intrigued many people. Evolutionary biologists have been studying pigment patterning as one of the most striking features to observe across species, as mutations in pigmentation usually have limited impact on survival but can co-evolve with other traits. Behavioral ecologists are fascinated by the fact that animals use their pigment patterning in mate selection, relative recognition and camouflage. Developmental biologists have used pigment as a model system to study the general problem of pattern formation and regenerative biology (Kelsh et al., 2009; Parichy, 2003). Geneticists study the genes and pigment cells that are responsible for regulating pigment cells specification, migration and survival.

Pigment patterning is defined by combinations of pigment cells that organize themselves on either epidermis or endoderm in animals and together display a recognizable colorful pattern for each species (Kelsh et al., 2009). The purpose of this section is to review vertebrate pigmentation, with a focus on the ontogenic development of melanocytes, which are the black pigment cells in vertebrate. Then this section will discuss pigmentary diseases, highlighting the importance of understanding pigment patterning from a therapeutic perspective. In the end, this section will examine the cell intrinsic and

environmental factors regulating pigment cell development.

1.1.2 Ontogenetic development of melanocytes

Overview

Melanocytes are the black pigment cells that are responsible for producing melanin. In human skin, melanocytes reside in the border between epidermis and dermis, accounting for the black pigmentation in the hairs, skins and eyes (Goding, 2007). Each melanocyte is connected to the neighboring keratinocytes in the overlying epidermis and to the fibroblasts in the underlying basal layer (Figure 1). Human skin is mainly comprised of those three types of cells, which are highly collaborative and all together regulate skin function and appearance (Yamaguchi et al., 2007).

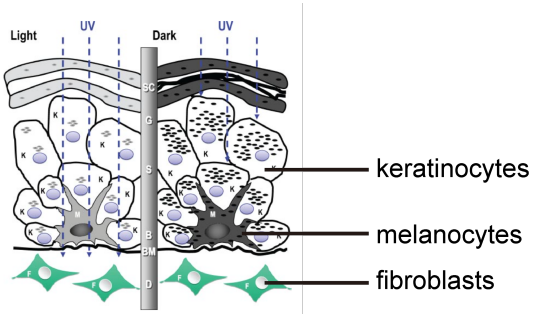

Figure 1. Human skin is composed of keratinocytes, melanocytes and fibroblasts. Right side is light-pigmented skin and Left side is dark-pigmented skin. Melanin granule number and content regulate skin color. From top to bottom: SC, stratum corneum; G, stratum granulosum; S, stratum spinosum; B, stratum basale; BM, basement membrane; D, dermis. Cell types: K, keratinocyte; M, melanocyte; F, fibroblast; shaded oval, melanin granule. Figure adapted from (Yamaguchi et al. 2007).

Melanocytes are derived from neural crest

Melanocytes are originated from neural crest cells and migrate to the junction between epidermis and dermis, as well as to the hair follicles (Thomas and Erickson, 2008). Neural crest cells are a pluripotent cell population unique to vertebrates that originates in the neural tube. Neural crest cells undergo extensive migration during epithelial to mesenchymal transition and differentiate into various structures including pigmented melanocytes in the skin (Figure 2) (Sommer, 2011). Melanocytes lineage specification is regulated in both spatial and temporal manners. In a traditional view, the melanocyte lineage is specified early on during neural crest development, as melanoblasts (the melanocytes precursor cells) has a fixed lineage program as soon as they are spatially separated from the other neural crest lineages (Sommer, 2011). Melanoblasts migrate on a dorsolateral pathway between the ectoderm for mice and avians (Thomas and Erickson, 2008), or on both dorsolateral and

ventral pathways in the case of zebrafish (Kelsh et al., 2009). Recently work has also suggested a dual neural crest origin of melanocytes, one is derived from neural crest cells by dorsolateral migration, and the other one is originated from a Schwann cell (glial)/melanoblast progenitor by ventral migration (Mort et al., 2015).

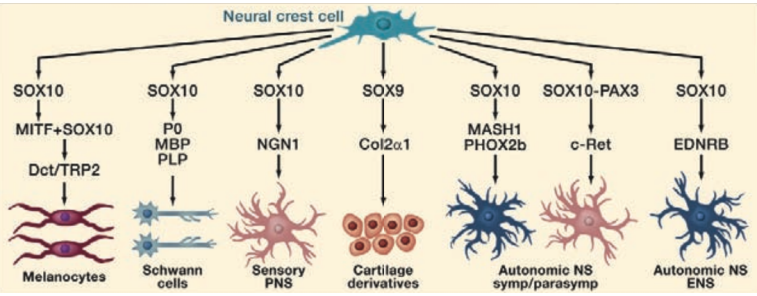

Figure 2. Neural crest cells differentiate into various progenity lineages, regulated by different combinations of transcription factors. Melanocyte lineage is specified by SOX10 and MITF. Figure adapted from (Sauka-Spengler and Bronner 2010).

The main function of melanocytes is to produces melanin

The maturation of melanocytes is marked by a process called melanogenesis, whereby melanocytes synthesize a group of pigmentation enzymes and structural proteins to reach a maturation structure and produce melanin within an intracellular organelle named the melanosome. The critical melanogenic enzymes include tyrosinase (TYR), tyrosinase related protein 1 (TYRP1), and DOPAchrome tautomerase (DCT) (Goding, 2007).They catalyze biochemical reactions to synthesize melanin starting from the substrate by hydroxylating tyrosine. Melanocytes can make two different types of melanin, which are yellow/red soluble pheomelanin (predominantly for individuals with red skins and skin, in whom skin cancer is more frequently observed) and dark brown/black insoluble eumelanin (the major pigment in individuals with dark skin and hair and is more efficient in UV protection) (Figure 3) (Ebanks et al., 2009). The key structural proteins include PMEL (Hellström et al., 2011;

McGlinchey et al., 2009) and MART1 (De Mazière et al., 2002; Hoashi et al., 2005), both of which are critical for melanosome to reach a maturation structure. PMEL is proteolytically cleaved into small fragments, and those fragment then polymerize and form a fibrillar matrix inside the melanosome to allow melanin deposition and melanosome structure. MART1 forms a complex with PMEL inside melanocytes and is critical for PMEL expression and processing.

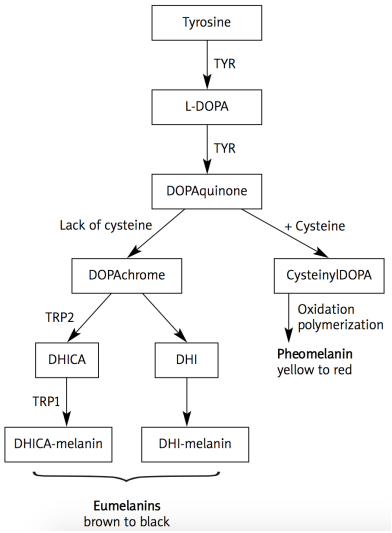

Figure 3. Melanin synthesis scheme. Melanin-making enzymes utilize tyrosine as a substrate to make two types of polymer of melanin in human: eumelanin (black-brown) and pheomelanin (yellow-red). Figure adapted from (Cichorek et al. 2013).

Melanocytes transfer melanin to keratinocytes through dendrites

Mature melanocytes secrete melanin-containing melanosome to 30~40 neighboring keratinocytes. Keratinocytes ingest the melanosome to form an umbrella structure around their nucleus to protect against UV-induced damage (Yamaguchi et al., 2007) (Figure 4). Therefore, melanins in both melanocytes

(a sparse cell population) and the upper layer keratinocytes together constitute the skin color.

Melanosome delivery is carried out by a specialized melanocyte cell projection called dendrites. Dendrites are actin and microtubule containing structures and their formation is regulated by keratinocyte-secreted growth factors and peptide hormones especially under UV stimulation (Kippenberger et al., 1998). Even though the exact molecular basis for dendrite formation is not known, the growth factors and peptide hormones generally converge on the cAMP second messenger pathway, and protein kinase C and MAP kinase pathway inside melanocytes (Hara et al., 1995; Hirobe, 1978). Small GTP-binding proteins such as Rac and Rho are known to regulate melanocyte dendrite formation, through a fine-tuned balance between Rho (which stimulates dendrite retraction) and Rac (which stimulates dendrite formation) (Scott, 2002), similar to what occurs in neuronal cells. Dendricity and pigmentation are the two key hallmarks for melanocyte differentiation. However, unlike pigmentation, how dendrites are acquired in concert with melanocyte differentiation during development is poorly understood.

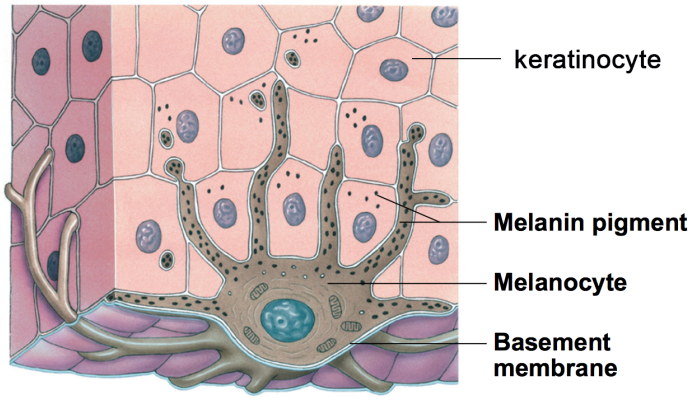

Figure 4. Melanocytes extend dendrites to transfer melanin pigment (inside melanosomes) to neighboring keratinocytes. Melanins form an umbrella shape around the keratinocyte nucleus to protect them from UV-induced damage. Figures adapted from 2012 Pearson Education.

Pigment diseases

Human pigment disorders highlight the importance of understanding pigment biology and has triggered an extensive search for therapeutic opportunities. Vitiligo is a hypopigmentation disorder characterized by patches of the skin losing their pigment. Vitiligo patients do not have functional melanocytes and multiple mechanism might contribute to this loss, with autoimmune disease triggering genetic susceptibility thought to be the main one (Picardo et al., 2015). Waardenburg syndrome is another hypopigmentation disease with loss of pigmentation in skin patches and deafness. It is an autosomal dominant disorder with mutations of genes required for the melanocyte development pathway (such as *EDN3*, *EDNRB*, *MITF*, *PAX3*, *SNAI2*, and *SOX10*) (Bondurand et al., 2000; Edery et al., 1996; Tassabehji et al., 1994). Patients

do not have melanocytes and have pigment defects in the skin, hair, eyes and problems with hearing. Albinism is a congenital disorder with patients are complete or partial lack of pigment in the skin, hair and eyes and are experiencing problematic vision. In the most severe form, Type 1 (oculocutaneous) albinism there is an absence of tyrosinase (the key enzyme making melanin) due to a mutation in *TYR* gene (Oetting and King, 1999). Albinism patients have melanocytes but are not able to produce melanin. Finally, melanoma is an extreme example of a pigment disorder where melanocytes are transformed because of oncogenic mutations and become malignant (Bandarchi et al., 2010). Melanoma will be discussed extensively in chapter 3.1.

1.1.3 Cell intrinsic mechanisms of melanocyte development

Melanocyte specification

Neural crest cells give rise to melanocytes, during which a tightly-regulated cell intrinsic program is activated to ensure proper cell specification. Microphthalmia-associated transcription factor (MITF) is the master transcription factor that has pleiotropic effects in melanocyte specification, differentiation and survival. MITF marks melanoblasts as soon as neural crest cell emigration from the neural tube (Hou and Pavan, 2008). Mutations in *MITF* are the cause of many pigment disease such as Waardenburg syndrome (Sun et al., 2017). Mice with MITF mutation display severe reduction of the early melanocyte marker DCT (Nakayama et al., 1998), while zebrafish with MITF loss of function fail to develop melanocytes (Lister et al., 1999). These all together suggest MITF plays a critical role in melanocyte specification.

But what factors activate MITF to pave the road for melanocytes? It was shown that PAX3 (Bondurand et al., 2000) and SOX10 (Lee et al., 2000) act synergistically to bind to the MITF promoter and activate MITF transcription in neural crest cells, with SOX10 being the major player (Elworthy et al., 2003) (Figure 5). Mice null for SOX10 have absence of melanocyte markers MITF and DCT in the dorsolateral pathway (Britsch et al., 2001), while PAX3 null leads to greatly reduced number of DCT+ melanocytes. These data suggests that SOX10 directly regulates MITF expression while PAX3 collaborates with these process during early melanoblast expansion (Hornyak et al., 2001).

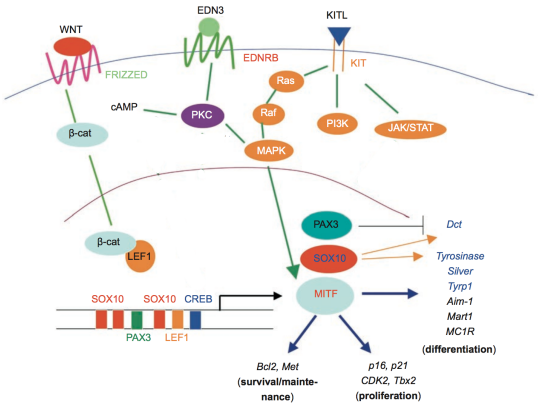

Figure 5. Melanocyte development is regulated by several key signaling pathways. Three major signaling pathways (WNT, KIT, and EDNRB) are stimulators to activate *Mitf*. Mitf subsequently transcriptionally turns on target genes, which include genes involved in cell survival, cell proliferation and differentiation. Figure adapted from (Hou and Pavan 2008).

However, glial cells can also co-express SOX10 and PAX3. What additional factor helps distinguish melanoblasts? Forkhead transcription factor FOXD3 has been shown to serve as negative regulator of the melanocyte lineage by repressing MITF expression. FOXD3 is expressed in all neural crest cells except for cells destined for the melanocytic lineage (Kos et al., 2001). In addition, overexpression of FOXD3 in quail neural crest cell cultures leads to glial cells while inhibiting melanocyte marker expression (Thomas and Erickson, 2009). In zebrafish, neural crest cells give rise to three different types of pigment cells: melanophores (fish orthologue of melanocytes), iridophores and xanthophores. Enforced expression of *foxd3* in pigment progenitors represses *mitfa* expression and induces iridophores generation in zebrafish (Curran et al., 2009; Ignatius et al., 2008), while in mice FOXD3 is contributing to glia and neurons cell fate. These together suggested an

elegant network where SOX10 and PAX3 activate MITF expression to prompt melanocytes specification and FOXD3 negatively inhibits this process.

Melanocytes differentiation

Differentiated melanocytes synthesize melanin and acquire dendritic cell morphology. Melanocytes pigmentation is regulated via the cell intrinsic factor MITF. MITF directly activates numerous targets that are important for melanocytes differentiation. These include genes encoding melanin synthesis enzymes, such OA1 (Vetrini et al., 2004), TYR, and TYRP1 (Lowings et al., 1992) and DCT (Schwahn et al., 2005); genes important for melanosome maturation, such as PMEL and MART1 (Du et al., 2003). What factors serve as the cue to activate MITF to trigger melanocyte differentiation? Pro-opiomelanocortin (POMC) is a precursor polypeptide that is produced in keratinocytes and cleaved into the small peptides α-MSH and ACTH (Paus et al., 1999; Tsatmali et al., 2000). In response to UV stimulation, keratinocytes secrete α-MSH (α-MSH can also be secreted systematically by the anterior pituitary gland) (Schauer et al., 1994) and α-MSH subsequently binds to the melanocortin 1 receptor (MC1R), a G protein–coupled receptor expressing on melanocyte cell membrane through paracrine signaling (Mountjoy et al., 1992). Agonist-bound MC1R activates adenylyl cyclase and the second messenger cAMP, which leads to phosphorylation of cAMP responsive-element-binding protein (CREB). CREB then transcriptionally activates MITF (Figure 5). MITF expression is enriched significantly within one day of UV exposure, while the downstream transcriptional targets such as TYR, PMEL, and DCT respond within 1–3 weeks after UV exposure (Levy et al., 2006; Videira et al., 2013).

Melanocyte pigmentation in response to UV exposure therefore can take several days to weeks to occur.

Melanocyte migration

Melanocytes are highly migratory populations, with KIT and endothelin receptor type B (EDNRB) playing vital roles during these process. KIT is known as stem cell growth factor receptor and it is highly expressed in both melanoblast and melanocytes (Wehrle-Haller, 2003). Zebrafish with KIT null mutations have defective melanocyte migration and subsequently undergo apoptosis. Mice with KIT mutation or KIT ligand mutation leads to a dominant white *spotting (W)* or *Steel (Sl)* phenotype with absence of melanocytes (Cable et al., 1995; Geissler et al., 1988; Wehrle-Haller, 2003).

EDNRB and its ligand EDN3 are required for melanoblast proliferation and migration in the dermis. Mice with mutations or deletions any of these two genes lead to *piebald lethal* and *lethal spotting* mutants phenotypes respectively (Hosoda et al., 1994). Both mutant mice have white color, except for spotted regions in the head and rump. Mice is lacking enteric ganglia in the distal colon and die at juveniles from megacolon. The zebrafish null mutant for EDNRB has normal embryonic pigmentation but defective normal numbers of melanocytes and iridophores during metamorphosis and exhibit a disrupted pigment pattern (Krauss et al., 2014; Parichy et al., 2000).

The best example to illustrate melanocytes migration is in the process of epidermis invasion. In mice, melanocytes migrate through dorsolateral pathway in the dermis, sequentially invade into the epidermis and then the into the hair follicle, where they colonize and differentiate. Melanoblast invasion of

the epidermis is coincident with epidermal stratification marked by different expression of the cell adhesion molecules E-cadherin and P-cadherin (Koster and Roop, 2007). For example, when melanocytes are invading, they express the same cadherins and subvide themselves based on their epidermis/dermis location. In epidermis, both keratinocytes and melanocytes expressed high level of E-cadherin; while dermal fibroblasts and melanocytes are low for both E-cadherin and P-cadherin; melanocytes in the hair matrix are E-cadherin low and P-cadherin high (Hirai et al., 1989). It is likely that the same process regulating epidermal stratification is also hijacked by melanocytes to invade.

Melanocyte proliferation

Epidermal black melanocytes are considered as a very quiescent population which normally rarely divide. To increase melanocyte number, developing animals usually increase proliferation of unpigmented melanoblasts or melanocytes stem cells, followed by differentiation into visible mature melanocytes.

For example, in mice, melanoblasts undergo first waves of proliferation in the dermis before invading into epidermis, followed by a second waves of rapid proliferation in the epidermis (Jordan and Jackson, 2000; Mackenzie et al., 1997; Nishikawa et al., 1991). At the hair follicle, melanocyte stem cells will then transiently proliferate and then differentiate into black melanocytes with each hair cycle and so add color to the hair (Nishimura et al., 2002, 2005). In zebrafish, most pigmented embryonic melanocytes are derived directly from neural crest/melanoblast differentiation, with a small population of black cells that maintain their proliferative capacity (Taylor et al., 2011). In adult zebrafish,

most melanocytes are derived from melanocyte stem cell differentiation (Hultman et al., 2009; Iyengar et al., 2015; Tryon and Johnson, 2012). In humans, a small percentage of melanoblasts have evidence of cell division during wound-healing related regeneration to restore the pool of black melanocytes. Once melanocytes are differentiated, it is generally thought that those cells lose proliferative potential.

However, recently data also suggested there could a transient population where melanocytes are both differentiating and proliferative. Those cells (Kim et al., 2017) are not terminal differentiated yet therefore still maintain active proliferation potential. MITF activity is fine tuned in those populations as very high levels of MITF can halt cell division while absent or low MITF is anti-differentiation (Carreira et al., 2006; Hoek and Goding, 2010).

While black melanocytes *in vivo* rarely divide, tissue culture experiments suggest the evidence of actively dividing pigmented melanocytes and therefore help shed light on the mechanism regulating melanoblast/melanocyte proliferation. MAPK-kinase signaling, α-MSH/cAMP/PKA, Endothelin/PKC signaling pathways all promote cell proliferation (Costin and Hearing, 2007), while TGF-β, INF-β, IL-1 and IL-6 counteract these effect (Sulaimon and Kitchell, 2003).

1.1.4 Environmental factors regulating melanocyte development

Keratinocytes are the most well-known cell type regulating melanocyte development

Keratinocytes accounts for 90% of the cells found in epidermis (Müller et al., 2014). It undergoes keratinization to form the dead superficial layer of the human skin. Once the superficial keratinized cells are dead, the actively dividing keratinocytes from the basal layers will move upward to replenish the pool. Keratinocytes are known potent regulators for melanocyte development through paracrine signaling, as they secrete growth factors such as endothelin 1-3 (EDN1-3) (Hara et al., 1995; Saldana-Caboverde and Kos, 2010) and kit ligand (KITL) (Belleudi et al., 2010; Grichnik et al., 1998). These factors work on the corresponding receptors on melanocytes to regulate entire life-cycle of melanocytes as mentioned above, such as melanoblast specification, differentiation, proliferation and melanocytes migration. In response to UV, keratinocytes upregulate p53 expression which then subsequently induces POMC activity to secrete more a-MSH and ACTH (Cui et al., 2007). a-MSH and ACTH act upon the MC1R on melanocytes membrane to induce pigmentation during tanning. Besides p53, keratinocytes can secrete more interleukin-1 in an autocrine fashion to increase the production of ACTH, MSH, endothelin 1 and bFGF (Brenner and Hearing, 2008). During tanning, keratinocytes also exert protective effects on melanocytes by secreting NGF to prevent melanocyte apoptosis following UV exposure (Kadekaro et al., 2003).

Interestingly, keratinocyte-derived factors share similar identity with those important in blood vessel formation (such as EDN, KITL and HGF). It is hypothesized that melanocyte migration is influenced by the same factor released from blood vessels which prime the dependence of melanocytes on the same factors post colonization.

Fibroblasts are a novel player regulating melanocytes development

Fibroblasts are stromal cells that synthesize the extracellular matrix and collagen in dermis. Together with keratinocytes and melanocytes, they constitute the three major cell types in human skin. A few studies highlight the contribution of fibroblasts in the regulation of pigmentation (Duval et al., 2014). In the 1990s, scientists have discovered the roles of fibroblast produced-extracellular matrix (ECM) in altering melanocyte morphology and significantly increasing melanogenic activity (Buffey et al., 1994). Recently, Dikkopf 1(DKK-1) produced by fibroblasts in the palms and soles was shown to repress melanocyte growth and inhibit melanosome transfer, resulting in lighter color in patch of skin (Yamaguchi et al., 2008, 2009). Fibroblasts also have melanogenic effects by secreting bFGF, neuregulin-1 (NGR-1), SCF, hepatocyte growth factor (HGF) or keratinocyte growth factor (KGF) to promote melanocyte pigmentation (Imokawa, 2004) (Figure 6).

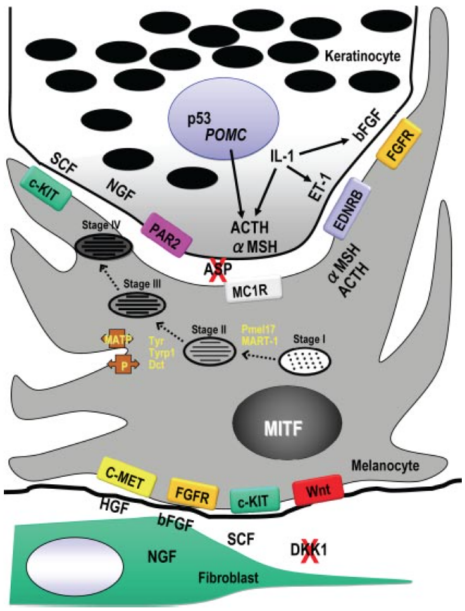

Figure 6. Hunan skin pigmentation is regulated by receptors, ligands and other factors. Keratinocytes and fibroblasts communicate with melanocytes through paracrine signaling. Figure adapted from (Yamaguchi et al. 2007).

UVR is the most important extrinsic factor inducing tanning

UVR induces melanocytes pigmentation mainly through the keratinocyte-melanocyte paracrine signaling as mentioned above (Furuya et al., 2002). There are two types of skin tanning response, immediate tanning and delayed pigmentation. Immediate tanning appears 5 min to 10 min after UV exposure and can disappear days later. Immediate tanning is triggered by melanin redistribution from melanocytes to upper layer keratinocytes, and is largely due to UVA damage. Delayed pigmentation, in the other hands, takes days to weeks to occur. It is mainly caused by both UVA and UVB radiation, and results from transcriptional upregulation of genes in involved in melanin

synthesis (Costin and Hearing, 2007; Schiaffino, 2010; Tadokoro et al., 2005; Thody and Graham, 1998). UVR is also known to induce melanocyte dendricity, which serves as the channel to transfer melanosomes during photo protection (Jian et al., 2014).

Sex hormones

Although less is known about the molecular mechanism, the connection between hormone and pigmentation has been noticed for centuries. For example, pregnancy has long been linked with increases in skin pigmentation, commonly known as melasma.

Natale et al have shown that physiologic concentrated estrogen (17b-estradiol) increases melanin synthesis while progesterone counteract this effect (Natale et al., 2016). Sex steroids modulate melanin synthesis pathway through a classical signal transduction similar to α-MSH, which activates adenylate cyclase increases cAMP and leads to phosphorylation of CREB. CREB then transcriptionally activates MITF. Using both primary human melanocyte culture and 3D skin models, they proposed that estrogen and progesterone stimulate G protein-coupled estrogen receptor (GPER) and progestin and adipoQ receptor 7 (PAQR7) on melanocyte membrane respectively (Hirobe, 2011; Natale et al., 2016). These findings suggested a rich and complex components of GPCRs other than MC1R on melanocyte membrane that could affect melanin production. They also noticed the presence of others GPCRs such as histamine and leukotriene receptors with unknown functions.

Using immunochemistry and RT-PCR, Tadokoro et al located the androgen receptor expression in the nuclei of cultured human genital melanocyte cells. Furthermore, they reported that androgen is another stimulator for pigmentation by increasing tyrosinase activity in human genital melanocytes cells (Tadokoro et al., 1997), revealing one mechanism to explain the enhanced pigmentation after puberty.

Thyroid hormone

Hyperpigmentation is one of the side-effect from hyperthyroidism which could be attributed to an elevated secretion of pituitary adrenocorticotropic hormone compensating for accelerated cortical degradation (Diven et al., 1989). In cattle, T4 addition has been shown to affect pigmentation and hair growth (Safer, 2011). Recently in zebrafish, thyroid hormone has been shown to influence pigmentation cell patterning by promote xanthophores differentiation (a fish specific pigment cell type) while attenuating melanophores (fish ortholog of melanocytes) proliferation and survival (Guillot et al., 2016; McMenamin et al., 2014).

Fatty acids

Fatty acid is recently shown to regulate tyrosinase ubiquitination and tyrosinase proteasomal degradation. Specifically, linoleic acid (an unsaturated fatty acid) increases tyrosinase degradation whereas palmitic acid (a saturated fatty acid) counteracts this effect and increase tyrosinase activity in mouse melanoma cells (Ando et al., 2004). Therefore, many other saturated fatty acids such as palmitic acid, palmitoleic acid and stearic acid could induce B10 melanocytes differentiation (Hirobe, 2011).

1.2 Zebrafish as a model organism

1.2.1 Background

Scientists could not appreciate the beauty of basic molecular and cell biology without the aid of model organisms (Davis, 2004). Back in the eighteenth century, biologists approached many problems using observation, where they looked for evidence of divergence and convergence across species and came to a general solution to explain the mechanism. These efforts have led to many of early discoveries, such as linnaean classification, evolution by natural selection and embryology. By the end of the nineteenth century, more rigorous experimental biological approaches led to a standardized system to study general biological principles. These boosted the utilization of peas (which contributed to classical genetics), *Arabidopsis* (which serves as a multicellular form system to study plant biology) (Somerville and Koornneef, 2002), roundworm (*Caenorhabditis elegans*, with which scientists elegantly showed the course of development at the level of individual cell) (Ankeny, 2001; Brenner, 1974; White, 2013; White et al., 1986), fruit fly (*Drosophila melanogaster*, which gave rise to a groundbreaking of phenotypic and genetic information) (Nüsslein-Volhard and Wieschaus, 1980), E. coli, Salmonella and phages (which made molecular biology experiments approachable) and mice (which represent a mammalian system with relevance to human disease) (Paigen, 2003). All those model organisms have shared advantages with a relatively smaller size, easy to maintain in laboratory and most importantly, the availability of mutants. Through the study of numerous mutants, biologists mapped chromosomes, deciphered the genetic basis of each phenotype and put together signalling and transcriptional pathways.

In the late 1960s, G. Streisinger, a phage geneticist who had previously had tremendous success in understanding the genetic code and intracellular development of phage T4, decided to switch into developmental biology using something he was interested as a hobby: zebrafish (*Danio rerio*) (Grunwald and Eisen, 2002). Zebrafish began to thrive in the scientific community when researchers realized they need a vertebrate system to advance what they learned in *C. elegans* and Drosophila. This chapter will discuss the unique advantages with zebrafish as a genetic tool, then focus on the history of using zebrafish to study pigmentation, an obvious decision derived from the "zebra"-"fish" name. Finally, this chapter will touch on using zebrafish as a model to study human disease especially cancer.

1.2.2 Advantages of the zebrafish system

Cost effective

Zebrafish is a cost effective model organism. Zebrafish has a relatively small size (3–4 cm long as an adult) (Figure 7), which make them very easy to maintain in large quantity in the laboratory environment. Zebrafish have a relatively short sex maturation time with 2-3 month old fish being able to breed, which makes genetic studies possible. Moreover, a pair of zebrafish adults are able to produce a few hundreds eggs in one morning, allowing for enough animals in a high throughput experiment. Once fertilized, zebrafish embryos are develop quickly with the majority of organs being formed by 48 hours post fertilisation (hpf). More importantly, both embryos and adult (because of the engineered mutant *casper*), are transparent (White et al.,

2008), which made direct observation down a dissecting microscope possible (Patton and Zon, 2001).

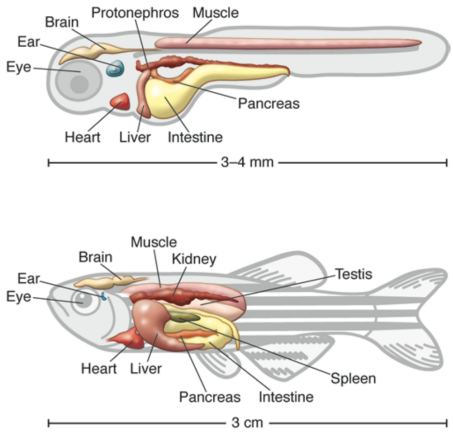

Figure 7. Zebrafish share similar organs with human. Shown are larval at 3dpf (Top) and adult (Bottom) zebrafish organs. Figure adapted from (Santoriello and Zon 2012).

Chemical screens

Zebrafish are highly suitable for chemical screens. As mentioned above, zebrafish can produce thousands of embryos per morning. Moreover, zebrafish embryos are small enough to be screened directly in multi-well plates. Compared to traditional screening using cell lines, zebrafish are better suited for drug discovery as they are living intact animals that possess a fully functional digestive and metabolism system (Tamplin et al., 2012). In addition, with abundant mutants available (Kettleborough et al., 2013), it is easy to combine zebrafish mutants with compounds to perform suppressor or enhancer screen. Screening for compound that can rescue a mutant phenotype into a wildtype (WT) is called a suppressor screen (Peterson et al., 2000, 2004; Stern et al., 2005) (Figure 8). Screening for drugs that could bring out a new phenotype in a sensitized background is called an enhancer screen,

where the targets are thought to be essential in promoting a phenotype in combination with the sensitized genotype in the case of an agonist as a hit.

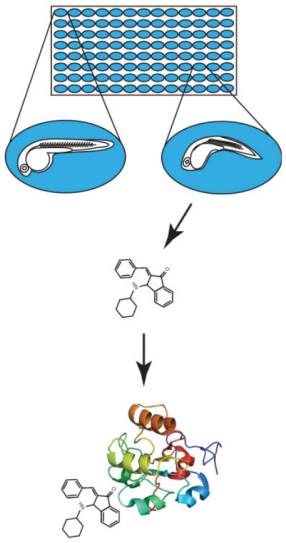

Figure 8. Chemical screen to look for compounds alternating a certain phenotype. Zebrafish embryos are tested in a 96-well place format. Compounds from an established library are added to each well to assay for their effects on a certain developmental phenotype. The hit compound that reaches desired phenotype would be retrieved from the library and reconfirmed. Figure adapted from (Tamplin et al. 2012).

Rich tools are available for genome editing

It is relatively straightforward to make transgenic zebrafish by microinjection of plasmids into a 1-cell stage embryo. Because of the large number of embryos, scientists can generate a large number founders to study gene expression in vivo. With the emergence of genome-editing tools, such as TALENs (Dahlem et al., 2012), zinc finger nuclease (Foley et al., 2009) and CRISPR-Cas9 (Irion et al., 2014), researchers now routinely perform gene knockout and gene knock-in reverse genetic experiments in zebrafish. Zebrafish can be also used in forward genetic screen using random N-ethyl-N-nitrosourea (ENU) mutagenesis (de Bruijn et al., 2009), which generates a large number of

mutant and enables identification of novel genes associated with a desired phenotype (Driever et al., 1996; Haffter et al., 1996).

1.2.3 Zebrafish have a long history in pigmentation research

The zebrafish has a beautiful layout of adult pigment cells with alternating black and white stripes, corresponding to a "zebra-like" pattern. Like other vertebrates, zebrafish possess pigment cells that arise from two distinct embryonic sources: one derived from neural crest cells and located between the dermis and epidermis; and those that originate from the optic cup and comprise the retinal pigment epithelium (RPE) (Mort et al., 2015). Zebrafish have three classes of pigment cells: black melanophores, yellow xanthophores, and silvery iridophores. Dark stripes contain melanophores and iridophores, whereas light stripes include xanthophores and iridophores (Parichy, 2003).

Zebrafish have a two waves of pigment cell formation to pattern the embryonic pigmentation and adult pigmentation, with both of them being derived from a SOX10+ neural crest cells. The embryonic pattern is formed by melanocytes that directly specified from SOX10+ neural crest into an SOX10+/MITF+ melanoblast. The adult melanoblasts originate from a melanocyte stem cell population that is set aside during embryo stage and re-activated during metamorphosis. Melanocyte stem cells reside at the dorsal root ganglia and is dependent on ERB and KIT pathway for specification and survival (Hultman et al., 2009).

Zebrafish have clearly defined pigment phenotypes and share conserved pathways regulating melanocytes biogenesis. Scientists recovered many pigment mutants from pet stores stock and from there started pigment genes research. These are some of early zebrafish pigment mutants that paved the road for pigment research (Figure 9) (Kelsh et al., 1996; Streisinger et al., 1986).

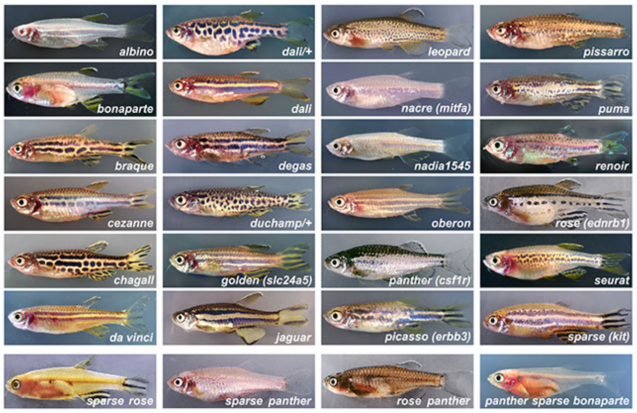

Figure 9. Zebrafish mutants with pigment cell abnormalities. Figures adapted from Dr. David Parichy's website.

Albino

Albino, a mutant in *slc45a2* gene. Streisinger recovered the first described albino mutant *alb*^{b4} (Streisinger et al., 1986). *Albino* fails to melanize by 2 days post fertilization and does not have pigmentation in neither RPE nor neural crest-derived melanophores. The human orthologous gene is involved in human skin color disease OCA4 (Newton et al., 2001). *slc45a2* regulates melanosomal pH homeostasis, with defective proper pH homeostasis leads to tyrosinase enzymatic activity quenching (Dooley et al., 2013).

Golden

Golden, a mutant in *slc24a5* gene. Lamason et al characterized this mutant and showed that *golden* zebrafish has delayed and reduced development of melanin pigmentation. At approximately 48 hpf when there is evident melanin deposition in melanophores, *golden* are still pale. By 72 hpf and all the way into adult, *golden* melanophores and RPE begin to develop pigmentation that is lighter than that of wild type. *slc24a5* is a melanosome-enriched calcium exchanger that is critical in regulating melanosome number and structure (Lamason et al., 2005). Importantly, this gene is responsible for a large amount of the variation in human skin color between Caucasian and African populations (Lamason et al., 2005).

Sparse

Sparse corresponds to a mutation in the *c-kit* gene. Parichy (Parichy et al., 1999) et al showed that *sparse* embryos initially have normal melanized melanophores but by 11 days post fertilization (dpf) all the melanophores are dead. As the early melanophores fail to migrate, this suggests that *c-kit* is vital for melanophore migration and survival. As a consequence, *sparse* adults have half the number of melanophores compared to WT animals.

Rose

Rose has mutation in the *ednr1b* gene. Parichy et al showed that *rose* mutants have normal embryonic pigment but fail to develop normal numbers of melanocytes and iridophores during metamorphosis and therefore exhibit a disrupted adult pigment pattern. EDNRB binds to all three endothelin ligand (EDN1-3) with equal affinity. Activated EDNRB1 protein leads to phosphorylation of protein kinase C (PKC), mitogen-activated protein kinase

(MAPK) and CREB, which turn on MITF mediated melanocyte differentiation (Parichy et al., 2000).

Leopard

Leopard is due to a mutation in the *connexin41.8* gene. Watanabe et al showed that *leopard* mutants have spotted skin pattern instead of stripes. There are different leopard alleles, such as leo^{t1}, leo^{tq270} and leo^{tw28} with each showing different skin-pattern phenotypes. Those mutations have defective channel function of connexin41.8, causing loss of cell to cell interactions (Watanabe et al., 2006).

Nacre

Nacre corresponds to mutation in the *mitfa* gene. *Nacre* mutants lack melanophores from embryos to adults, but have an approximate 40% increase in the number of iridophores at 3dpf. MITFA is the master transcription factor that specify the melanophore lineages, and lack of MITFA therefore leads to absence of melanophore cell phate (Lister et al., 1999).

1.2.4 Zebrafish is a unique system to model melanoma

Melanoma is a malignant skin cancer originating in transformed melanocytes. 50%–60% of melanoma have BRAFV600E mutations which leads to uncontrolled activation of BRAF/MEK/ERK signaling pathway (Ascierto et al., 2012). Patton et al. took advantages of those clearly defined genetic disorders in melanoma and generated the first transgenic melanoma model, where the BRAFV600E oncogene is specifically expressed in melanocytes under MITFA promoter; the tumor suppressor P53 is inactivated in this model to release

melanocytes from oncogene-induced senescence. Fish with only BRAFV600E developed moles similar to human nevi, whereas the double mutants of BRAFV600E and p53$^{-/-}$ form melanoma starting at four months with 100% penetrance (Figure 10).These melanomas closely resemble human cancers at the morphological, mRNA expression and genomic alteration levels (Patton et al., 2005).

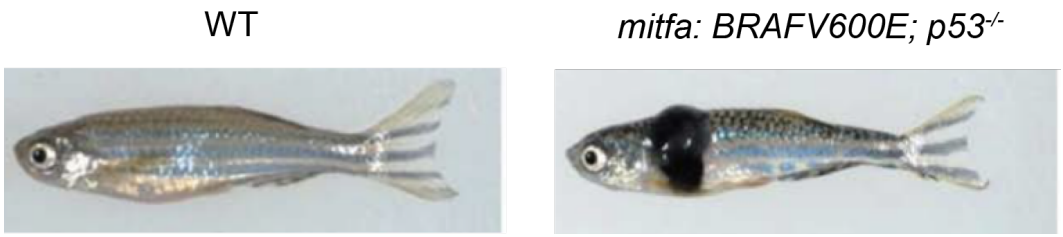

Figure 10. A transgenic zebrafish melanoma model (*mitfa:BRAFV600E; p53*$^{-/-}$), with the human oncogene *BRAFV600E* driven by a zebrafish melanophore specific promoter *mitfa*. Adult zebrafish form spontaneous tumors in a time window from 2 to 24 months, with 100% penetrance. Figure adapted from (White et al., 2011).

White et al. used this transgenic model to identify a transcriptional signature of early melanomas. This revealed a significant overexpression of neural crest related genes, particularly the embryonic neural crest marker *crestin* as well as other genes such as BACE2. They then performed a chemical suppressor screen to identify compounds which suppressed this neural crest signature. They identified inhibitors of dihydroorotate dehydrogenase (DHODH) which could suppress *crestin*+ neural crest signature and inhibit melanoma growth for human cells (White et al., 2011). DHODH inhibitor leflunomide is currently being tested in phase I/II clinical trials and this translational finding suggested how scientists could take advantages of the abnormal dependence on embryonic gene programs to suppress melanoma growth. Moreover, these

observations led to additional work showing the importance of neural crest genes such as SOX10 as important for melanoma initiation (Kaufman et al., 2016).

Ceol et al. further modified the tumor model by breeding them into a *mitfa* null mutant *nacre*. In these animals, they could couple melanocyte rescue with oncogene overexpression and examine the consequence of oncogene expression specifically only in transformed melanocyte. They identified that *setdb1* as histone methyltransferase as recurrently amplified in melanoma which accelerates melanoma (Ceol et al., 2011).

Transplantation-based methods have a big impact in tumor biology, where tumors can be dissected off from a transgenic tumor-bearing animal or from patient-derived xenografts (PDXs), and then serially transplanted into recipient animals. Zebrafish proves themselves to be applicable for those techniques (White et al., 2013). White et al have established a stable, fluorescently-labeled zebrafish melanoma cell line (ZMEL-color) with an easily manipulated genome. Transplantation of ZMEL-color cell into transparent zebrafish *casper* for both embryos and adults, allows for highly sensitive measurement of melanoma cell behavior at single cell resolution (Figure 11). The ZMEL-color line is completely unpigmented in vitro, but once transplanted into casper, 100% of the locally engrafted skin tumors regain pigmentation within ~7-14 days after transplant, which is a reflection of melanocytic differentiation. Using this assay, they can visualize the gradual differentiation over time and study the influence of differentiation on tumor morphology, primary tumor growth, and metastasis (Heilmann et al., 2015; Kim et al., 2017).

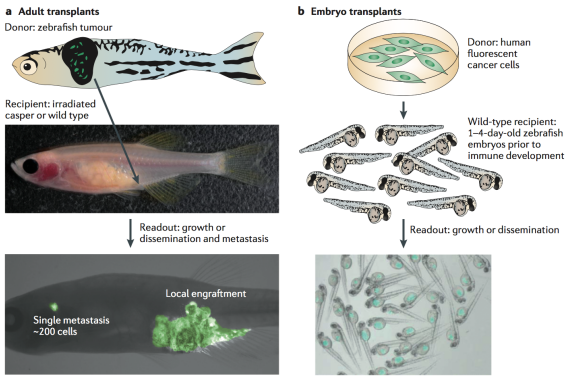

Figure 11. Tumor transplantation in zebrafish. (A) Transplant a primary tumor dissected from a tumor-bearing fish into a transparent adult *casper* mutant (middle) gives the resolution to observe single cell metastasis in a live animal (bottom). (B) Color labelled donor cells are transplanted into zebrafish embryos. Recipients can be used to test chemical efficacy in a high-throughput screen, and to study the interplay between host fish genetic mutations with cancer cells. Figure adapted from (White et al. 2013).

1.3 BACE2

1.3.1 Background

Beta-site amyloid precursor protein cleaving enzyme 2 (BACE2) is a transmembrane aspartic protease that belongs to β-secretase family. BACE2 is also previously referred to as MEMAPSIN 1 or ASP1. BACE2 cleaves substrates to exert biological functions (Figure 12). This chapter will talk about *BACE2* gene location and transcripts expression, known substrates and functions, its relevance to homolog *BACE1* and then focus on the potential roles of BACE2 in melanocytes as a lineage factor.

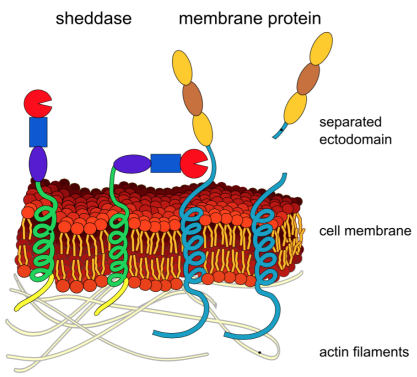

Figure 12. Diagram of ectodomain shedding. Membrane-bound sheddase cleaves its substrates and sheds them off from membrane. Figure adapted from art work of Armin Kübelbeck, distributed under a CC BY-SA 3.0 license (Wikimedia Commons).

1.3.2 BACE2 gene location and transcripts expression

The human *BACE2* gene is located on chromosome 21 in the Down's syndrome region at 21q22.3. This region is triplicated in the genome of Down's syndrome patients and also contains the APP gene (Acquati et al., 2000; Bennett et al., 2000). Human BACE2 has 518 amino acids, with 20 amino acids long N-terminal signal peptide and a propeptide domain immediately following after. BACE2 has two highly conserved aspartic protease enzymatic sites with sequence D(T/S)G(T/S) that are required to endocleave substrates (Ahmed et al., 2010). BACE2 has three disulfide bonds and shares similar tertiary structures with BACE1 (Bennett et al., 2000), with the aspartic protease active site facing the lumen or the extracellular environment. BACE2 has a transmembrane domain followed by a carboxyl-terminal 80 amino acids long cytosolic tail (Bennett et al., 2000). These features suggested that BACE2 belongs to type one transmembrane protein with single pass

transmembrane domain and has its N-terminus targeted to the ER lumen during synthesis. Intracellularly, BACE2 is localized either to the plasma membrane, endoplasmic reticulum, trans-Golgi network, endosomes and lysosomes, with a broad pH range for enzymatic activity while most effective at pH=3.5 (Kim et al., 2002).

BACE2 is highly expressed in pancreas, colon, placenta, kidney, prostate, trachea, stomach and pigment cells, but has low or undetectable level in adult whole brain and most brain sub regions (Bennett et al., 2000).

1.3.3 BACE2 function

BACE2 is known to cleave the following substrates.

Self-cleavage of BACE2

BACE2 contains a prodomain that requires cleavage during post translational modification to become an active enzyme. BACE2 undergoes self-processing to remove its prodomain (Hussain et al., 2001; Yan et al., 2001).

APP

BACE2 was initially speculated to be a β secretase APP cleaving enzyme and responsible for generating Aβ through a series of *in vitro* experiments, similar to its homologue BACE1 (Hussain et al., 2000). However, further *in vivo* study suggested BACE2 instead behave like an α secretase and cleave APP protein at residues A-Phe19 and A-Phe20 (which occurs within the Aβ sequence), however BACE1 could not cleave at the same site. α site cleavage lowers the levels of Aβ and mediates the degradation of Aβ but not production of the Aβ-

fibrils (Abdul-Hay et al., 2012; Ahmed et al., 2010; Fluhrer et al., 2002; Yan et al., 2001). Moreover, BACE1 null mice nearly abolished Aβ peptides production while the intact copy of BACE2 was still present, suggesting there is limited function of BACE2 in Aβ production. Moreover, there is little expression of BACE2 mRNA in the mouse neurons which suggests a limited complementation to BACE1. These all together imply that BACE2 works like an α-secretase and is not responsible for producing Aβ peptides in Alzheimer's disease.

PMEL

In melanocytes, PMEL forms the sheet-like matrix of amyloid fibrils to allow melanin deposition. PMEL forms the amyloid fibrils through a series of proteolytic cleavages inside the melanosome. PMEL amyloidogenesis occurs during stage I and II of melanosome maturation and controls the ellipsoidal shape and striated ultrastructure of melanosomes. Melanosome structure integrity is essential for melanocyte health likely by sequestering toxic ROS produced during melanin synthesis.

PMEL proteolytic cleavage is a multistep process: the full length PMEL is first cleaved by proprotein convertase (PC) into a Mα fragment and a Mβ fragment, connected by disulfide bonds. Then Mβ fragment is cleaved by BACE2 to be divided into a N terminal fragment and a transmembrane C-terminal fragment (CTF). CTF is cleaved through intramembrane proteolysis γ-secretase complex. Mα is also processed by unknown proteases into smaller fragments to form fibrils in melanosome (Kawaguchi et al., 2015). BACE2 is one of the key proteases that facilitate PMEL maturation inside melanosome. Lack of

BACE2 leads to defective formation of PMEL derived amyloid fibrils, altered early-stage melanosome morphology and silvery coat color mice (Rochin et al., 2013; Shimshek et al., 2016).

TMEM27

BACE2 cleaves TMEM27 in pancreatic β cells. TMEM27 normally increases pancreatic β cells proliferation, cell mass and augments glucose-stimulated insulin secretion. TMEM27 content on plasma membrane is negatively regulated by BACE2 shedding. Absence of cleavage stabilizes TMEM27 level in pancreatic β cells and leads to an increased β-cell mass, increased insulin levels, and eventually to reduce blood glucose levels (Esterházy et al., 2011; Stützer et al., 2013).

1.3.4 BACE2 shares distinct functions compared to BACE1

BACE1 and BACE2 shares 64% similarity in amino acids. Unlike other aspartic proteases, BACE1 and BACE2 both belong to type one transmembrane protein with a single pass transmembrane domain and a short cytosolic tail, which imply the membrane-bound nature of their substrates (Bennett et al., 2000). However, BACE1 and BACE2 have non-overlapping characteristics. Firstly, they localize to different compartments inside cells. BACE2 is diffusely expressed throughout both the early and late Golgi compartments while BACE1 is limited to the late Golgi and TNF (Yan et al., 2001). Secondly, they have distinct tissue enrichment. BACE1 is highly expressed in neuronal cells, while BACE2 is more enriched in peripheral secretory tissues, such as pancreas, prostate, stomach, thyroid and pigment cells (Bennett et al., 2000). The differences in intracellular location and

expression suggest that BACE21 and BACE2 have different substrates profiles and possess distinct physiological functions. BACE1 is important in nerve cell myelination, retinal integrity and neuromast development (Venugopal et al., 2008), while BACE2 plays roles in enteric neural crest migration, melanocyte development, choroidal vasculature and insulin secretion.

1.3.5 BACE2 is a potential lineage factor in melanocyte

Lineage factors are genes that are preferentially enriched in a certain lineage of cells, important in fate decision, differentiation and survival (Cao et al., 2011; Cheung and Nguyen, 2015; Garraway et al., 2005). They can be the initial transcription factors that activate a network of downstream proteins to specify this lineage, such as SOX10 and MITF in melanocytes (Harris et al., 2010; Levy et al., 2006). Lineage factors can also be genes that produce cell type specific features such as melanin synthesis genes in melanocytes. In addition, lineage factors can also be the survival genes that are critical to maintain cell survival to deal with a changing environment, such as KIT in melanocytes. Finally, lineage factors can also be genes that fine-tune cell's response to growth factors and hormone, to add on a cell type specific response to a general circulating factor.

BACE2 is highly expressed in melanocytes as well as melanoma, probably due to its enzymatic activity to cleave PMEL in melanocytes (Barretina et al., 2012; Rochin et al., 2013). In mice, *BACE2* null melanocytes displaying abnormally melanosome structure and "silvery" coat color further confirm this. In zebrafish, *bace2*$^{-/-}$ mutant display a striking melanocyte morphological

phenotype that is distinct from *pmela*$^{-/-}$ mutant (van Bebber et al., 2013; Walter, 2013), suggesting BACE2 could have alternative function in melanocytes and act as a lineage factor in regulating melanocyte morphology.

1.4 insulin/PI3K/mTOR signaling

1.4.1 Background

PI3K/AKT/mTOR signalling are critical in a wide range of cellular process such as cell growth, survival and nutrients metabolism (Figure 13). The major players in the pathway: phosphatidylinositide 3-kinases (PI3Ks), AKT and the mechanistic target of rapamycin kinase (mTOR) are essential in development as loss any of the major genes results in embryonic death (Napolitano and Ballabio, 2016; Zarogoulidis et al., 2014). Moreover, the pathway is frequently activated or amplified in cancers and has been an important focus of cancer research (Engelman, 2009; Porta et al., 2014).

Insulin is a circulating hormone that classically known to be released by pancreatic β cells into the bloodstream. Insulin regulates glucose and lipid homeostasis by binding to the insulin receptor tyrosine kinase (IR), which phosphorylates and recruits different substrate adaptors such as the insulin receptor substrates (IRS). Phosphorylated IRS then provides binding sites for numerous signaling partners, such as PI3K. PI3K then activates AKT which phosphorylates mTOR. mTOR has numerous downstream effectors, (which reflects the pleiotropic functions of mTOR), such as 4EBP1 and P70S6 kinase (S6K). They regulate translation initiation necessary for cell metabolism (Lizcano and Alessi, 2002).

This chapter will first discuss the specific structure and function of four major players in this signaling cascade: insulin, insulin receptor, PI3K and mTOR. Then this chapter will focus on the involvement of Insulin/PI3K/mTOR in embryonic development, with specific emphasis on cytoskeleton organization. Finally, this chapter will examine the regulation of insulin receptor level and activity.

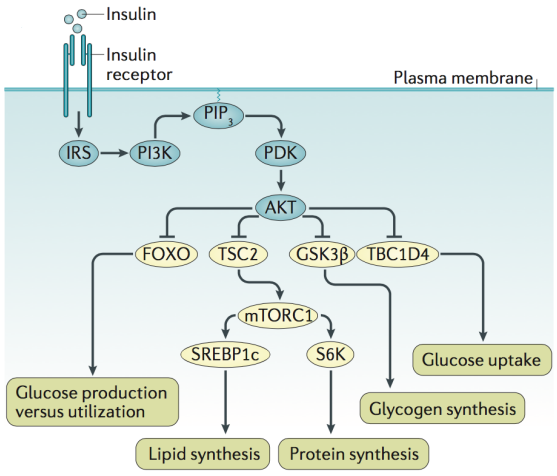

Figure 13. Overview of insulin signaling. Figure adapted from (Haeusler et al. 2018).

1.4.2 Structure and function of insulin, insulin receptor, PI3K and mTOR

Insulin

Human insulin is a 51 amino acid peptide composed of A and B chains. A chain and B chain are 21 and 30 amino acids long respectively, with A chain's N- and C-terminal helices linked to the central helix of the B chain via two disulphide bonds (Weiss et al., 2000).

Insulin is known to be synthesized inside the β cells of the pancreatic islets as pre-proinsulin and then processed into proinsulin. Pre-proinsulin synthesis occurs in the rough endoplasmic reticulum, as a 100 amino acid long peptide consisting of a signal peptide, the B chain, the connecting (C) peptide and then the A chain. The signal peptide is removed in the endoplasmic reticulum to form proinsulin. Proinsulin is transferred by secretory vesicles from rough endoplasmic reticulum to Golgi (Fu et al., 2013). Proinsulin is further wrapped inside storage vesicle to leave Golgi, during which proinsulin is converted into mature insulin. Insulin is packed inside dense-core granules and is released from the islet into the portal veins in response mainly to glucose (Hou et al., 2009).

Elevation of blood glucose is a strong stimulus to release insulin in two phases: an initial rapid insulin secretion and a 2nd mild but sustained release (Wilcox, 2005). β cell glucokinase is the key sensor for glucose level. When glucose enters β cell, glucokinase phosphorylates glucose to glucose-6-phosphate (G6P), generating ATP. ATP production results in closure of K+-ATP dependent channels and leads to membrane depolarization. Voltage-dependent calcium channels are open because of the depolarized membrane and lead to an increase in intracellular calcium concentration. Elevated calcium level eventually triggers pulsatile insulin secretion (Wilcox, 2005). Secreted insulin acts on muscle and adipocytes cells by inducing glycogen and lipid synthesis and reducing lipolysis and gluconeogenesis (MacDonald et al., 2005).

Insulin receptor

The insulin receptor belongs to the receptor tyrosine kinase (RTKs) family that can be activated by various ligands: insulin, IGF-1 and IGF-II (Ward and Lawrence, 2009). INSR gene encodes insulin receptor with two isoforms IR-A and IR-B due to alternative RNA splicing of exon 11. Both isoforms undergo post-translational proteolytic cleavage and results in α and β subunit, which could assembled by disulfide-linked to form a 320 kDa transmembrane insulin receptor (Belfiore et al., 2009). Each monomer is made of eight domains (Smith et al., 2010), as shown in Figure 14.

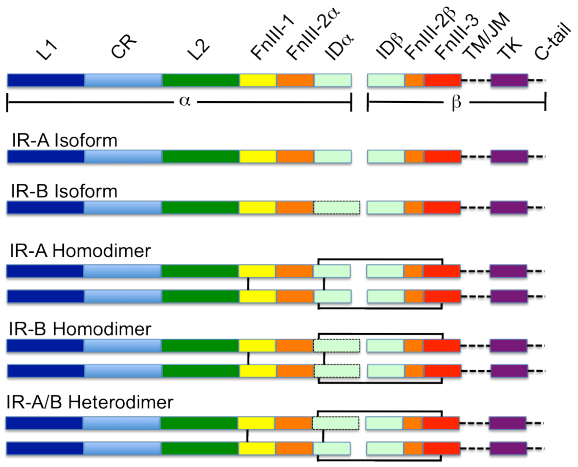

Figure 14. Insulin receptor structure. Figure adapted from art work of Fletcher01, distributed under a CC BY-SA 3.0 license (Wikimedia Commons).

Ligand binds to the α subunit which leads to insulin receptor conformational changes and ATP binding to the β subunit. ATP binding then triggers phosphorylation of the specific Tyr residues in the β subunit and confers tyrosine kinase activity (Wilcox, 2005). Phosphorylated β subunit further phosphorylates intracellular insulin receptor substrate (IRS) which can bind other signaling molecules (such as PI3K) to mediate downstream cellular actions of insulin (Haeusler et al., 2018).

In mammals, the insulin receptor is produced as a precursor protein, which is then proteolytically cleaved by the furin protease into α and β subunit, which together form a functional insulin receptor. An unknown protease further cleaves of the β subunit into a C-terminal fragment (CTF) (Kasuga et al., 2007), analogous to PMEL processing.

PI3K

Phosphatidyl-inositol-3-kinases (PI3Ks) are a lipid kinase family that can phosphorylate the inositol ring 3′-OH group in inositol phospholipids. Activated RTKs or GPCR can recruit PI3K to the adaptor proteins (such as insulin receptor substrate) by directly binding to phosphotyrosine consensus residues through one of the two SH2 domains in the adaptor subunit. Activated PI3K converts the substrate phosphatidylinositol-4,4-bisphosphate (PI-4,5-P2) into phosphatidylinositol-3,4,5-triphosphate (PI3,4,5-P3). PI3,4,5-P3 acts as a second messenger and recruits a subset of signaling proteins (such as AKT) harboring PH domains to the membrane (Porta et al., 2014).

There are three classes of PI3K due to their difference in structure and substrate specificities in mammalian cells. Among the Class I, there are further division of subclasses IA and IB due to various regulation modes (Figure 15). Class IA PI3Ks include PI3Kα, PI3Kβ and PI3Kδ. While each isoform has its own p110 catalytic subunit from α to δ respectively, they can associate with any of the five regulatory isoforms: p85α, p85β and p55γ, all called p85-type regulatory subunits (Thorpe et al., 2015).

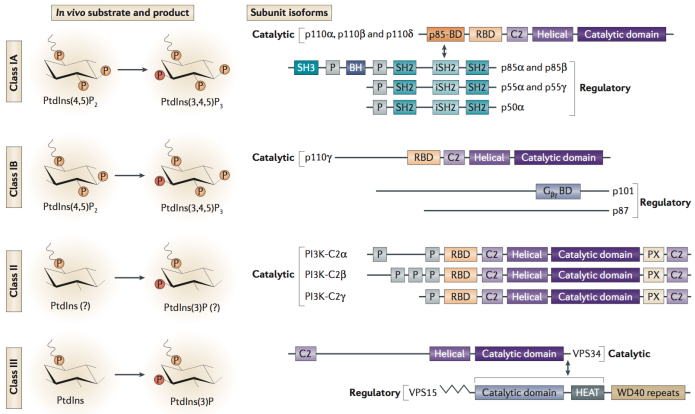

Figure 15. Different isoforms in PI3K family. PI3K is divided into three classes based on different compositions and *in vivo* substrates, with class I further divides into Class IA and IB. Abbreviations: P: proline-rich domains. C2: membrane-interacting domains. PX: Phox homology domain. p85-BD: p85-binding domain. RBD: RAS-binding domain. iSH2: inter-SH2 domain. BH: breakpoint cluster homology. Figure adapted from (Thorpe et al. 2015).

Class IB PI3Kγ are heterodimers that contain a p110γ catalytic subunit and coupled with regulatory subunits such as p101 or p87. Class I PI3K has different expression profile, with p110α and p110β are ubiquitously expressed and p110δ and p110γ are limited to leukocytes (Shymanets et al., 2013; Thorpe et al., 2015).

When PI3K is inactive, regulatory subunit inhibits p110 kinase activity; when receptor tyrosine kinase (RTK) or GPCR is activated, class I PI3Ks are recruited to the cell membrane and the inhibition effect from the regulatory subunit is relieved and p110 phosphorylates PtdIns(4,5)P2 to generate PtdIns(3,4,5)P3 (Engelman, 2009).

mTOR

Mechanistic target of rapamycin kinase (mTOR) is an essential protein for life, conserved from yeast to human. mTOR is a serine/threonine protein kinase that regulates protein synthesis, nutrient sensing and autophagy. Deregulated mTOR signaling contributes to cancer progression, diabetes and aging (Laplante and Sabatini, 2009). There are two complexes in the mTOR family: mTORC1 and mTORC2. The mTORC1 complex is made up of mTOR, Raptor, mLST8, and PRAS40. It distinguishes itself by sensitivity to rapamycin. It activates S6K and inactivates 4EBP1 to promote translation initiation for cell metabolism. The mTORC2 complex is made of mTOR, Rictor, Sin1, and mLST8. It is known to activate AKT, insulin receptor and insulin-like growth factor 1 receptors, thereby promoting cell proliferation and survival (Porta et al., 2014).

mTOR promotes protein synthesis through two main downstream effectors: p70S6 Kinase 1 (S6K1) and eIF4E Binding Protein (4EBP). mTORC1 directly phosphorylates S6K1 to activate several substrates that promote mRNA translation initiation, such as eIF4B, a positive stimulus of the 5'cap binding eIF4F complex, and ribosomal protein S6 (rpS6), a component of the 40S ribosomal subunit. Phosphorylated rpS6 activates translation of the TOP mRNAs, which are mRNAs that contain an oligopyrimidine tract at their 5′-terminus (5'-TOP). TOP mRNAs are mRNAs that are involved in translational machinery, such as ribosomal proteins and translation factors. Therefore mTOR-S6K1-rpS6 cascade is highly involved in the regulation of cell size, metabolism, proliferation and glucose homeostasis. mTORC1 phosphorylates

4EBP and releases the translation inhibition effects from 4EBP (Laplante and Sabatini, 2012; Saxton and Sabatini, 2017).

1.4.3 Involvement of Insulin/PI3K/mTOR in early development

Mice with germline loss of PI3K/mTOR often leads to embryonic lethality, therefore other model organisms serve as alternatives to dissect the roles of PI3K/mTOR in early development. In yeast (*S. cerevisiae*), TOR1 and TOR2 control cell size and sense nutrient availability, as rapamycin treatment or TOR1 and TOR2 depletion arrests yeast growth in the early G1 phase and induces an inhibition of translation initiation showing characteristic of starved cells entering stationary phase (G0) (Barbet et al., 1996; Di Como and Arndt, 1996). In fly (*D.melanogaster)*, TOR or S6K null animals are lethal in embryo accompanied by smaller cell sizes (Montagne et al., 1999; Oldham et al., 2000; Zhang et al., 2000). In zebrafish (*Danio rerio*), TOR is expressed ubiquitously in the early embryo. Rapamycin treatment or TOR knockdown leads to mild developmental delay up to 72 hpf and an arrested digestive tract development at the primitive gut tube stage (Makky et al., 2007). In mice, a germline mutation in the intronic region of *TOR* (which resulted in abnormal mRNA splicing and maintained 20% of mTOR kinase activity) leads to defective cell proliferation in the telencephalon and fails in rotation movement around the body axis and mice is lethal at 12.5 days post coitum. TOR null mice die shortly after implantation due to defective cell division in embryonic as well as extraembryonic cells (Hentges et al., 1999, 2001).

1.4.4 Involvement of PI3K/mTOR in cytoskeleton organization

In mammals, Rho family of GTPases is well known to affect cytoskeleton organization by regulating F-actin maturation (Tapon and Hall, 1997). PI3K/mTOR has recently been implicated to be involved in cytoskeleton organization by rearranging actin filament.

TOR2 is initially thought to be the only class in the mTOR family that regulates actin cytoskeleton through Rho GTPases. Factors known to activate mTOR signaling could induce cells spreading into the substratum and assembling of F-actin fibres, while mLST8 and mAVO3 siRNA knockdown (which are components only in TORC2) inhibited this process in NIH 3T3 cells. TOR2 KD induced F-actin assembly inhibition can be rescued using an active form of Rac or Rho (Jacinto et al., 2004). Moreover, Jacinto et al proposed that TORC2 is important in the formation of GTP-bound Rac1 as pull-down assay showed that there is 20–30% decrease in GTP-bound Rac1 in TORC2 siRNA-transfected cells. Rictor knockdown cells (a component of TORC2) display a flatter and a square-like cell morphology, due to a reduced amount of phosphorylation of Protein Kinase C (PKC) which is known to affect accumulation of thick actin fibers in the cytoplasm (Sarbassov et al., 2004).

Dendrites are the primary interaction sites between neuronal cells and different neurons have distinct dendrites morphology and pattern. PI3K is known to promote neurite outgrowth and retraction in neuronal cell (Leemhuis et al., 2004). There is evidence that PI3K-AKT-mTOR cascade induces the growth and branching of dendrites in hippocampal neurons *in vitro*. Inhibition of PI3K or knockdown of mTOR or p70 ribosomal S6 kinase greatly reduce

dendritic complexity (Jaworski et al., 2005). The upstream small GFPase Ras is also involved as constitutively active mutants of Ras could rescue dendrites growth from mTOR inhibition (Jaworski et al., 2005; Kumar et al., 2005).

TORC2 regulation of cytoskeleton has an impact on neuron morphology (Angliker and Rüegg, 2013). Ablation of rictor (the core component in TORC2) in brain decreases the mean total neuronal dendritic length by 15%. The soma size of *RICTOR* null neurons is only 70% of the control neurons and has less complex neurites. Thomanetz et al further extended this observation into a mechanistic study where they proposed that TORC2 is important for PKC isoforms activation and expression, since PKCs are known to play a role in spinocerebellar ataxia and in shaping the actin cytoskeleton. *RICTOR* null neuron leads to reduced level of PKC and a reduced activation of GAP-43 and MARCKS (Thomanetz et al., 2013).

TORC1 is also proposed to control the protein expression of the GTPases RhoA, Cdc42, and Rac1; rapamycin could inhibit this effect. 4EBP1 and S6K1 are the intermediate effectors as expression of constitutively hypophosphorylated 4EBP1 or downregulation of S6K1 suppress expression of the GTPases family. Rapamycin-resistant and constitutively active S6K1 could also partially prevent rapamycin inhibition effect (Liu et al., 2010).

1.4.5 Regulation of insulin receptor function

Defective insulin receptor signaling is one of the cause for insulin resistance which leads to type II diabetes. The insulin receptor is the bridge connecting extracellular ligand and intracellular signal transduction, and proper regulation

of Insulin receptor activity therefore is vital for systematic glucose homeostasis. Mutations in the insulin receptor gene are rare and is not likely to contribute to the reductions in insulin receptor function observed physiologically (Gao et al., 2013). Physiologically, there are multi-level regulations of insulin receptor activity: (1) regulation of insulin receptor enzymatic activity, or (2) regulation of insulin receptor content on plasma membrane at the level of transcription or post-translational modification (Youngren, 2007).

Much is known about the regulators involved in modulating insulin receptor tyrosine kinase activity. Multiple proteins are known to affect insulin receptor autophosphorylation, which is the first event occured post insulin binding. PC-1, also known as ectonucleotide pyrophosphatase phosphodiesterase 1, can directly bind to insulin receptor to block autophosphorylation (Maddux and Goldfine, 2000). LAR and PTP-1B are skeletal muscle specific tyrosine phosphatases that contribute to insulin receptor dephosphorylation (Ahmad and Goldstein, 1995). Phosphorylation of insulin receptor substrate (IRS) is the 2nd step in ligand binding. IRS is reported to be serine phosphorylated to inhibit its ability to serve as a substrate of insulin receptor, via JNK (Aguirre et al., 2002). Post-translational modification can also affect insulin receptor's enzymatic capacity. In pancreatic β cells, glucosamine increases O-glycosylation of both the insulin receptor and IRS-1, which leads to reduced insulin receptor autophosphorylation (D'Alessandris et al., 2004). Interaction of Grb14 with the insulin receptor does not affect insulin receptor autophosphorylation but still results in reduced IRS-1 phosphorylation, suggesting that tyrosine kinase activity can be uncoupled from its own

autophosphorylation level (Bérézíat et al., 2002; Hemming et al., 2001; Kasus-Jacobi et al., 1998). Insulin receptor activity can also be regulated at the level of RNA alternative splicing. Insulin receptor has two isoforms IR-A and IR-B due to splicing of exon 11, with IR-A having an increased responsiveness to IGF-I and IGF- II (Yamaguchi et al., 1991).

Regulation of the number of insulin receptors on plasma membrane is another way to regulate its function. Mice that are double heterozygous for the insulin receptor and IRS have reduced insulin sensitivity and glucose tolerance (Brüning et al., 1997). This underlies the importance of having adequate insulin receptors on the plasma membrane.

Transcription regulation of the insulin receptor is less understood. FOXO1 is proposed to function as a transcription activator that mediates insulin receptor transcription by binding to its promoter directly (Puig and Tjian, 2005). Moreover, insulin itself is also well known to decrease the amount of insulin receptor by promoting insulin receptor internalization and degradation (Okabayashi et al., 1989).

Recently, E3 ubiquitination is identified as a novel mechanism negatively regulating insulin receptor level. E3 ubiquitin ligase MARCH1 ubiquitinates insulin receptor to decrease cell surface insulin receptor level, inducing protein degradation. As a consequence, loss of MARCH1 enhances hepatic insulin sensitivity while overexpression of MARCH 1 impairs it in mice (Nagarajan et al., 2016).

CHAPTER 2: DISTANT INSULIN SIGNALING REGULATES VERTEBRATE PIGMENTATION THROUGH THE SHEDDASE BACE2

2.1 Introduction

Vertebrate pigmentation is an essential component of mate selection, camouflage and protection against UV damage(Price et al., 2008; Yamaguchi et al., 2007). Pigment cell patterning during development involves a precise spatiotemporal control of cell number, differentiation and localization. This patterning requires close coordination of both short-range and long-range extracellular factors with cell-intrinsic melanophore gene programs.

The major pigment cell type in humans is the black melanocyte, which corresponds to the black melanophore found in teleosts such as zebrafish. Across vertebrates, a cell-intrinsic transcriptional hierarchy orchestrates specification and differentiation(Mort et al., 2015). Melanocytes are derived from the neural crest, a population of *sox10*+ pluripotent cells that eventually give rise to lineage-restricted *mitf*+ melanoblasts(Ernfors, 2010; Sommer, 2011). *mitf* itself activates pigment genes such as *dct*, *tyr* and *tyrp1* and the melanoblasts then differentiate into melanocytes/melanophores. These cells are characterized by black melanin production and formation of cell dendrites, which in mammals transfers melanin packets into surrounding keratinocytes(Goding, 2007; Lin and Fisher, 2007).

Local environmental factors crosstalk with these intrinsic melanophore gene programs to instruct their development. One example of this interaction is short range communication between endothelins (EDN1, EDN3) produced by keratinocytes after UV exposure(Garcia et al., 2008; Hara et al., 1995;

Imokawa et al., 1992), which then act on nearby melanophores with endothelin-B receptor EDNRB on the membrane(Baynash et al., 1994; Parichy et al., 2000). Keratinocytes can also secrete other short range factors such as alpha-MSH which act on melanocortin receptors (MC1R) on the melanophores(Abdel-Malek et al., 1995; Chakraborty et al., 1991). These short-range factors act as strong positive regulators of melanophore proliferation and differentiation, and their effects are ultimately abrogated when the UV signal inducing their expression is reduced. Interactions between neighboring pigment cells also regulates their survival and localization(Hamada et al., 2014; Mahalwar et al., 2016). Adjacent xanthophores can exclude melanophores during stripe consolidation by extending specialized cell projections called airinemes which interact with microenvironmental macrophages(Eom and Parichy, 2017; Eom et al., 2015; Nakamasu et al., 2009).

Longer range factors such as endocrine hormones, can also control pigment patterning. Growth hormone/insulin growth factor (IGF) can induce melanophore proliferation and differentiation(Edmondson et al., 1999; Tavakkol et al., 1992) and melanin concentrating hormone released from the pituitary modulates melanosome trafficking to facilitate camouflage(Logan et al., 2006; Richardson et al., 2008). Thyroid hormones are critical to promote xanthophore differentiation while attenuating melanophore proliferation and survival(McMenamin et al., 2014). Because these hormones can pass through the bloodstream, it remains unclear how these more “general” factors are regulated within the melanophore lineage in a spatiotemporal manner, and how the melanophore turns off this signal. Such negative regulation is

essential to proper patterning, as excess melanophores could dramatically alter the appearance of the animal and render them susceptible to neoplastic growth. One hypothesis for this negative regulation is that these extracellular factors depend on lineage-specific gene programs within the melanophore to regulate their activity.

In this study, we utilized the zebrafish to study the role of distant factors in melanophore patterning. The zebrafish is an ideal system to address this question since it allows for facile genetic manipulation and chemical genetic strategies in a whole-organism context. Using this system, we characterized a mutant called *wanderlust* that has a disruption of normal melanophore patterning, with an excess number of hyperdendritic, hypermigratory melanophores. This mutant harbors an inactivating mutation in the sheddase Bace2, a melanophore-enriched gene that has been linked to abnormal migration but through an unknown mechanism(van Bebber et al., 2013). Here, we show that Bace2 acts to negatively regulate insulin/phosphatidylinositol 3-kinase (PI3K) signaling within the melanophores. This occurs due to the ability of Bace2 to cleave and degrade the insulin receptor specifically on melanophores. When Bace2 is lost, this leads to unregulated melanophore proliferation and migration, suggesting a mechanism that connects distant hormonal signaling to melanophore-specific gene programs.

2.2 Result

2.2.1 The zebrafish *wanderlust* mutant has hyperdendritic melanophores due to a loss of Bace2

In order to identify processes involved in pigment patterning, we characterized a zebrafish mutant called *wanderlust* that has a nonsense mutation in the sheddase *bace2(van Bebber et al., 2013)* (allele: *bace2*^{hu3332}). This leads to an early stop codon in exon 1 (Figure 16). During normal embryonic development, *mitf*+ melanophore precursors emerge from the neural crest from 16 to 24 hr post fertilization (hpf) and then migrate along the dorsolateral migration pathway, where they move first caudally and then ventrally along the somite boundaries(Kelsh et al., 2009). At the point of maximal migration, approximately 48 hpf, melanophores are highly dendritic, but by 72 hpf, after they have mostly ceased migration, the melanophores become compact and retract their dendrites(Cooper and Raible, 2009). In contrast, the *wanderlust* mutant has extensively hyperdendritic melanophores throughout development. These melanophores appear in atypical locations and abnormally migrate into the caudal tail fin (Figure 17A). The hyperdendritic phenotype is maintained throughout embryogenesis and into adulthood (Figure 17B). Consistent with this, during metamorphosis we find an increased number of ectopic melanophores in the inter-stripe region in the *wanderlust* mutant (Figure 17C-D). Transient knockdown of Bace2 using morpholinos (MO) in wild type (WT) embryos recapitulates the *wanderlust* embryo phenotype (Figure 17E), as does pharmacologic inhibition of Bace2 with the compound PF-06663195 (Figure 17F). Measurement of the tailfin melanophores shows that *wanderlust* melanophores occupy a larger cell area compared to WT embryos (Figure

17G). Collectively this demonstrates that it is the loss of Bace2 function that leads to the defect in melanophore localization and morphology.

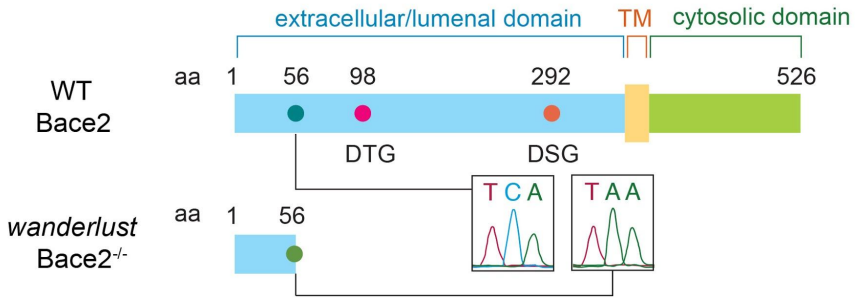

Figure 16. Bace2 protein diagram.
Schematic representation of zebrafish WT and Bace2$^{-/-}$ protein as found in the *wanderlust* mutant. Zebrafish Bace2 is a type I integral membrane β secretase that contains two DTG and DSG protease sites within its extracellular/lumenal domain. The *wanderlust* mutant (Bace2$^{-/-}$) has a C to A nonsense mutation leading to a truncated protein with size of 56 amino acids (aa), lacking both protease sites. TM=Transmembrane domain.

Figure 17. The zebrafish *wanderlust* mutant has hyperdendritic melanophores due to a loss of Bace2.
(A) Brightfield imaging shows that the *wanderlust* melanophores are hyperdendritic compared to WT fish (arrowhead) in the tail fin at 72hpf. Labeling of the melanophore cell membranes (bottom panel) using the *Tg(tyrp1b: membrane-mCherry)* line demonstrates that this is due to a change in cell morphology rather than a redistribution of melanin.
(B) These hyperdendritic melanophores are maintained into adulthood, and yield irregular stripe boundaries (arrowhead).
(C-D) *wanderlust* mutants develop melanophores outside of the stripe during metamorphosis at 24 days post fertilization (dpf) (arrowhead). Inter-stripe melanophores number are quantified in (D); fish number: n(WT)=5, n(*wanderlust*)=5, two-tailed t test, **P<0.01.
(E-F) Bace2 loss of function using morpholino knockdown (E) or pharmacological inhibition (F) phenocopies the *wanderlust* mutant. WT embryos are treated with Bace2 inhibitor (PF-06663195,100μM) from 48-72hpf.
(G) *bace2*$^{-/-}$ melanophores have larger cell area in the tail fin at 72hpf. Melanophore cell area is defined as the surface area covered by melanophores in the tailfin. Data are from five independent experiments, with total fish numbers: n(WT)=80, n(*bace2*$^{-/-}$)=105, two-tailed t test, ****P<0.0001. All bar graphs are presented as mean ± s.e.m. Scale bars, 100μM (A, B middle and bottom panel, C, E, F), 0.5cm (B top panel).

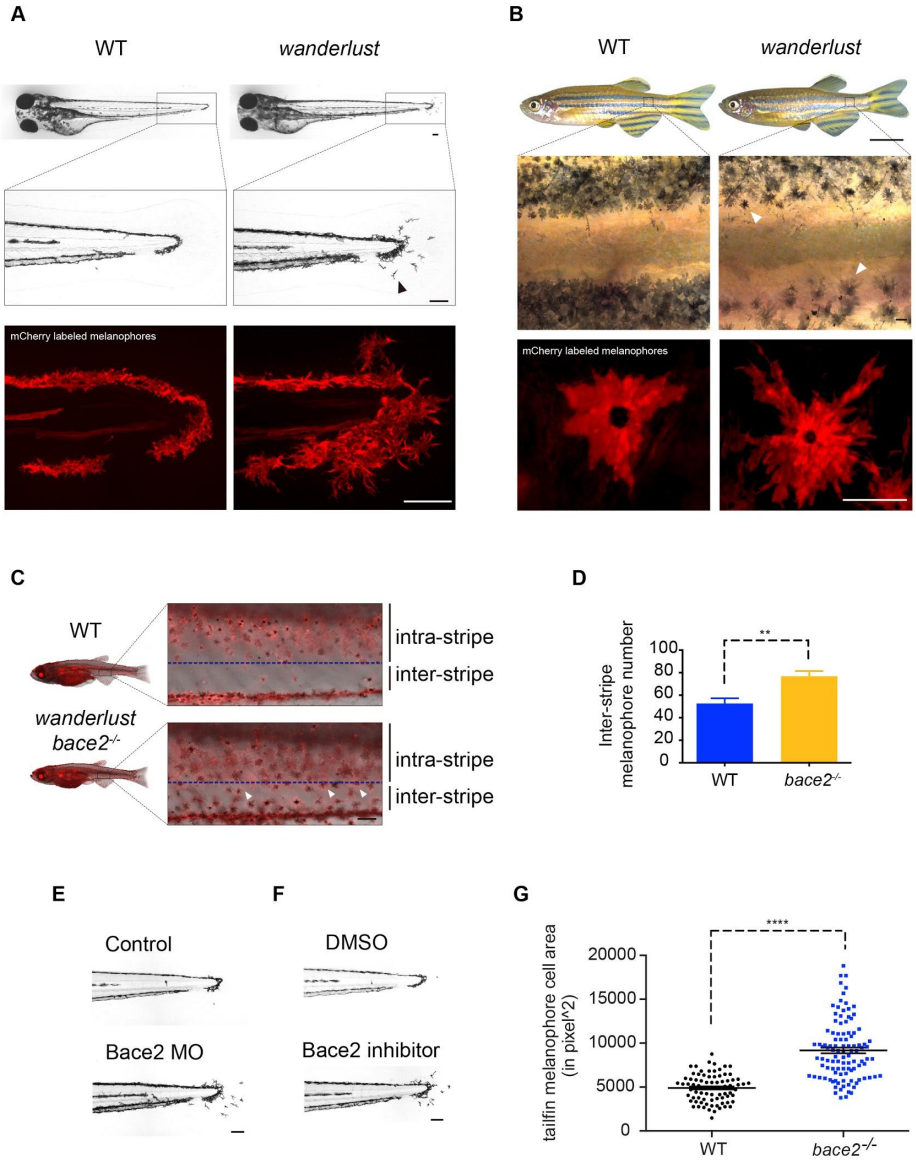
A
WT
wanderlust
mCherry labeled melanophores
B
WT
wanderlust
mCherry labeled melanophores
C
WT
intra-stripe
inter-stripe
wanderlust
bace2-/-
intra-stripe
inter-stripe
D
Inter-stripe melanophore number
100
80
60
40
20
0
**
WT
bace2-/-
E
Control
Bace2 MO
F
DMSO
Bace2 inhibitor
G
tailfin melanophore cell area (in pixel^2)
20000
15000
10000
5000
0
****
WT
bace2-/-

2.2.2 Bace2 acts during melanophore differentiation

We used a panel of neural crest and melanophore markers to determine when during development Bace2 is required using whole mount *in situ* hybridization (ISH). Whereas expression of the neural crest markers *crestin* and *sox10* at 24 hpf was normal in the *wanderlust* mutant (Figure 18A), by 72 hpf we noted an increase in pigmentation genes such as *dct*, *pmela*, *tyr* and *tyrp1b* in the mutant (Figure 18B), especially noticeable in the head region. This increase in pigmentation gene expression corresponds to an increase in visibly pigmented melanophores in the head region (Figure 18C-D). To determine whether these excess head melanophores were due to proliferation, we utilized a previously developed assay(Hultman and Johnson, 2010; Lee et al., 2010b; Lévesque et al., 2013; McMenamin et al., 2014) that uses existing melanin as a lineage tracer. In this assay, the animals are treated with the small molecule PTU, which prevents *de novo* melanin synthesis but does not affect existing melanin, so the appearance of new cells with melanin is indicative of division of a previously pigmented cell (Figure 19A-C). Using this assay, we find that PTU treatment did not prevent the increase in pigmented cell number, suggesting that Bace2 loss results in excess cell division of melanized cells (Figure 19D-E). To more precisely define the timing in which Bace2 acts, we treated WT embryos with Bace2 inhibitor PF-06663195 at various time windows from shield stage to 72hpf, and found that application from 48-72hpf is sufficient to give rise to the *wanderlust* phenotype (Figure 18E), coinciding with the period when the melanophores are actively pigmenting and differentiating.

Figure 18. Bace2 acts during melanophore differentiation.
(A) At 24hpf, ISH shows the *bace2*$^{-/-}$ mutants have unaffected expression for neural crest markers and melanocytes markers.
(B) But at 72hpf, ISH shows mRNA for the pigmentation genes *dct, pmela, tyr* and *tyrp1b* are elevated in *bace2*$^{-/-}$ mutants, especially in the head (arrowhead).
(C-D) Consistently, *bace2*$^{-/-}$ mutants have increased numbers of pigmented melanophores in the head (arrowhead). Fish number n(WT)=55, n(*bace2*$^{-/-}$)=30, two-tailed t test, **P<0.01.
(E) Treatment of WT embryos with 100μM Bace2 inhibitor (PF-0666195) from 48-72 hpf is sufficient to phenocopy *bace2*$^{-/-}$. Data are from two independent experiments, with total fish numbers: n(DMSO)=21, n(shield-24h)=45, n(shield-48h)=56, n(shield-72h)=72, n(24h-48h)=58, n(24h-72h)=40, n(48h-72h)=49; One-way ANOVA followed by Holm-Sidak's multiple comparisons test, **P<0.01. All bar graphs are presented as mean ± s.e.m. Scale bars, 200μM.

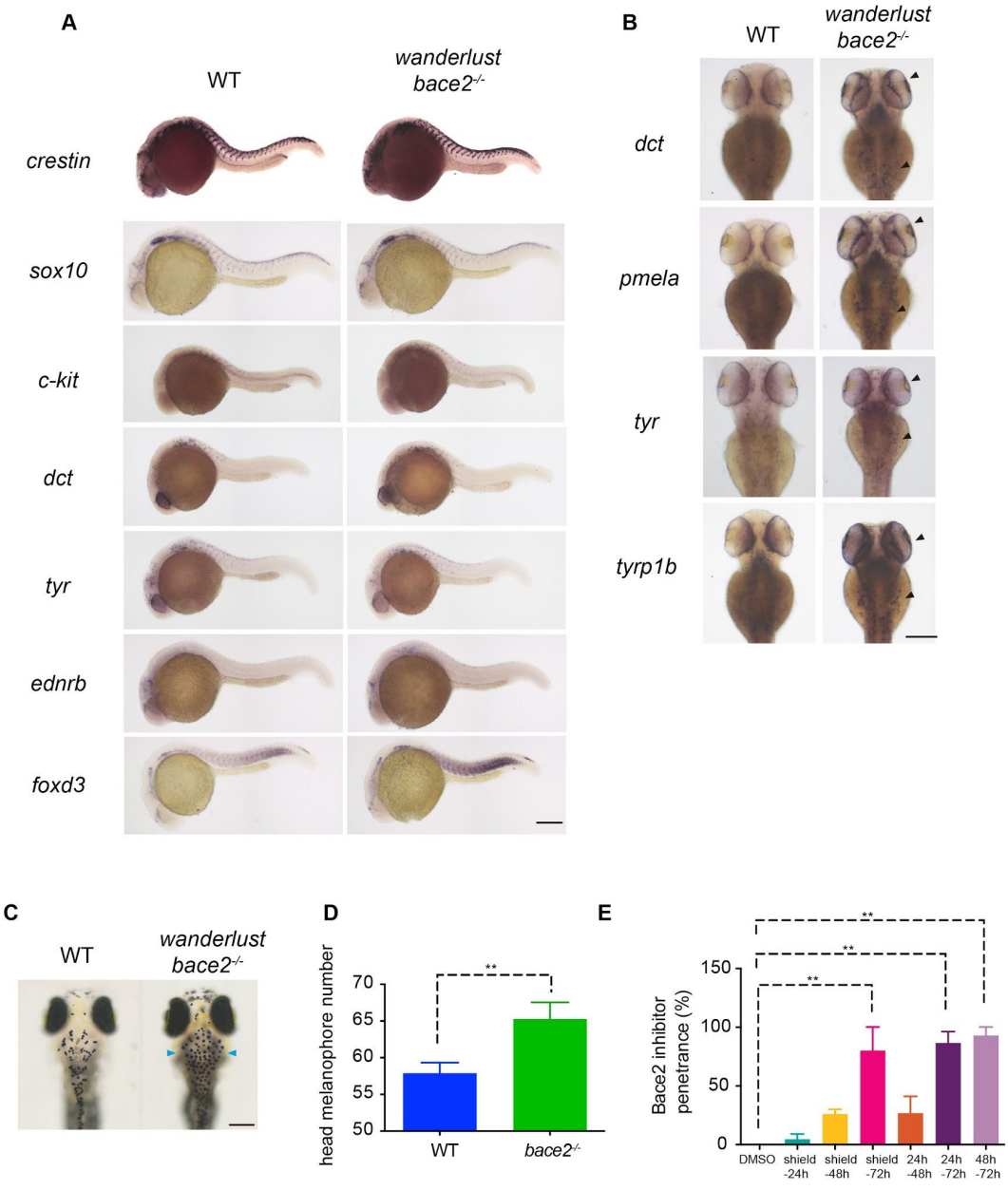
A
WT
wanderlust
bace2-/-
crestin
sox10
c-kit
dct
tyr
ednrb
foxd3
B
WT
wanderlust
bace2-/-
dct
pmela
tyr
tyrp1b
C
WT
wanderlust
bace2-/-
D
head melanophore number
70
65
60
55
50
**
WT
bace2-/-
E
Bace2 inhibitor
penetrance (%)
150
100
50
0
**
**
**
DMSO
shield
-24h
shield
-48h
shield
-72h
24h
-48h
24h
-72h
48h
-72h

Figure 19. Bace2 deficiency leads to increased melanophore cell division.
(A) Schema for testing the mechanism of increased melanophore cell number when Bace2 is loss. WT embryos were treated from 3-5dpF with 300μM PTU and/or 100μM Bace2 inhibitor (PF-06663195). PTU is a tyrosinase inhibitor that prevents new melanin synthesis to allow visualization only of previously pigmented melanophores.
(B-C) Schema for two possible scenarios. If Bace2 loss of function induces pigment cell division as shown in (B), co-treatment with the Bace2 inhibitor and PTU would still increase melanophore cell number the same way as Bace2 inhibitor treatment alone. This is because PTU would not affect pre-existing melanin and the newly derived daughter cells would inherit melanin from their mother cell. If Bace2 loss of function induces differentiation of unpigmented precursor cells as shown in (C), co-treatment with the Bace2 inhibitor and PTU would not increase visible melanophores cell number, as PTU would inhibit any new melanin from synthesis.
(D-E) Co-treatment with the Bace2 inhibitor and PTU led to an increase in the number of pigmented melanophores, which necessarily must have come from previously pigmented cells division due to the effects of PTU, quantified in (E). The data are from three independent experiments, one-way ANOVA followed by Holm-Sidak's multiple comparisons test; fish number n(DMSO)=53, n(Bace2 inhibitor)=56, n(PTU)=54, n(Bace2 inhibitor+PTU)=61. **P<0.01, ****P<0.0001. Epinephrine (5mg/ml) was used to aggregate melanin to facilitate cell counting. All bar graphs are presented as mean ± s.e.m. Scale bars, 200μM.

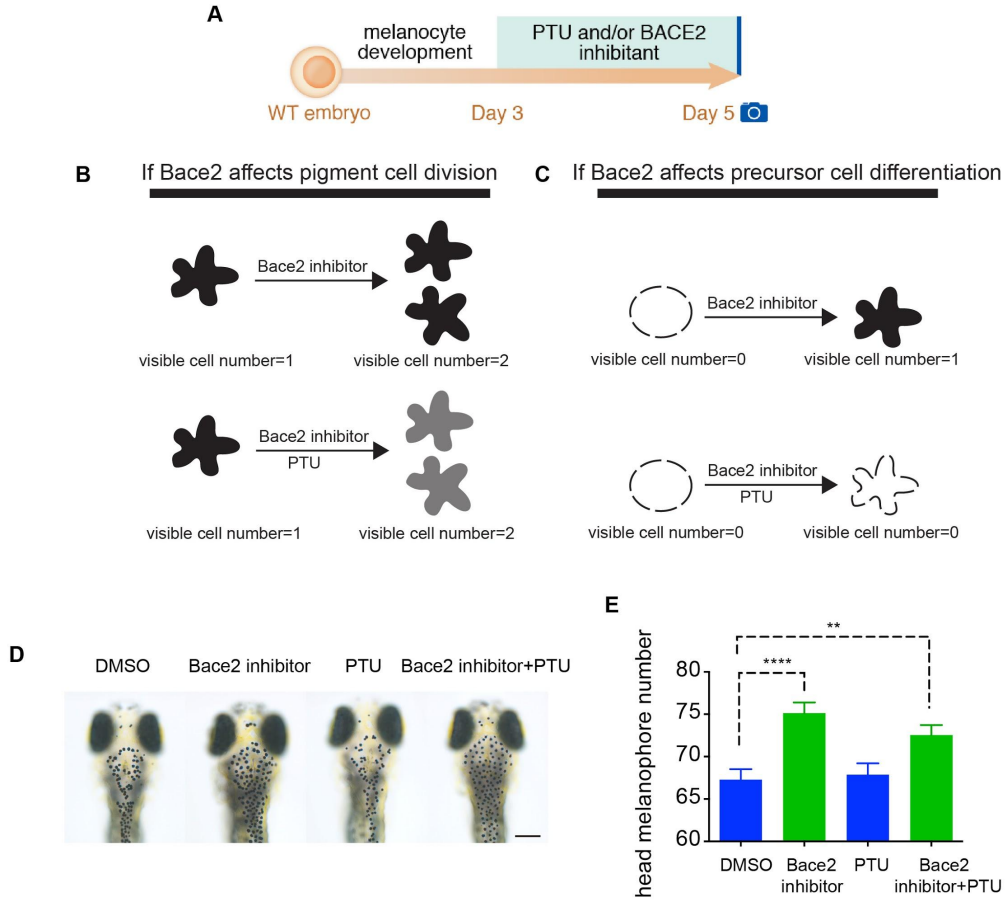
A
melanocyte development
PTU and/or BACE2 inhibitant
WT embryo
Day 3
Day 5
B
If Bace2 affects pigment cell division
Bace2 inhibitor
visible cell number=1
visible cell number=2
Bace2 inhibitor
PTU
visible cell number=1
visible cell number=2
C
If Bace2 affects precursor cell differentiation
Bace2 inhibitor
visible cell number=0
visible cell number=1
Bace2 inhibitor
PTU
visible cell number=0
visible cell number=0
D
DMSO
Bace2 inhibitor
PTU
Bace2 inhibitor+PTU
E
head melanophore number
80
75
70
65
60
**
****
DMSO
Bace2 inhibitor
PTU
Bace2 inhibitor+PTU

2.2.3 Bace2 acts cell-intrinsically within the melanophore lineage

To test if Bace2 was acting cell-intrinsically within the melanophore lineage, we examined expression of *bace2* by ISH and noted that it strongly overlaps with *crestin*, a pan neural crest marker that has been previously shown to mark all derivative lineages including melanophores (Figure 20A)(Kaufman et al., 2016; Luo et al., 2001; Rubinstein et al., 2000; White et al., 2011). To more directly test whether Bace2 was acting cell-intrinsically, we created a stable rescue transgenic line in which the fugu *dct* promoter(Budi et al., 2011) drives WT Bace2. When crossed into the *wanderlust* mutant, we see a complete rescue of the melanophore defect in both the tail and head regions, consistent with a cell-intrinsic effect of Bace2 loss (Figure 20B-D).

Taken together, these data indicate that Bace2 acts inside melanophore lineage and Bace2 deficiency leads to a hyperdendritic melanophore with increased proliferative and migratory capacity.

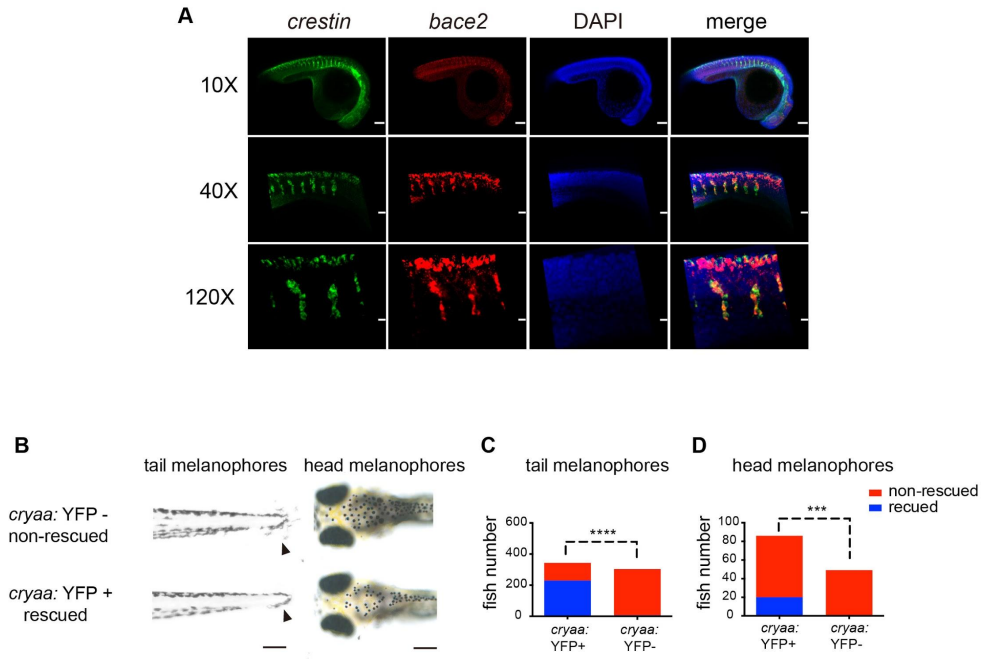

Figure 20. Bace2 acts cell-intrinsically within the melanophore lineage. (A) At 24hpf in WT embryos, double fluorescent ISH against the pan neural crest marker *crestin* (green) and *bace2* (red) shows *bace2* expression overlaps with *crestin*, suggesting *bace2* is highly enriched in the neural crest lineage from which the melanophores are derived.
(B-D) Melanophore-specific transgenic rescue of the *bace2*$^{-/-}$ mutant. A stable transgenic line was created in which the *dct* promoter drives Bace2 in the melanophores (along with a *cryaa*: YFP transgene marker). Founders were identified by expression of the YFP marker in the eye. Founders were crossed into other uninjected *bace2*$^{-/-}$ adult to generate F1 embryos. F1 embryos were scored for dendritic tail melanophore rescue at 3dpF (B, arrowhead) or for rescue of the head melanophores at 5dpF. F1 were divided into four groups: rescued, non-rescued, YFP positive and YFP negative. Chi-square with Yate's correction was performed to associate rescue phenotype with YFP positive eye (quantified in C and D). ***P<0.001, ****P<0.0001.All bar graphs are presented as mean ± s.e.m. Scale bars, 10μM (A 120X), 30uM (A 40X), 100μM (A 10X, B left panel), 200μM (B right panel).

2.2.4 Pmela is a substrate for Bace2 but is not responsible for the *wanderlust* phenotype

Bace2 is a transmembrane aspartic protease that acts as a sheddase, typically cleaving extracellular fragments to be released into the local microenvironment. Numerous BACE2 substrates have been previously described, including PMEL in melanocytes(Rochin et al., 2013; Shimshek et al., 2016) and TMEM27 in pancreatic β cells(Esterházy et al., 2011; Stützer et al., 2013). In mammals, the cleavage of PMEL by BACE2 is required for proper melanosome formation. Similarly, we found that in the zebrafish, Bace2 is sufficient to cleave Pmela (Figure 21A) and loss of Bace2 leads to disrupted melanosomes as seen by electron microscopy (Figure 21B). However, genetic knockout of *pmela* (Figure 21C), or morpholino knockdown of *pmela*/*pmelb(Burgoyne et al., 2015; Schonthaler et al., 2005)* does not phenocopy the hyperdendritic/proliferative phenotype of the *wanderlust* mutant (Figure 21D-E). This suggests a Pmel-independent role for Bace2 in melanophore patterning and morphology.

Figure 21. Pmel is a substrate for Bace2 but is not responsible for the *wanderlust* phenotype.
(A) zebrafish Bace2 cleaves Pmela. We constructed a fusion protein of zebrafish Pmela and a C-terminal Flag tag to detect cleavage by immunoblotting using Flag antibody. Expression of the fusion protein in HEK 293T cells reveals an immature core-glycosylated P1 form of Pmela (~150 kDa), the Mβ (~47 kDa), and the CTF (~18 kDa) when treated with γ secretase inhibitor DAPT (1μM), in a similar manner to human PMEL protein. Inhibition of human BACE2 using BACE inhibitor IV (1μM) increases the relative abundance of Mβ and decreases the abundance of the CTF, suggesting Bace2 cleaves Mβ and gives rise to CTF. Co-expression of the fusion protein and zebrafish Bace2 (zBACE2) leads to accumulation of cleavage product CTF, suggesting zebrafish Bace2 is sufficient to cleave zebrafish Pmela.
(B) Electron microscopy of 72hpf embryos tail melanophores showed a difference in melanin distribution as well as melanosome (M) shape. Melanosomes in WT are round with a smooth outline and homogeneously filled with melanin (yellow arrow). *bace2*$^{-/-}$ melanophores have a darker hue in the cytosol (red arrow) and irregular melanosome membrane (yellow arrow), suggesting a leakage of melanin out of melanosomes into the cytosol.
(C) Knockout of *pmela* using CRISPR-Cas9 in WT zebrafish leads to pale but not dendritic melanophores, similar to previously published *fading vision* mutant. This suggests that loss of *pmela* does not result in hyperdendritic melanophores. Melanophore membrane structure is visualized using *Tg(tyrp1b: membrane-mCherry)* strain at 3dpF.
(D-E) Knockdown of *pmelb* alone (D) or co-knockdown of *pmela* and *pmelb* (E) using morpholinos in WT embryos does not lead to the hyperdendritic melanophore phenotype as seen in the *bace2*$^{-/-}$ mutant. Scale bars, 100 nM (B bottom panel), 1μM (B top panel), 100μM (C-E).

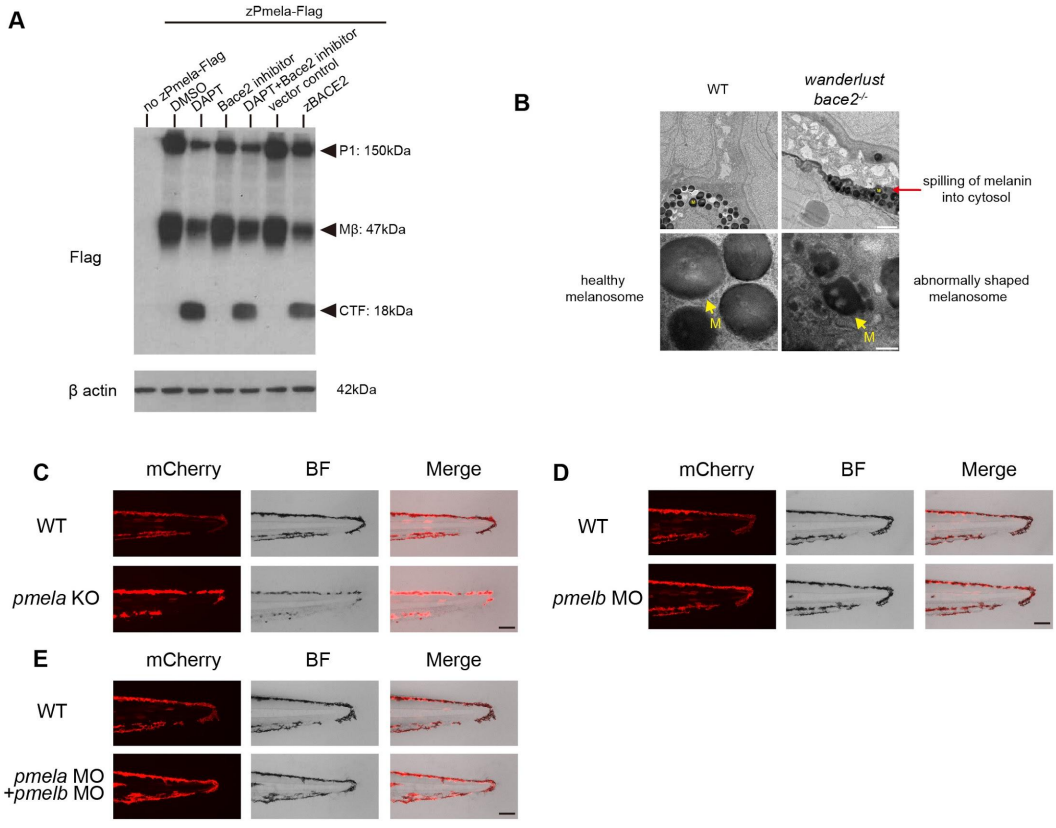
A
zPmela-Flag
no zPmela-Flag
DMSO
DAPT
Bace2 inhibitor
DAPT+Bace2 inhibitor
vector control
zBACE2
P1: 150kDa
Mβ: 47kDa
CTF: 18kDa
Flag
β actin
42kDa
B
WT
wanderlust
bace2-/-
spilling of melanin into cytosol
healthy melanosome
abnormally shaped melanosome
M
M
C
mCherry
BF
Merge
WT
pmela KO
D
mCherry
BF
Merge
WT
pmelb MO
E
mCherry
BF
Merge
WT
pmela MO +pmelb MO

2.2.5 Bace2 regulates melanophore dendricity via PI3K/mTOR signaling

Because sheddases can affect a wide variety of substrates, we therefore wished to functionally look for factors that could rescue the melanophore defects in *wanderlust*. To do this, we performed a chemical genetic screen to identify suppressors of the *wanderlust* phenotype (Figure 22A). We screened 1,280 chemicals using the Sigma LOPAC library to identify compounds that could rescue the hyperdendritic mutant phenotype. For the screen, we quantified the area of tailfin melanophores at 72 hpf and identified chemicals which significantly reduced this in the mutant and scored these on a scale from 0 (no rescue) to 5 (complete rescue) (see Figure 23A for examples). Similar to our experience with prior chemical screens(White et al., 2011), we found that most chemicals had either no effect (~90.3%) or were broadly toxic (~8.9%) (Figure 22B). We identified four chemical hits that strongly rescued the mutant phenotype, all of which converge on PI3K/mechanistic target of rapamycin kinase (mTOR) signaling. Three PI3K inhibitors (AS605240, Wortmannin, LY-294,002) and one mTOR inhibitor (Temsirolimus) abrogated the hyperdendritic melanophore phenotype (Figure 22C-D). PP242, another mTOR inhibitor that is structurally distinct from Temsirolimus, phenocopied Temsirolimus. These compounds also rescued the structure of the hyperdendritic membrane structure, as seen using the *tyrp1b:*membrane-mCherry transgenic line (Figure 23B and Movie 1-4). We determined if this rescue could be reversed by performing washout of the drugs at 72 hpf, but found that the rescue persisted up to 108 hpf (Figure 23C). To a much lesser extent, WT melanophore dendrites are responsive to inhibition of the pathway, especially during the time points when they are normally most dendritic (i.e. 48 hpf) (Figure 24A-B).

We performed genetic knockdown experiments to determine the level at which this pathway caused the hyperdendritic phenotype. Among the small molecules we identified in our screen, the drug AS605240 was by far the most potent in rescuing the phenotype, which is a relatively selective inhibitor of the PI3K γ isoform. Consistent with this, we found that genetic knockdown of PI3K γ using a previously characterized morpholino(Li et al., 2015; Yoo et al., 2010), but not PI3K α, β or δ , rescued the melanophore dendricity (Figure 22E-F, Figure 32A). Morpholinos to mTOR itself resulted in near complete rescue of the phenotype (Figure 2E,G, Figure 32B-C). This is similar to what has been described for neuronal axon and dendrite patterning, in which PI3K signaling regulates downstream Rac/CDC42 signaling to drive dendrite neuronal morphology(Jiang et al., 2005; Markus et al., 2002; Shi et al., 2003). Our data suggest a specific role for PI3K/mTOR signaling in melanophore dendricity, which is exaggerated in the *wanderlust* mutant background.

Figure 22. Bace2 regulates melanophore dendricity via PI3K/mTOR signaling.
(A) Scheme for chemical suppressor screen of the *bace2*$^{-/-}$ mutant. 24hpf *bace2*$^{-/-}$ embryos were treated with each compound from the Sigma LOPAC 1280 library at 30μM for 48 hours, in order to identify chemicals which could rescue the melanophore defects.
(B) Compounds were scored with a range of 0 (non-rescued, mutant-like) to 5 (fully rescued, WT-like).
(C) Top hits from the screen (with score of 4 and 5) converge on PI3K/mTOR signaling pathway. PI3K inhibitors AS605240 (110nM), Wortmannin (230nM), LY-294,002 (15μM), and mTOR inhibitors Temsirolimus (30μM), PP242 (15μM) all fully rescue the *bace2*$^{-/-}$ hyperdendritic melanophores.
(D) Quantification of tailfin melanophore cell area at 72hpf with hits from the screen (n=each fish, one-way ANOVA followed by Holm-Sidak's multiple comparisons test, ****P<0.0001).
(E-G) Morpholinos knockdown of the PI3K γ isoform and mTOR in *bace2*$^{-/-}$ mutants rescue the phenotype analogous to what is seen with compounds from the screen, and the resulting tailfin melanophore cell area is quantified in (F) and (G). The data are from three independent experiments. Uninjected *bace2*$^{-/-}$ siblings (Control) are scored in the same manner, two-tailed t test, ****P<0.0001. All bar graphs are presented as mean ± s.e.m. Scale bar, 100μM.

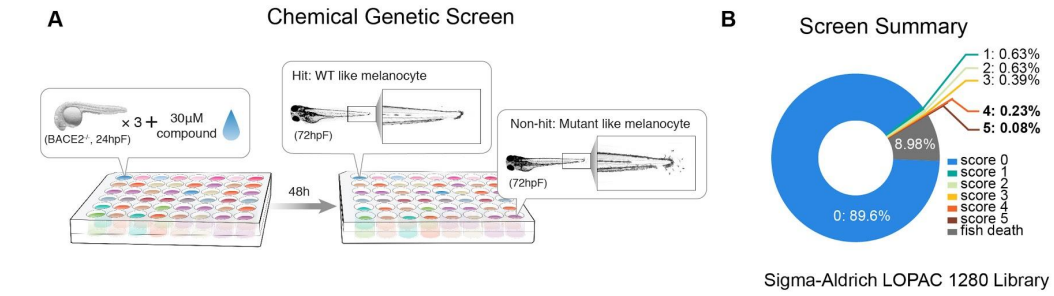
A
Chemical Genetic Screen
× 3 +
30μM
compound
(BACE2-, 24hpF)
Hit: WT like melanocyte
(72hpF)
Non-hit: Mutant like melanocyte
(72hpF)
48h
B
Screen Summary
1: 0.63%
2: 0.63%
3: 0.39%
4: 0.23%
5: 0.08%
8.98%
0: 89.6%
score 0
score 1
score 2
score 3
score 4
score 5
fish death
Sigma-Aldrich LOPAC 1280 Library

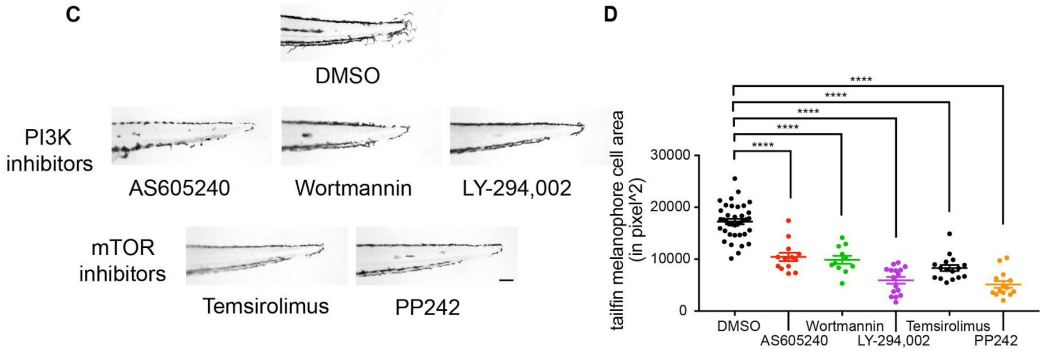
C
DMSO
PI3K
inhibitors
AS605240
Wortmannin
LY-294,002
mTOR
inhibitors
Temsirolimus
PP242
D
tailfin melanophore cell area
(in pixel^2)
30000
20000
10000
0
****
DMSO
AS605240
Wortmannin
LY-294,002
Temsirolimus
PP242

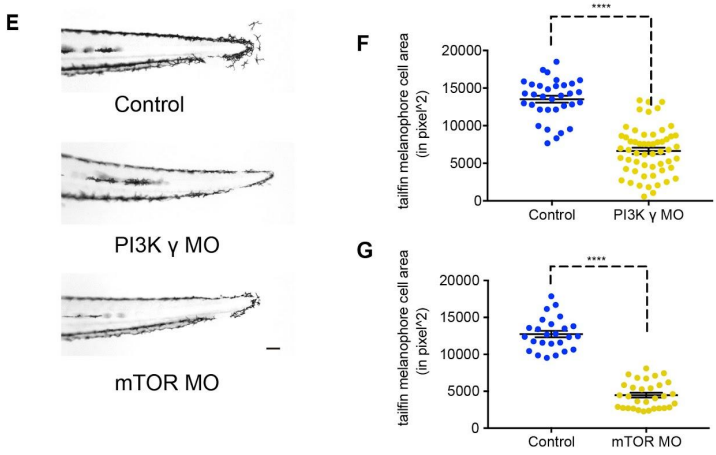
E
Control
PI3K γ MO
mTOR MO
F
tailfin melanophore cell area
(in pixel^2)
20000
15000
10000
5000
0
****
Control
PI3K γ MO
G
tailfin melanophore cell area
(in pixel^2)
20000
15000
10000
5000
0
****
Control
mTOR MO

Figure 23. PI3K/mTOR inhibition rescues dendritic melanophores in *bace2*$^{-/-}$.
(A) Representative pictures of melanophores with chemical screen scores from 0 (non-rescued, mutant like) to 5 (fully rescued, WT like).
(B) Confocal pictures high magnification view of tailfin melanophores in response to PI3K inhibitor AS605240 (110nM), mTOR inhibitor PP242 (15μM) and insulin receptor inhibitor NVP-AEW541 (60μM). *Tg(tyrp1b: membrane-mCherry)* fish were treated from 24hpf to 72hpf to visualize melanophore membrane structure. Also see Supplemental Movie 1-4.
(C) PI3K/mTOR/Insulin receptor inhibitors effect on tail melanophore phenotype is not reversible by drug washout. *wanderlust* mutants were treated with inhibitors from 24hpf to 72hpf, then inhibitors were washed off extensively and embryos were imaged at 108hpf. Scale bars, 30μM (B), 100μM (A, C).

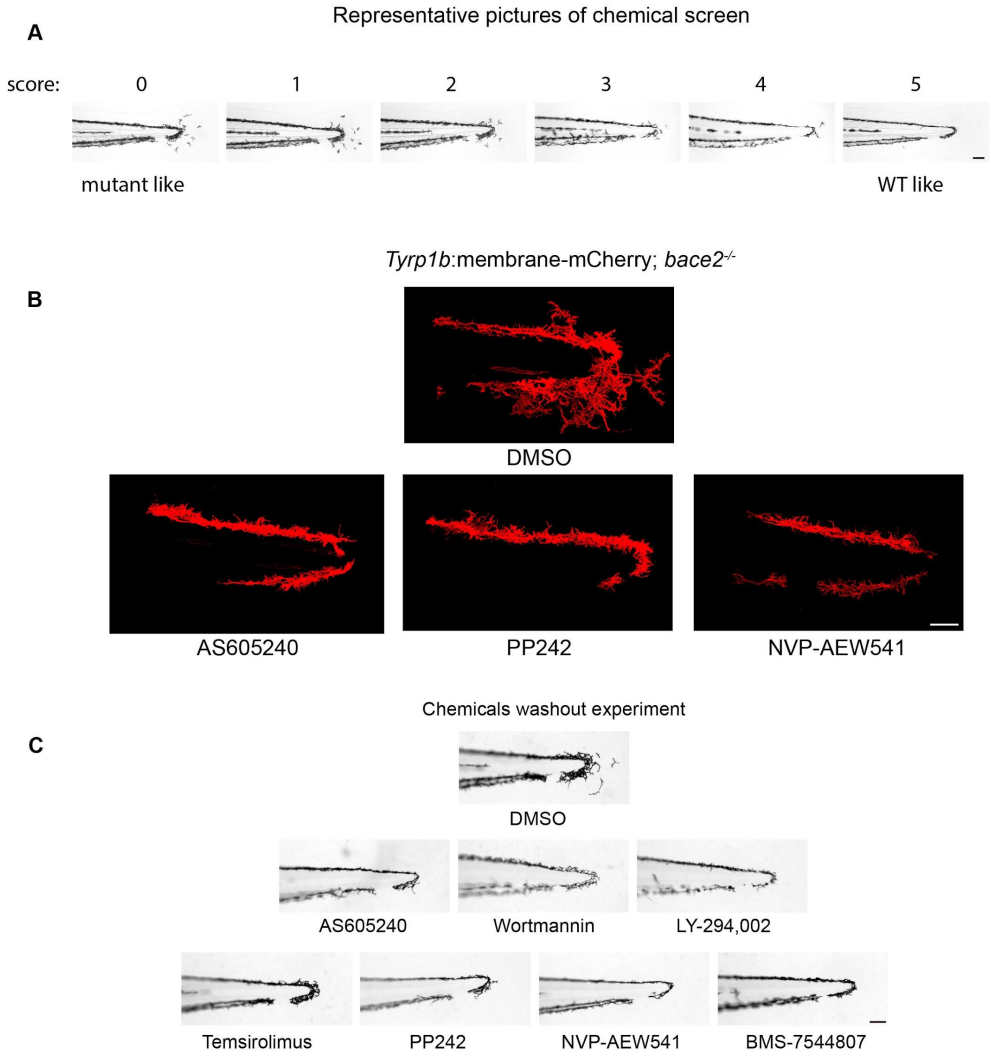
A
Representative pictures of chemical screen
score:
0
1
2
3
4
5
mutant like
WT like
B
Tyrp1b:membrane-mCherry; bace2-/-
DMSO
AS605240
PP242
NVP-AEW541
C
Chemicals washout experiment
DMSO
AS605240
Wortmannin
LY-294,002
Temsirolimus
PP242
NVP-AEW541
BMS-7544807

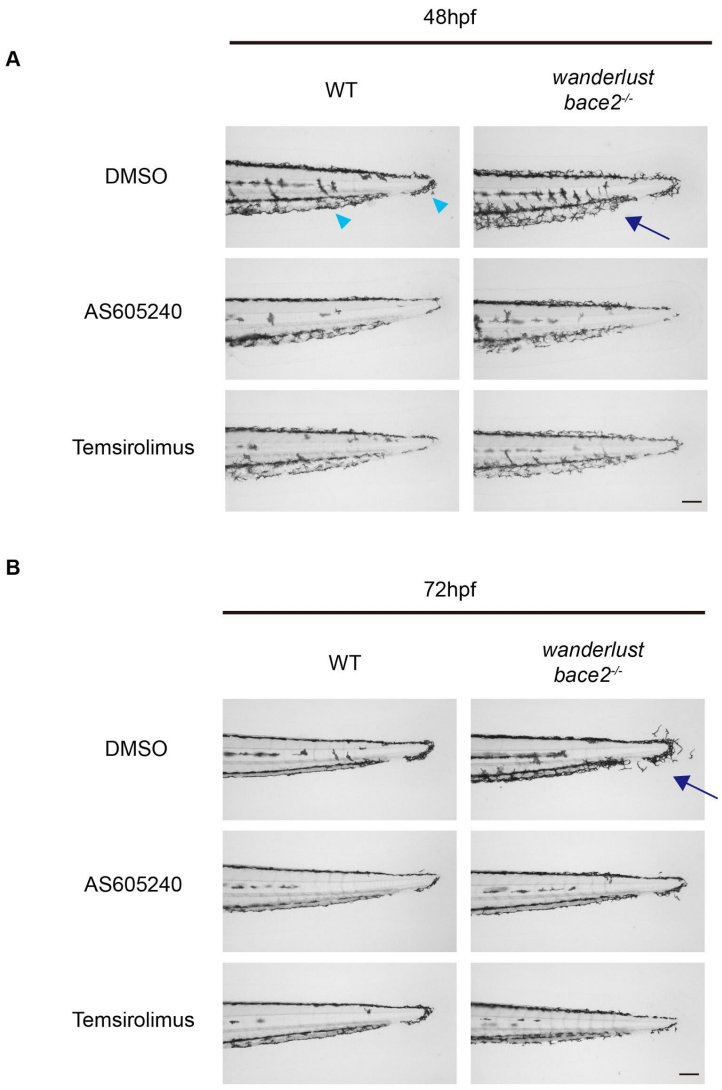

Figure 24. *bace2*$^{-/-}$ is hypersensitive to PI3K/mTOR inhibition compared to WT fish.
PI3K/mTOR inhibition reduced WT melanophore dendricity at 48hpf (A, arrowhead), but the *bace2*$^{-/-}$ melanophores are more sensitive to this effect at both 48hpf and 72hpf (A and B, arrow). Treatment of WT and *bace2*$^{-/-}$ embryos with the PI3K inhibitor AS605240 (110nM) or mTOR inhibitor Temsirolimus (30μM) from 24-48hpf (A) or from 24-72hpf (B).

2.2.6 *bace2*$^{-/-}$ mutants have increased PI3K/mTOR activity

To directly assess whether the hyperdendritic melanophores in the *wanderlust* mutant had abnormalities of downstream PI3K/mTOR signaling, we performed immunostaining for phospho-S6 ribosomal protein (p-S6) in the WT versus mutant fish. We quantified the p-S6 signal intensity in the melanophores from 24-72 hpf by examining co-staining with fluorophore-labeled melanophores. This revealed a significant increase in p-S6 staining in the mutant from 48-72 hpf (Figure 25A-C), and showed specific p-S6 staining pattern in the dendrites themselves at 72 hpf (Figure 25D). These data are indicative of increased output of the PI3K/mTOR pathway in the hyperdendritic melanophores of the *wanderlust* mutant.

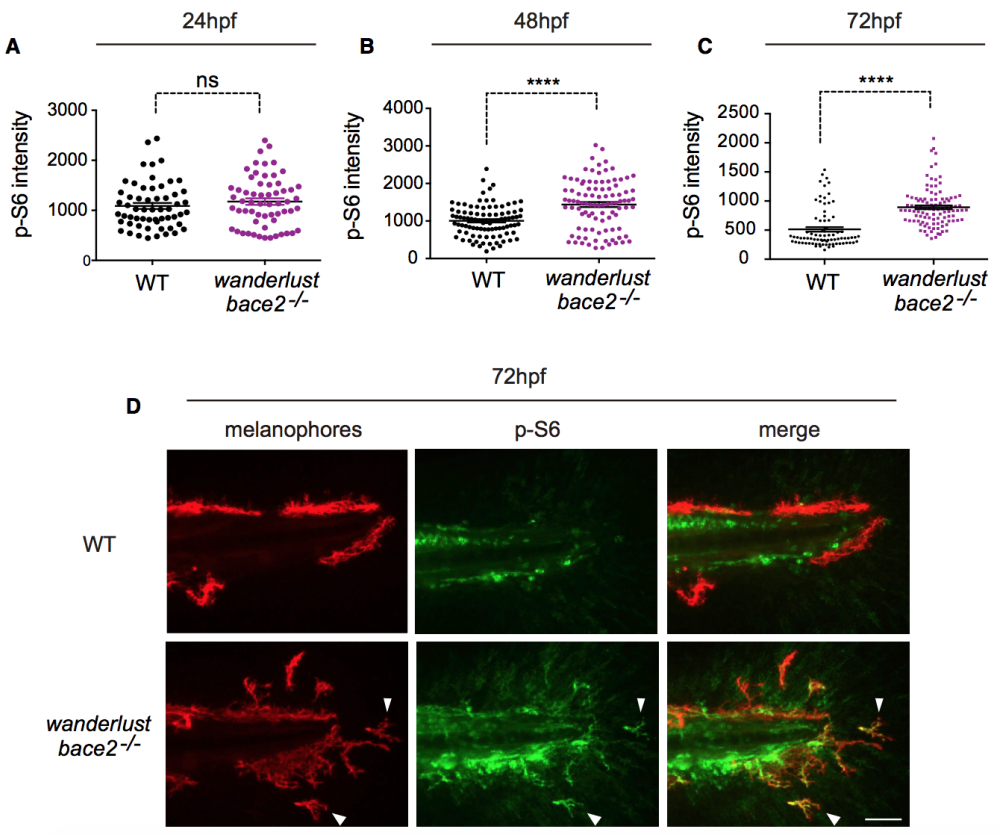

Figure 25. *bace2*$^{-/-}$ mutants have increased PI3K/mTOR activity. Immunostaining against phospho-S6 ribosomal protein(p-S6), a downstream readout of PI3K/mTOR activity, shows elevated p-S6 signal that overlaps with fluorophore-labelled melanophores at 48hpf (B) and 72hpf (C). A representative pictures of 72hpf is shown in (D) and overlapping signals are marked by arrowhead. The data are from three (A), five (B) and five (C) independent experiments, two-tailed t test, ****P<0.0001, ns=not significant. All bar graphs are presented as mean ± s.e.m. Scale bar, 50μM.

2.2.7 The insulin receptor is a substrate for Bace2 and regulates melanophore dendricity

The PI3K/mTOR pathway can be activated by numerous growth factor signaling pathways. We turned our attention to the insulin pathway, a canonical regulator of PI3K, because human BACE2 is known to regulate trafficking of the insulin receptor in pancreatic β cells(Casas et al., 2010) and can cleave the closely related family member IGF2R(Stützer et al., 2013). This led us to hypothesize that insulin receptor signaling drives the PI3K pathway in the hyperdendritic melanophores. To test this, we treated *wanderlust* mutants with the insulin receptor inhibitors BMS-754807 and NVP-AEW541, and found that both inhibitors were able to rescue the mutant phenotype (Figure 26A-B). Due to a teleost genome duplication, zebrafish have two insulin receptors (Insra and Insrb)(Toyoshima et al., 2008), so we used morpholinos to knockdown both of these receptors. Whereas each receptor itself was able to mildly rescue the mutant phenotype, the combined knockdown was much more effective (Figure 26C-D, Figure 32D).

Insulin receptors are broadly expressed in multiple cell types(Garofalo and Rosen, 1988; Toyoshima et al., 2008; Uhlén et al., 2015), including melanophore lineage cells(Kim et al., 2017; Morvan et al., 2012). It is unclear how a general factor such as insulin can exert cell-type specific effects on cells such as melanophores. In mammals, the insulin receptor is produced as a precursor protein which is then proteolytically cleaved by the furin protease into α and β chains, which together form a functional insulin receptor(Bravo et al., 1994). Further cleavage of the β chain to a C-terminal fragment (CTF) has been variously ascribed to a lysosomal protease(Massague et al., 1981), a

thiol protease(Knutson, 1991) or ADAM proteases(Kasuga et al., 2007). Given that Bace2 is a transmembrane β protease, we hypothesized that Bace2 is a melanophore-enriched protease that can cleave the insulin receptor β chain to dampen insulin/PI3K signaling. To test this, we expressed a fusion protein of the zebrafish insulin receptor and a C terminal c-Myc tag (Insr-Myc) along with zebrafish Bace2 in HEK293 cells (which do not express any fish proteins). Expression of the Insr-Myc fusion protein alone revealed the full-length insulin receptor (~180 kDa) and the β chain (~90 kDa) product of furin cleavage (Figure 26E-F). This fusion protein is robustly cleaved by concomitant expression of Bace2, as shown by an accumulation of the CTF for both Insra (Figure 26E) and Insrb (Figure 26F). This effect was not seen with the catalytically-dead Bace2, and can also be abolished when cells are treated with Bace2 inhibitor PF-06663195. This demonstrates that Bace2 is sufficient to induce insulin receptor cleavage (Figure 27).

Since Bace2 can induce β chain cleavage, this raised the possibility that loss of Bace2 in melanophores could serve to stabilize the β chain. To test this, we identified an insulin receptor antibody that recognized the endogenous zebrafish insulin receptor β chain (Figure 32D), and then measured its level after Bace2 inhibition in the ZMEL1 cells. After 24 hours, we found a 37% increase in β chain of the insulin receptor in the Bace2 inhibited cells (Figure 26G-H), suggesting that Bace2 normally acts to limit insulin receptor levels on melanophores.

To directly test whether insulin receptor signaling itself is responsible for the *wanderlust* phenotype, we created a transgenic construct in which the fugu

tyrp1(Zou et al., 2006) promoter drives a dominant negative insulin receptor substrate 2 (dnIRS2) to inhibit insulin signaling only in the melanophores. We then quantified tail melanophore dendricity as we did in the screen, and found a significant decrease in the transgenic animals compared with controls (Figure 26I-J). We also found that CRISPR knockout of *insra*/*insrb* in ZMEL1 cells led to a significant decrease in the elongated/dendritic phenotype and cell number (Figure 28A-E). Taken together, these data are consistent with abnormal insulin receptor signaling induced by loss of *bace2.*

Figure 26. The insulin receptor is a substrate for Bace2 and regulates melanophore dendricity.
(A-B) Inhibition of the insulin receptor in *bace2*$^{-/-}$ embryos using the insulin receptor inhibitors BMS-754807 (7.5μM) and NVP-AEW541 (60μM) rescue the hyperdendritic melanophores in the mutant, quantified in (B). *bace2*$^{-/-}$ embryos are treated from 24-72hpf, and the data are from three independent experiments. One-way ANOVA followed by Holm-Sidak's multiple comparisons test, *P<0.1, ****P<0.0001.
(C-D) Morpholino knockdown of insulin receptor (*Insr*) in *bace2*$^{-/-}$ embryos rescues the hyperdendritic melanophores, quantified in (D). Insra and insrb morpholinos were co-injected into *bace2*$^{-/-}$ embryos to deplete all insulin receptors. The data are from three independent experiments, two-tailed t test, ****P<0.0001.
(E-F) Bace2 cleaves the insulin receptor. Expression of zebrafish Insra-Myc (E) and Insrb-Myc (F) fusion protein in HEK 293T cells give rise to full length insulin receptor and the β chain. Inhibition of γ secretase using DAPT (2μM, 24 hours treatment) prevents the CTF from being cleaved, leading to CTF accumulation. Expression of zebrafish Bace2 (zBace2) on top of the Insra-Myc fusion protein leads to production of single CTF band (E). zBace2 addition leads to the production of two fragments from Insrb-Myc, one that migrates similarly to the CTF and additional larger fragment designated as CTF* (F). This is not seen with the enzymatic dead version of Bace2 (zBace2 dead) or after Bace2 inhibition with PF-06663195 (24 hours treatment). zBace2 dead was constructed by site-mutagenesis of two conserved catalytic sites aspartic acids into alanines (D98A and D292A).
(G-H) Bace2 inhibition with PF-06663195 (25μM, 24 hours treatment) in ZMEL1 cells, which normally express both Bace2 and the insulin receptor, leads to accumulation of endogenous insulin receptor β chain, quantified in (H). The data are from five independent experiments, two-tailed t test, **P<0.01.
(I-J) Melanophore-specific inhibition of insulin signaling in *bace2*$^{-/-}$ mutants rescues melanophores hyperdendricity in the tail fin. A mosaic F0 transgenic line was created in which the fugu *tyrp1* promoter drives dominant negative insulin receptor substrate 2 (dnIRS2) fused to EGFP in the melanophores (along with a *cmlc2*: mCherry transgene marker). At 72hpf, tailfin melanophore cell area was quantified in uninjected control (Control) and transgene-positive injected embryos (J). The data are from three independent experiments, two-tailed t test, ****P<0.0001. All bar graphs are presented as mean ± s.e.m. Scale bar, 100μM.

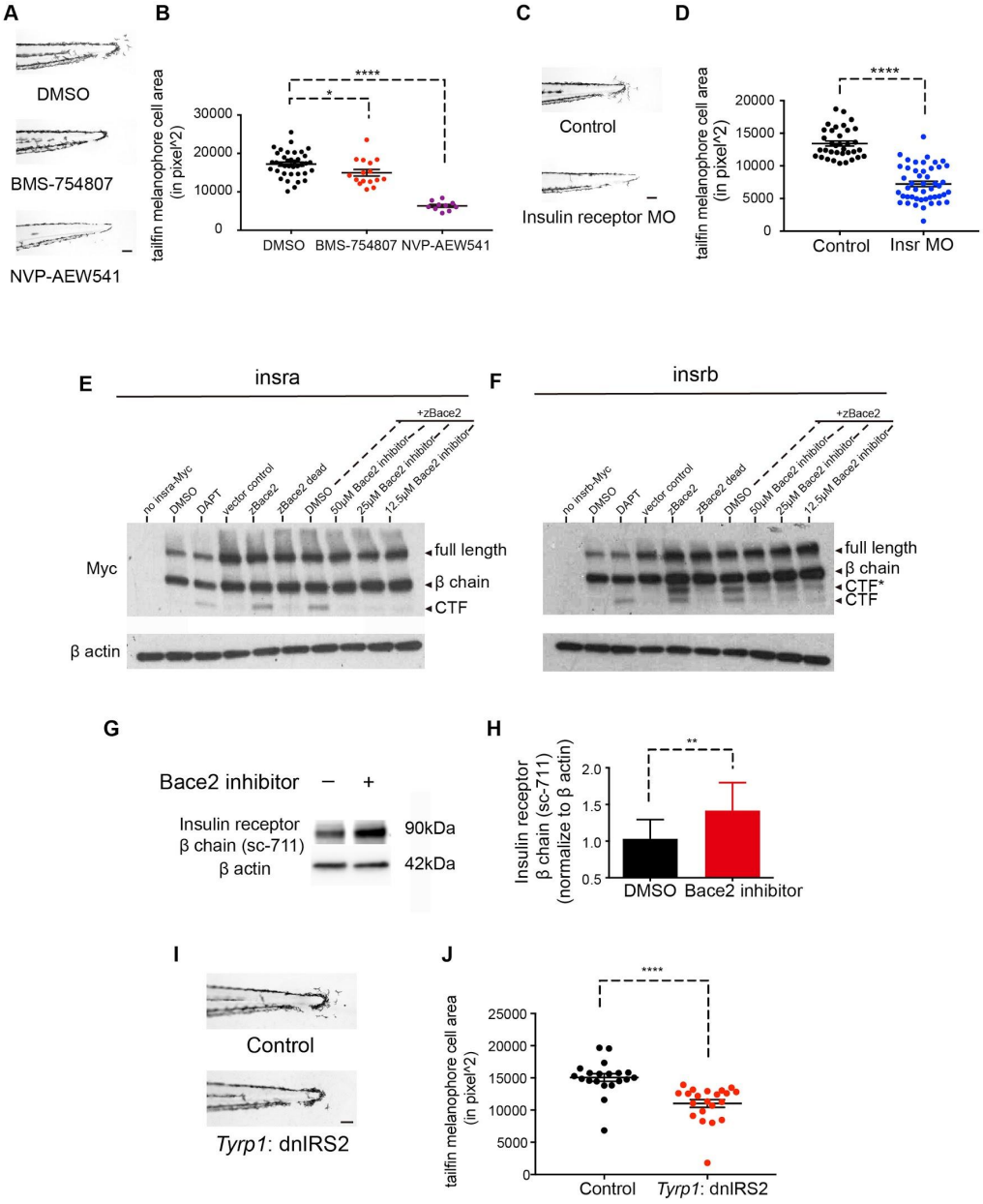
A
DMSO
BMS-754807
NVP-AEW541
B
tailfin melanophore cell area (in pixel^2)
DMSO
BMS-754807
NVP-AEW541
C
Control
Insulin receptor MO
D
tailfin melanophore cell area (in pixel^2)
Control
Insr MO
E
insra
no insra-Myc
DMSO
DAPT
vector control
zBace2
zBace2 dead
+zBace2
DMSO
50μM Bace2 inhibitor
25μM Bace2 inhibitor
12.5μM Bace2 inhibitor
Myc
full length
β chain
CTF
β actin
F
insrb
full length
β chain
CTF*
CTF
G
Bace2 inhibitor
Insulin receptor β chain (sc-711)
β actin
90kDa
42kDa
H
Insulin receptor β chain (sc-711) (normalize to β actin)
DMSO
Bace2 inhibitor
I
Control
Tyrp1: dnIRS2
J
tailfin melanophore cell area (in pixel^2)
Control
Tyrp1: dnIRS2

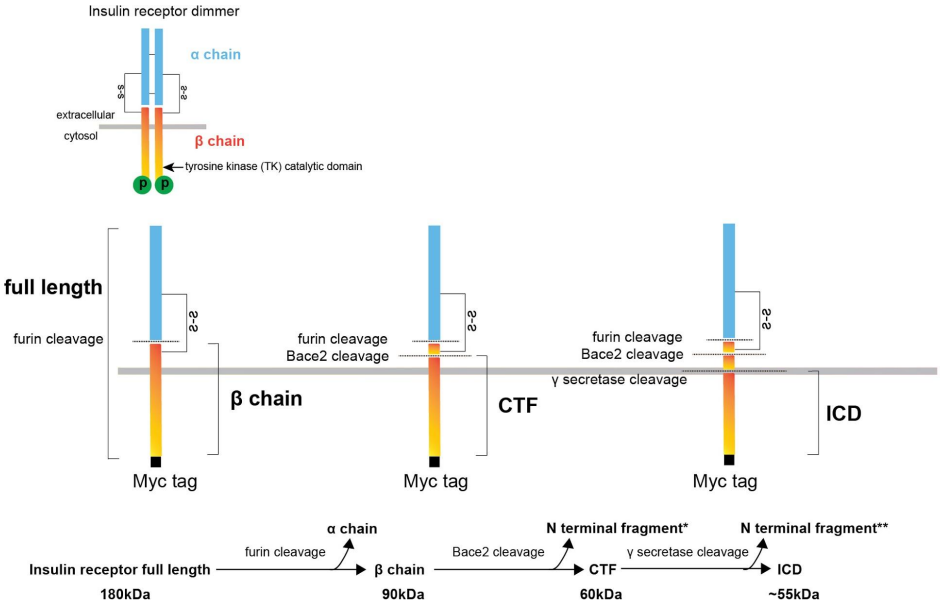

Figure 27. Schematic representation of the protease cleavage steps of the insulin receptor.
Insulin receptors are dimerized to form a functional unit as shown in the top panel. The full length monomer is first cleaved by furin, to yield the α and β chains. The β chain is then cleaved by Bace2 to yield the C-terminal fragment (CTF), which is then cleaved by γ secretase. When Bace2 is abundant, there is an accumulation of the CTF as cleavage product. When Bace2 is inhibited, there is an accumulation of the β chain. The ICD is not detectable in this experiment because it is unstable and quickly degraded by proteasome.

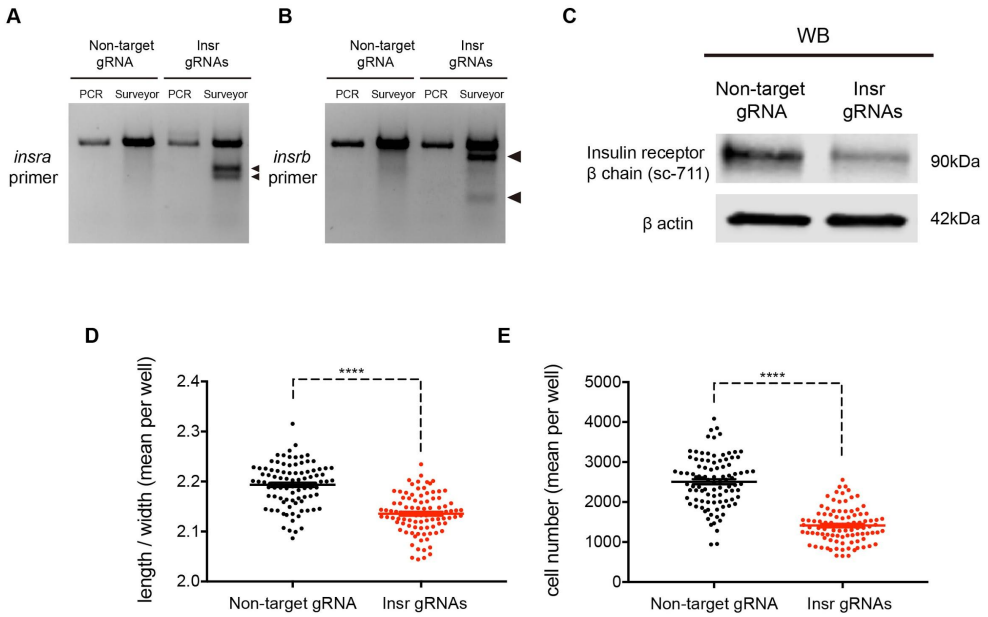

Figure 28. Insulin receptor regulates melanophore morphology and number in ZMEL1 cells. Two guide RNAs (gRNAs) targeting zebrafish *insra* and *insrb* respectively were co-nucleofected into ZMEL1 cells together with tracrRNA and recombinant Cas9 nuclease. A non-targeting gRNA was included as negative control. Surveyor nuclease assay was used to detect mutations in the *insra* (A) and *insrb* (B) genomic locus, resulting in two smaller digested PCR bands at the expected sizes (arrowhead). (C) Western Blot shows a pooled ZMEL1 knockout population leads to reduced Insr protein level. Membrane probed with antibody sc-711 recognizing insulin receptor β chain and β-actin as a loading control. Knockout of both insulin receptors in ZMEL1 cell using Crispr-Cas9 leads to less elongated/dendritic cell morphology (D) and reduced cell number (E), data are from three independent experiments. All bar graphs are presented as mean ± s.e.m. two-tailed t test, ****P<0.0001.

2.2.8 Insulin b is the upstream ligand that drives melanophore dendricity in *wanderlust*

Finally, we wished to determine the source of the insulin ligand driving the *wanderlust* phenotype. Similar to the receptors, zebrafish have two insulin

ligands, Insa and Insb(Papasani et al., 2006), and we knocked these down using morpholinos. Knockdown of Insa had little to no effect, whereas knockdown of Insb had a significant rescue of the *wanderlust* phenotype (Figure 29A-B, Figure 32E).

In humans, insulin is primarily produced in the pancreatic β-cells, whereas in teleosts and Drosophila, insulin peptides can be produced from other areas including the brain(Papasani et al., 2006). Whether humans produce insulin in the brain, or it is imported into the brain from the periphery, has been a source of some controversy although it is clear that insulin can have CNS-specific effects(Havrankova et al., 1979; Schwartz et al., 1992). To assess this in zebrafish, we performed whole-mount ISH for *insa* and *insb* ligand mRNA, and found that as predicted the *insa* transcript is exclusively produced in the pancreas (Figure 30A-B). In contrast, *insb* is initially expressed ubiquitously early in development but becomes gradually restricted to the head region and brain by 48-72 hpf (Figure 29C-E). To functionally exclude a role for pancreatic insulin in the *wanderlust* dendricity phenotype, we used morpholinos against *pdx1(Kimmel et al., 2015)* and *hb9(Harrison et al., 1999; Kimmel et al., 2011)* to completely ablate the pancreas. Whereas this maneuver led to a complete loss of Insa in the pancreas (Figure 30C), it had no effect on the *wanderlust* dendricity phenotype (Figure 30D). In addition, we find no consistent change in the size of the pancreas in the *wanderlust* mutants (Figure 30E). These data indicate that it is the Insb ligand, which is enriched in the head, that drives the melanophore dendricity, highlighting how a long-range factor can influence pigment patterning.

Taken together, these data demonstrate that the sheddase Bace2 modulates melanophore morphology in a cell-type specific manner by regulating insulin receptor cleavage and accumulation, which alters sensitivity to distant ligands such as insb (see Figure 31 for model).

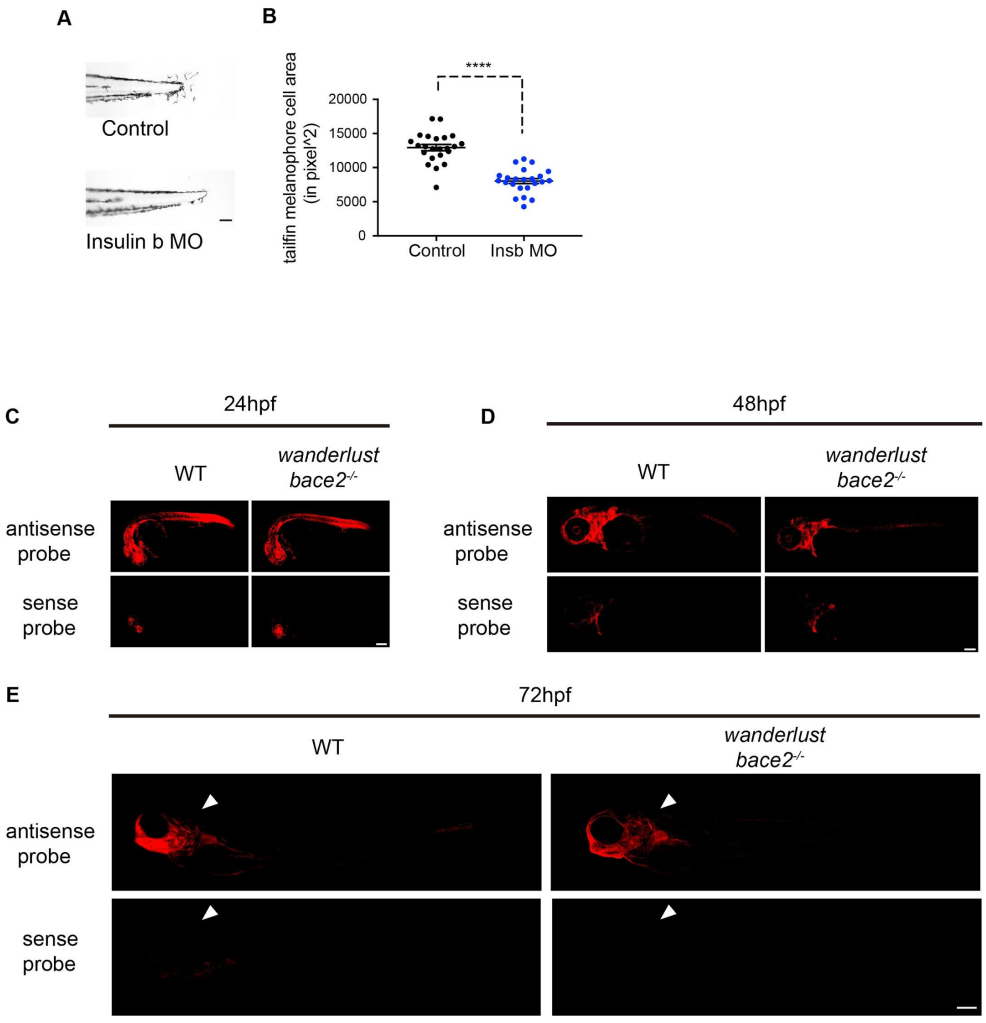

Figure 29. Insulin b is the upstream ligand that drives melanophore dendricity in *wanderlust.*

(A-B) Morpholino knockdown of the ligand insulin B (*insb*) in *bace2*$^{-/-}$ embryos rescues the hyperdendritic melanophores, quantified in (B). The data are from three independent experiments, two-tailed t test, ****P<0.0001.

(C-E) Fluorescent ISH shows zebrafish *insb* ligand mRNA is initially expressed ubiquitously at 24hpf and then restricted to the head/brain region (arrowhead) in *bace2*$^{-/-}$ embryos at 48-72hpf, sense probe controls for background signal. All bar graphs are presented as mean ± s.e.m. Scale bar, 100μM (A), 150μM (C, D), 200 μM (E).

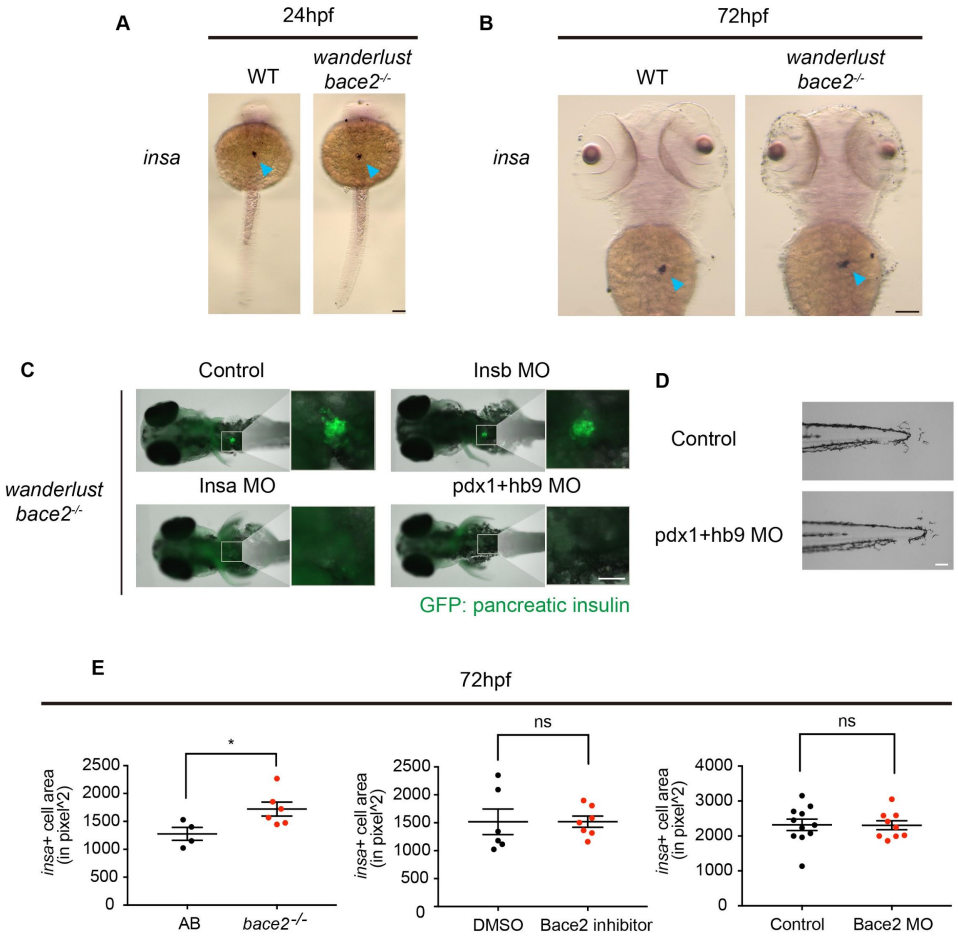

Figure 30. Pancreatic *insa* ablation does not rescue the *bace2*$^{-/-}$ phenotype.

(A-B) ISH shows *insa* mRNA is specifically expressed in pancreas at 24hpf (A) and at 72hpf (B) for both WT and *bace2*$^{-/-}$ embryos (arrowhead).

(C) Immunostaining shows knockdown of either *insa* or *pdx1/hb9* in *bace2*$^{-/-}$ mutants completely ablates insulin staining in the pancreas, while *insb* knockdown does not change pancreatic insulin level at 72hpf. Whole embryos were stained with anti-insulin antibody.

(D) Co-knockdown of *pdx1* and *hb9* in *bace2*$^{-/-}$ mutants fails to rescue dendritic melanophores at 72hpf.

(E) *wanderlust* mutant have slightly increased *insa* positive cell area compared to WT embryos at 72hpf, but Bace2 inhibitor and Bace2 morphant do not show significant differences to the control group, suggesting Bace2 loss of function does not consistently alter pancreatic β cell mass at 72hpf. n=each fish, two-tailed t test, *P<0.05. All bar graphs are presented as mean ± s.e.m. Scale bars, 50μM (C), 100μM (A, B, D).

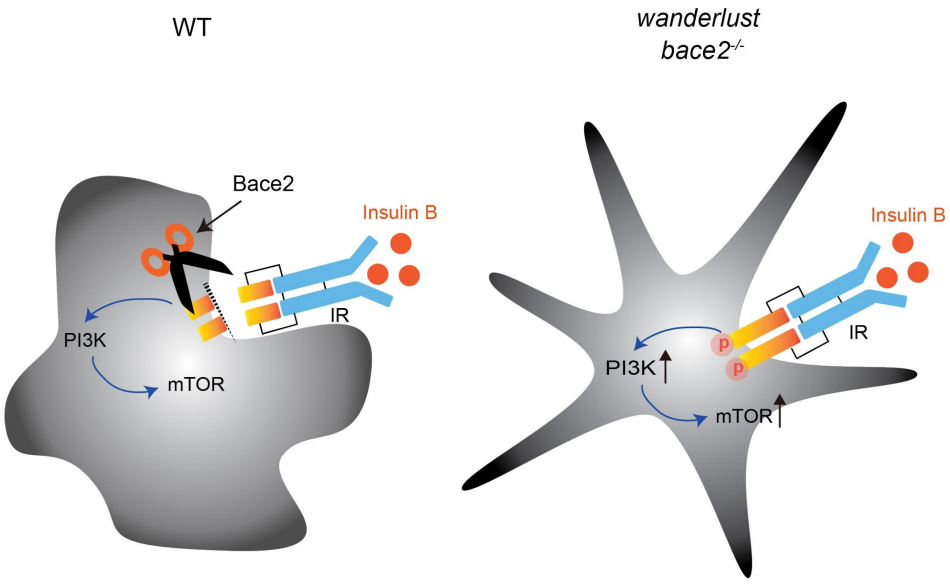

Figure 31. Graphical Abstract.
Bace2 normally cleaves the insulin receptor (IR) to decouple the α chain (blue bar) from the tyrosine kinase domain in the β chain (yellow bar) on melanophore cell membrane. *wanderlust* mutants are deficient in Bace2 and fail to cleave the insulin receptor, which leads to an accumulation of the β chain. Defective insulin receptor cleavage results in increased PI3K/mTOR signaling and sensitizing the melanophores to the effects of insulin B. PI3K/mTOR inhibition is sufficient to rescue *wanderlust* into resembling the wild-type melanophores.

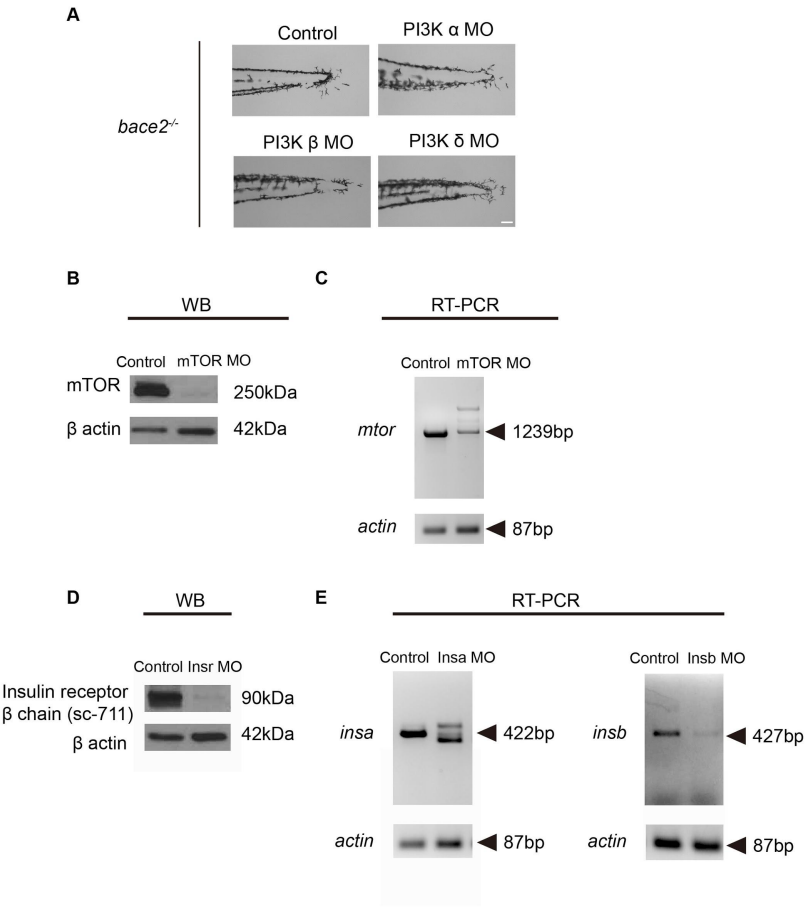

Figure 32. Control experiments for morpholino knockdown.
(A) Knockdown of PI3K α, β or δ isoforms using morpholinos does not rescue *bace2*$^{-/-}$ dendritic melanophores to the same extent as PI3K γ morpholinos, as shown in Figure 22E.
(B) Knockdown of mTOR using mTOR splicing morpholino leads to depletion of mTOR protein in Western blot. Membrane probed with anti-mTOR antibody and β-actin as a loading control.
(C) RT-PCR shows knockdown of mTOR using mTOR splicing morpholino leads to abnormal mRNA splicing. *mtor* fragment is amplified using primers adjacent to morpholino target sites. *actin:* input control.
(D) Western blot shows co-knockdown of insra and insrb using morpholinos leads to decrease insulin receptor protein. Membrane probed with antibody sc-711 recognizing insulin receptor β chain and β-actin as a loading control.
(E) Knockdown of *insa* (Left) and *insb* (Right) using splicing morpholinos lead to abnormal mRNA splicing and expression in RT-PCR. Fragments are amplified using primers adjacent to morpholino target sites. *actin*: input control. Scale bars, 100μM.

2.3 Discussion

It is increasingly recognized that vertebrate coloration is due to continuous interactions between pigment producing cells and their neighboring cells(Nakamasu et al., 2009);(Eom et al., 2015; Walderich et al., 2016). Although this has long been considered to consist primarily of short-range interactions (i.e. melanophore-iridophore, etc)(Frohnhöfer et al., 2013; Patterson and Parichy, 2013), recent data have highlighted a role for thyroid hormone in pigment patterning(McMenamin et al., 2014), and Aqp3a as a pore that can communicate with the external environment(Eskova et al., 2017). What has remained unclear is the manner in which long-range environmental factors interact with lineage-specific gene programs to regulate pigment pattern formation. Our data would suggest that a distant hormonal signal, insulin, can play a major role in this patterning by interacting with a melanophore-enriched gene, *bace2*.

A major question our study addresses is how circulating hormonal factors like insulin can ultimately yield cell-type specific phenotypes. One explanation for such specificity is that each cell type has a set of lineage-restricted genes that regulates the level and activity of the insulin receptor. In the present study, we identify Bace2 as one such candidate lineage factor in melanophores. Our data indicate a model in which the endogenous role of Bace2 in melanophores is to dampen insulin/PI3K signaling, and loss of Bace2 activity leads to hyperactivation of the pathway. This would be consistent with the phenotypes we observe, including hyperdendritic, proliferative and migratory melanophores. PI3K/mTOR signaling is well known to regulate dendrite formation in other cell types such as neurons(Jiang et al., 2005; Markus et al.,

2002; Shi et al., 2003). Inactivation of PTEN, a negative regulator of PI3K, leads to highly migratory and metastatic melanoma cells(Dankort et al., 2009).

Sheddases such as Bace2 are membrane-bound proteases that cleave the extracellular domain of transmembrane proteins and shed the soluble ectodomain extracellularly. They can act as both positive or negative regulators of downstream signaling. Sheddases such as ADAM17 (also known as TACE) cleave and activate epidermal growth factor (EGF) ligands, and loss of ADAM phenocopies EGF ligand mutants(Luetteke et al., 1993; Peschon et al., 1998). Similarly, cleavage of the Notch receptor by ADAM10 and ADAM17 is required for release of the notch intracellular domain (NICD), where it can then move to the nucleus to influence downstream gene transcription(Brou et al., 2000; van Tetering et al., 2009). In contrast, sheddases can also act as negative regulators of receptor activity by quenching free ligands using the ectodomain from cleaved receptors. For example, the soluble form of the Mer proto-oncogene tyrosine kinase (MerTK) can bind to its ligand to limit Akt signaling downstream of endogenous MerTK(Cai et al., 2016; Sather et al., 2007). A more straightforward way to dampen down receptor activity is to physically cleave the receptor proteins. ADAM10 inhibition leads to hepatocyte growth factor receptor (HGF-R/MET) accumulation and subsequent activation by its ligand HGF in liver metastasis(Kopitz et al., 2007; Miller et al., 2013; Schelter et al., 2011). Similarly, ADAM10 and ADAM17 can proteolytically cleave receptor tyrosine kinases such as AXL, and loss of ADAM cleavage leads to AXL accumulation on cell membrane and results in increase in mitogenic signaling activity(Miller et al., 2016; Orme et al., 2016). Our data suggest that Bace2 primarily acts as a negative regulator of insulin signaling

by proteolytically cleaving the insulin receptor. Interestingly, it has been shown that downregulation of RTK cleavage can be hijacked by tumor cells to acquire drug resistance, suggesting that sheddases are also under dynamic feedback regulation(Miller et al., 2016).

In mammals, BACE2 has been shown to be enriched in pancreatic beta cells, where it cleaves TMEM27 and leads to increased secretion of insulin(Esterházy et al., 2011). BACE2 is also known to be expressed in mammalian melanocytes, where it serves to cleave PMEL to achieve melanosome maturation(Rochin et al., 2013; Shimshek et al., 2016). In contrast, our studies highlight a Pmel independent role for Bace2 in pigmentation, since we find that loss of function of *pmela/b* does not resemble the zebrafish *wanderlust* mutant. Instead, our data show that it is another substrate, the insulin receptor, which mediates the pigment phenotype. This highlights the functional plasticity of sheddases, which can have numerous different substrates to regulate cell-type specific effects. Whether Bace2 is important for zebrafish pancreas development remains to be determined, but pancreatic insulin is unlikely to play a role in pigment patterning since ablation of the pancreas with *pdx1*/*hb9* morpholinos failed to rescue the *wanderlust* phenotype. Moreover, we did not see a strong signal of *bace2* in pancreas during zebrafish embryogenesis by ISH, although this will need further study in the future. *Insb* is dynamically expressed. At 24 hpf it is expressed fairly ubiquitously, but then becomes gradually restricted to the head region by 48 to 72 hpf. We did not see a strong enrichment of *insb* in the pancreas as noted before(Papasani et al., 2006). Based on this, we also tried the same *insb* probe from(Papasani et al., 2006) but were not able to consistently see a

greater signal in the antisense versus sense probe in the pancreas. Although we do not understand the nature of this discrepancy, we decided to primarily focus on the probe published by(Junker et al., 2014) for our studies since it correlated closely with their RNA-sequencing topography analysis and consistently gave us an excellent antisense:sense signal.

It is likely that insulin cooperates with other long-range endocrine-related factors such as thyroid hormone(McMenamin et al., 2014). Although not specifically addressed in our study, one interesting consideration is how hyperinsulinemia leads to hyperpigmentation in humans, a well described phenomenon that typically occurs as part of the disease acanthosis nigricans(Hermanns-Lê et al., 2004). This is a condition specifically linked to other endocrinopathies such as diabetes mellitus, hypothyroidism, and polycystic ovarian syndrome, and thus the melanocyte responsiveness to insulin may be part of this pathophysiology.

BACE inhibitors are being evaluated in clinical trials, primarily for the prevention or treatment of Alzheimer's disease. This is due to the fact that BACE1 can cleave amyloid precursor protein, thought to be a major target in that disease. In contrast, BACE2 inhibitor may have utility for the treatment of diabetes, due to its capacity for increasing insulin secretion(Esterházy et al., 2011). Many of the molecules developed so far have some but not complete selectivity for either isoform. Our data would suggest that inhibition of BACE2, in the context of hyperinsulinemia, may have effects on pigmentation via the PI3K pathway, and may increase the migratory capacity of these hyperdendritic melanocytes. Whether this has clinical consequences,

especially in regard to melanoma development, remains to be determined, but is an important area for future exploration.

CHAPTER 3: BACE2 AS A POTENTIAL TUMOR SUPPRESSOR IN MELANOMA

3.1 Introduction

3.1.1 Melanoma is a heterogeneous tumor type

Melanoma, the deadliest form of skin cancer, is derived from pigment cells called melanocytes that arise from the neural crest (Uong and Zon, 2010). If diagnosed early, melanoma can often be cured by surgical resection. However, once it metastasizes, melanoma becomes extremely deadly (Gray-Schopfer et al., 2007). Melanoma cells are heterogeneous populations with a wide degree of morphology, differentiation status and transcriptomics, but this heterogeneity is not taken into account when deciding upon treatment (Albino et al., 1981; Egger et al., 2013; Houghton et al., 1982, 1987). Many factors that could contribute to this phenotypic heterogeneity, and we wish to test the hypothesis that melanoma heterogeneity reflects diversity in melanoma differentiation states.

3.1.2 The role of cellular differentiation in melanoma

Genetic profiling and immunohistochemistry of patients samples and cell lines suggest there are three distinct melanoma differentiation states: 1) an undifferentiated, invasive state similar to a neural crest progenitor, 2) a partially differentiated/proliferative state, and 3) a terminally differentiated/non-proliferative state (Chien et al., 2009; Eichhoff et al., 2010; Pinner et al., 2009; Tap et al., 2010). This model is sometimes called the “rheostat” model of melanoma in which cells both within and between patients can lie along a spectrum of differentiated states (Goding, 2011). Further, several *in vivo* studies show that melanoma cells can undergo phenotypic switching to

change their differentiation status (Eichhoff et al., 2010; Quintana et al., 2008, 2010). Phenotypic plasticity enables melanoma cells to adapt to the various challenges that arise during tumor progression. Initially, cells with greater proliferative abilities drive the expansion of the primary tumor. Subsequently, these cells can undergo dedifferentiation and a subpopulation of undifferentiated cells arises. Dedifferentiated cells have metastatic advantages that enable them to disseminate to distant organs (Hoek et al., 2008). Once there, success at nascent metastases depends on the cell's ability to partially differentiate in order to regain their former proliferative capacity and colonize. Indeed this mechanism explains the initially paradoxical observation that melanoma cells that are partially differentiated are also the most proliferative (Hoek and Goding, 2010; Hoek et al., 2008; Vandamme and Berx, 2014).

Both cell-intrinsic and microenvironmental factors have been hypothesized to control phenotype switching in melanoma, and emerging data has begun to identify some of these factors (Carreira et al., 2006). One central factor in phenotype switching is the transcription factor MITF (Hsiao and Fisher, 2014). MITF is a master regulator of melanocyte differentiation, and has been shown to be a lineage-specific oncogene amplified in malignant melanoma (Garraway et al., 2005; Goding, 2011). However, MITF has been shown to have a complex role in melanoma progression because it not only drives melanocytes into differentiation but also is essential in maintaining melanocyte survival (Garraway and Sellers, 2006; Hsiao and Fisher, 2014; Sáez-Ayala et al., 2013). Another important factor is SOX10, a neural crest progenitor gene essential for both melanoma initiation and progression that directly

upregulates MITF expression (Kaufman et al., 2016; Mohamed et al., 2013; Shakhova et al., 2012).

The clinical relevance of melanoma differentiation is an active area of investigation. "Differentiation therapy" by inducing terminal differentiation and cell cycle exit was previously attempted to treat melanoma but was not successful (Abdi et al., 1988; Friedman, 2008; Houghton et al., 1987; McArthur, 2014; Ravandi et al., 1999), possibly because undifferentiated cells were forced into a partially differentiated, more proliferative phenotype (Carreira et al., 2006). Further, differentiation signatures have an impact on drug sensitivity (Sáez-Ayala et al., 2013; Tap et al., 2010). BRAF-mutant melanomas with the undifferentiated, neural crest gene expression signature have the highest level of resistance to vemurafenib, a BRAF inhibitor, while melanomas with the terminally differentiated gene signatures are least resistant (Konieczkowski et al., 2014). Accordingly, these signatures are correlated with different levels of MITF, which modulates the intrinsic sensitivity of melanomas to MAPK pathway inhibitors. Taken together these data imply that differentiation state has a profound effect on the heterogeneous melanoma phenotype.

3.1.3 Bace2 in melanoma

Chapter 2 suggested that in normal physiology, Bace2 is part of a program that pushes melanophores into a terminally differentiated states where they no longer cycling. When Bace2 is absent, melanophores are locked in an actively differentiating/proliferative state, leading to aberrant melanophore migration, proliferation and deposition of melanin in the wrong places. This is because

Bace2 modulates the strength of PI3K/mTOR inside melanophores, by cleaving and inactivating insulin receptors on melanophore membrane. When Bace2 is present, the insulin receptor is cleaved into half and the signal is turned off; when Bace2 is absent,the insulin receptor is intact, and the signal is on.

Melanocytes are the precursor cells for malignant melanoma, and melanoma is known to inherit embryonic memory and addicted to lineage program (White et al., 2011). We would like to test if Bace2 as a lineage factor has an impact on melanoma proliferation and differentiation, and if these changes in differentiation status have a consequence on tumor progression.

3.2 Result

3.2.1 Bace2 expression in melanoma

In order to study the roles of Bace2 in melanoma, we first examined Bace2 expression and genomic alterations in melanoma. We crossed examine the Broad Institute Cancer Cell Line Encyclopedia (CCLE) and cBioPortal to check Bace2 expression and found that Bace2 is highly expressed in melanoma cell lines and melanoma tissues (Figure 33A-B) (Barretina et al., 2012; Gao et al., 2013). We do not see consistent changes in genomic deletion, amplification, copy number or hotspots mutation, compared to other known lineage factors (MITF, SOX10) or tumor suppressor (CDKN2A) in melanoma (Figure 33C-E). As Bace2 has dual roles in melanocytes (cleaving PMEL for melanosome maturation versus cleaving insulin receptor to regulate cells proliferation and differentiation), it is likely that the enrichment of Bace2 simply reflects its role in PMEL cleavage in pigment cells and therefore it is hard to predict the

carcinogenic function of Bace2 based on expression level alone (Rochin et al., 2013).

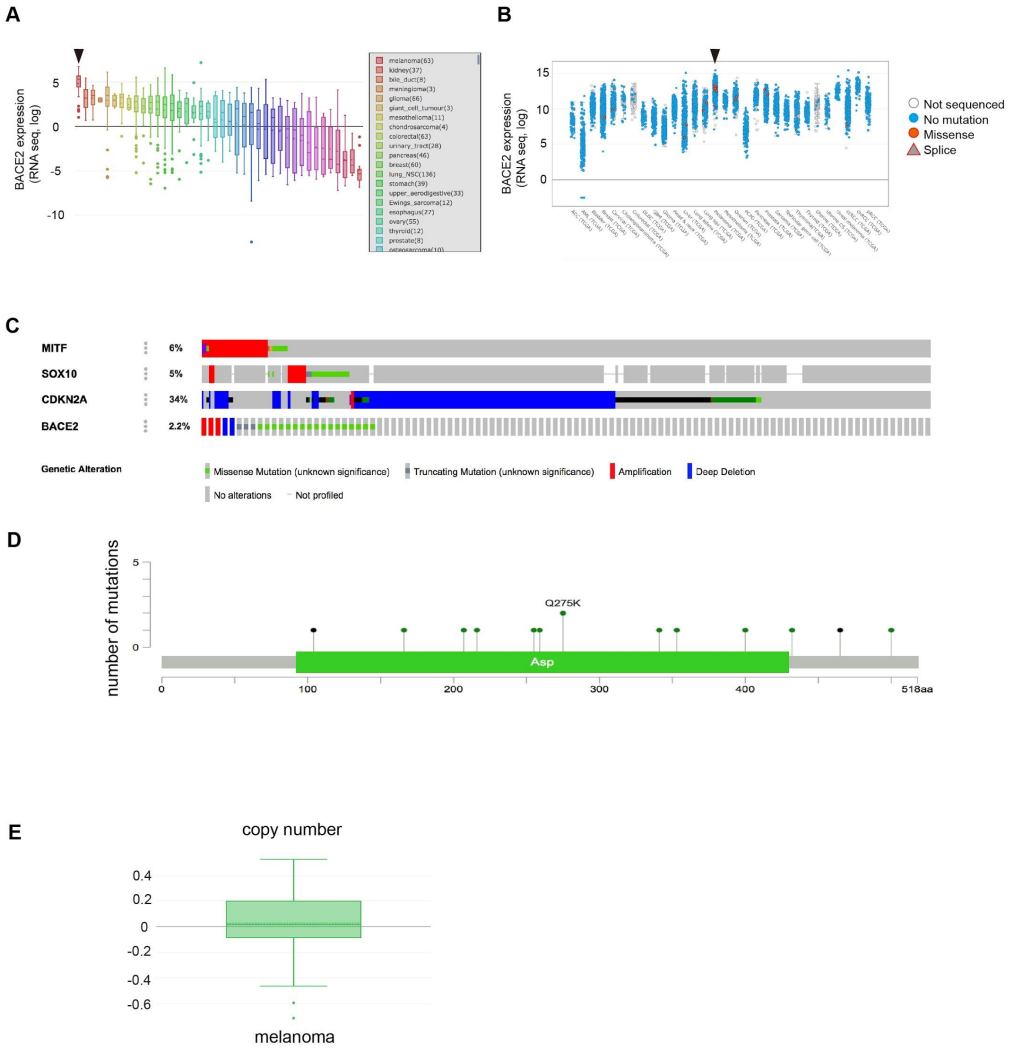

Figure 33. BACE2 is highly enriched in human melanoma cells, with little genomic alterations.
(A-B) *BACE2* mRNA is highly enriched in melanoma cell lines (marked by arrowhead) and in melanoma cell lines and patients samples (marked by arrowhead). Data is from CCLE (A) and cBioPortal (B).
(C) While other melanocyte-enriched lineage factors *MITF* and *SOX10* are significantly amplified and canonical melanoma suppressor gene *CDKN2A* is significantly deleted in melanoma, *BACE2* locus is altered at 2.2% across a panel of melanoma cells and samples, without enrichment of amplification or deletions. Data is from cBioPortal.
(D) *BACE2* (previously named *ASP*) locus does not have hotspot mutations. Data is from cBioPortal.
(E) BACE2 locus does not have copy number changes in melanoma cell lines. Data is from CCLE.

3.2.2 Loss of Bace2 increases zebrafish melanoma proliferation and differentiation, resulting in a highly invasive cells

We utilized the ZMEL1 cell line, which is a zebrafish-specific melanoma cell line expressing high levels of *bace2* along with other key pigment genes such as *mitfa*, *dct*, and *tyr* (Heilmann et al., 2015; Kim et al., 2017), to study if Bace2 loss of function could change tumor cell proliferation/differentiation in a similar to fish melanophores and more importantly, if the changes in cell lineage lead to enhanced cell migration and invasion. We treated the ZMEL1 cells with the Bace2 inhibitor PF-06663195, and found that inhibition of Bace2 in ZMEL1 cells caused a dose-dependent dendritic phenotype (Figure 34A-B), one of the hallmarks for melanoma cells differentiation. ZMEL1 dendricity is measured both by an increase in cellular length-to-width ratio. Bace2 inhibition also leads to a significant increase in cell number (Figure 34C). This increase in cell number is consistent with an increase in proliferation as measured by a significant increase in phospho-histone H3 (pH3) staining (Figure 34D) but no change in apoptosis as measured by caspase 3/7 activity (Figure 34E). Collectively, these suggested that Bace2 loss of function induces ZMEL1 differentiation (measured by changes in cell morphology) and proliferation, similar to what is seen *in vivo* during normal melanophores development. We further tested if the changes in cell lineage results in differences in cell migration. Using a transwell assay, we found that Bace2 inhibition leads to a strong increase in cell migration (Figure 34F), confirming our hypothesis that actively differentiating and proliferative cells still maintain a migratory capacity.

To further study the effects of BACE2 on tumor progression, we crossed the *bace2*$^{-/-}$ mutant with the previously developed transgenic melanoma model

(*mitfa:BRAFV600E; p53*$^{-/-}$) (Patton et al., 2005) , so that we can compare tumors derived from BACE2 WT or KO cells within a melanoma-prone background. *bace2*$^{-/-}$; *mitfa:BRAFV600E; p53*$^{-/-}$ fish have an early melanoma onset (Figure 34G) and histologically a very aggressive tumor compared to bace2^{WT}; *mitfa:BRAFV600E; p53*$^{-/-}$ sibling controls (Figure 34H). These together suggested that melanoma cells inherit the Bace2's influence on melanocytes, and loss of Bace2 leads to an actively differentiating, highly proliferative cells which results in early tumor onset and tumor invasion *in vivo*.

Figure 34. Loss of Bace2 leads to elongated zebrafish melanoma cells which are highly invasive and proliferative.
(A-C) The zebrafish melanoma cell line ZMEL1 was treated with 12.5μM or 25μM of the Bace2 inhibitor PF-06663195 for 72 hours, and resulted in hyperdendritic cells (arrowhead) similar to what was seen *in vivo*. A representative field of cells is shown in (A) and dendricity is quantified as an increase in cell length to width ratio (B), along with an increase in overall cell number (C). Data are from three independent experiments, one-way ANOVA followed by Holm-Sidak's multiple comparisons test, ****P<0.0001.
(D) The increased cell number induced by Bace2 inhibitor is due to increased ZMEL1 cell proliferation, as measured by increased phospho-histone H3 (pH3) immunostaining. Data are from three independent experiments, one-way ANOVA followed by Holm-Sidak's multiple comparisons test, ***P<0.001, ****P<0.0001.
(E) The increased cell number induced by Bace2 inhibitor is not due to changes in ZMEL1 apoptosis, as measured by caspase activity. Data are from three independent experiments, one-way ANOVA followed by Holm-Sidak's multiple comparisons test, ns=not significant.
(F) ZMEL1 treated with 25μM of the Bace2 inhibitor PF-06663195 for 48 hours have increased migration in Transwell assay. Data are from five independent experiments, two-tailed t test, ***P<0.001.
(G-H) Loss of Bace2 in zebrafish melanoma-prone background *Tg(mitfa: BRAFV600E; p53$^{-/-}$)* leads to early onset tumor, with 62% of one-year-old adult developed melanoma. Those tumor are highly invasive as shown by histology H&E staining in (H). Chi-square test with Yate's correction. All bar graphs are presented as mean ± s.e.m. Scale bars, 10μM.

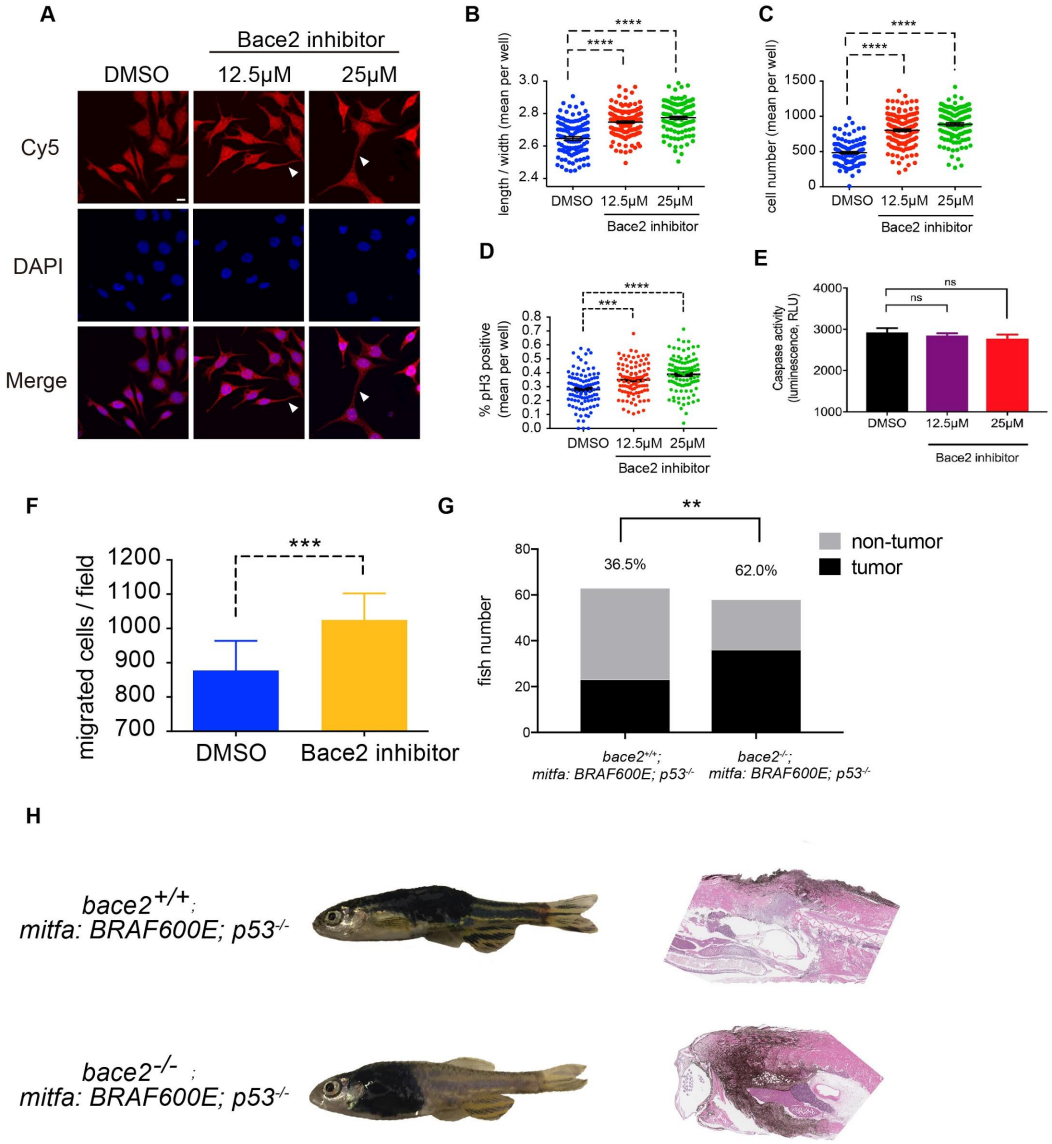
A
Bace2 inhibitor
DMSO
12.5μM
25μM
Cy5
DAPI
Merge
B
length / width (mean per well)
DMSO
12.5μM
25μM
Bace2 inhibitor
C
cell number (mean per well)
D
% pH3 positive (mean per well)
E
Caspase activity (luminescence, RLU)
ns
F
migrated cells / field
DMSO
Bace2 inhibitor
G
non-tumor
tumor
fish number
36.5%
62.0%
bace2+/+; mitfa: BRAF600E; p53-/-
bace2-/-; mitfa: BRAF600E; p53-/-
H
bace2+/+; mitfa: BRAF600E; p53-/-
bace2-/- ; mitfa: BRAF600E; p53-/-

3.2.3 Loss of BACE2 increases human melanoma cells invasion

Given that the zebrafish model of melanoma greatly resembles human melanoma, and the BACE2 protein sequence is highly conserved between zebrafish and human, we wish to validate our zebrafish studies in human melanoma. Because our preliminary data suggest that loss of Bace2 induces melanocyte differentiation in zebrafish, we hypothesize that BACE2 loss of functions will lead to more differentiated/proliferative, and invasive melanoma cells.

We generated a doxycycline-inducible lentiviral construct (Fellmann et al., 2013) to knockdown BACE2 and transduced this construct into human melanoma cell line A375. Upon addition of doxycycline, GFP is co-expressed with an shRNA targeting BACE2 or luciferase (negative control). We confirmed efficient BACE2 knockdown using Western blot analysis (Figure 35A) and measured cell proliferation and cell invasion. Interestly, BACE2 knockdown did not alter cell proliferation the same way in zebrafish (data not shown) but both shRNAs had significant increases in matrix degradation consistent with increased invasion (Figure 35B-C). Taken together, these data indicated that Bace2 deficiency leads to melanoma cells with increased migratory and invasive capacity.

The discrepancy in cell proliferation between zebrafish melanoma cells and human melanoma cells is unknown but likely to be real, as other human melanoma cell lines (SKMEL-28, MNT-1, MALME-3, MeWo) do not change

their proliferation behavior as well in response to BACE2 knockout, BACE2 knockdown or BACE2 inhibition (data not shown).

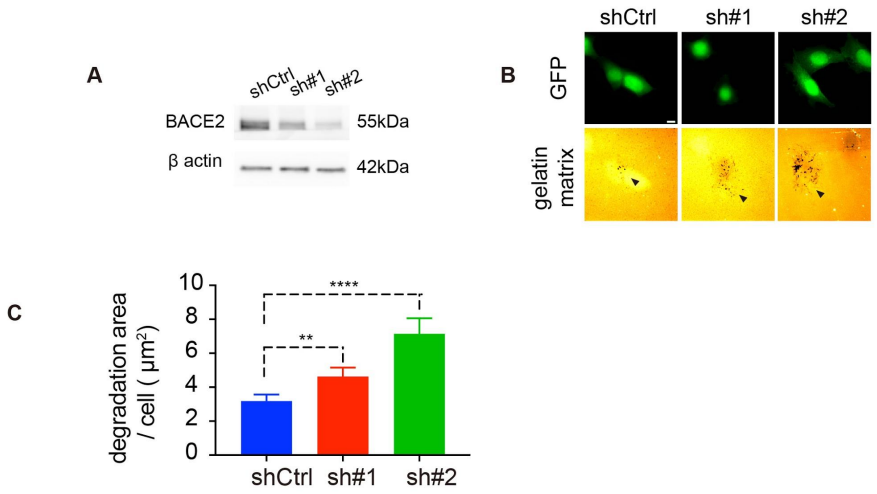

Figure 35. BACE2 Knockdown results in invasive human melanoma cells.
(A) Western blot analysis of BACE2 shRNA knockdown in A375 cells. Membrane probed with anti-BACE2 antibody and ß actin as loading control. (B) Knockdown of BACE2 in A375 led to increased invasion as measured through degradation of a collagen I/gelatin matrix. Top panel, cells expressing doxycycline-induced GFP. Bottom panel: representative matrix degradation (black spots with arrowhead).
(C) Quantification of degradation area / cell (μm^2). Data are from three independent experiments, > 90 fields analyzed per condition, Mann-Whitney test, **P<0.01, ****P< 0.0001. All bar graphs are presented as mean ± s.e.m. Scale bar,10µM.

3.3 Discussion

Melanoma is highly invasive tumor type and once metastatic it becomes extremely deadly. Previous literature provides evidence that suggested that cellular differentiation has a significant impact on the ability of melanoma cells to invade: while de-differentiated and neural crest like (MITF-low) cells are more invasive, partially differentiated cells (MITF-high) are more proliferative; and terminal differentiated cells are the least motile and become quiescent (Goding, 2011). A key question remaining in the melanoma metastasis field is how do the slow dividing, invasive pioneer melanoma cells resume proliferation once they land on a new site? Recently Kim et al proposed an alternative strategy that metastatic melanoma cells acquire differentiation after initial invasion and couple differentiation and proliferation to populate their number post seeding. This cell identity changes are under the regulation of microenvironmental morphogen endothelin, where endothelin induces a differentiated/proliferative state (Kim et al., 2017).

While this solved the limited cell number dilemma for micro-metastasis, it did not address if the resulting differentiated/proliferative cells still maintain their invasion capacity. It is also possible that a macro-metastasis could reach out to form a secondary metastasis (Rashidi et al., 2000). Whether the macro-metastasis cells undergo dedifferentiation to re-acquire invasion capacity, or themselves still maintain a migratory ability is poorly understood. In zebrafish both melanoblast and partially differentiating melanophores are highly migratory (Eom et al., 2012; Williams et al., 2018) also suggested that invasion is not uniquely linked to de-differentiated cells. *bace2* null melanophores in zebrafish are both highly proliferative and actively differentiating melanophores

and still migratory to ectopic sites, suggesting that differentiated/proliferative melanoma cells can still maintain their invasion capacity.

Our work shows that Bace2 loss of function in melanoma phenocopies melanocytes in a way that cells are still dendritic (a hallmark for differentiation) and proliferative (in the case of ZMEL1), and importantly the resulting melanoma cells are migratory, invasive and give rise to early tumor onset. This suggested that invasiveness is not solely linked to de-differentiated neural crest-like cells, and that actively differentiating and dividing cells still maintain invasion capacity. Our data would imply that solely targeting undifferentiated cell populations is likely to miss important players in metastasis, and maintaining BACE2 activity in melanoma is essential to push melanoma cells into terminal differentiation. Currently, BACE inhibitors (which mainly target BACE1 with some extent of BACE2 inhibition activity) are under clinical investigation for diseases such as Alzheimer's (Lopez Lopez et al., 2017; Mandal et al., 2016; Vassar, 2014). Our work would suggest that we should be cautious using inhibitors that against BACE2 as this would prevent terminal differentiation of melanocytes, expand the actively differentiating population and increase the risk for neoplastic transformation.

CHAPTER 4: CONCLUSION AND FUTURE DIRECTIONS

4.1 General conclusions and summary

Proper patterning of pigment cells is important for animals for mate selection, hiding from predators and protection against UV induced DNA damage. To achieve this, animals have developed a highly organized and evolutionarily conserved system to regulate pigment cell behavior. Pigmentation is also a versatile system as they change in response to environmental needs. Mammalian melanocytes transfer melanin to surrounding keratinocytes to protect the epithelial keratinocytes from UV-damaged (Boissy, 2003). In contrast, zebrafish, a specifies rarely exposed to direct sunlight, do not transfer melanin between cells but instead contract or aggregate melanosomes within melanophores to change their overall appearance very quickly during camouflage (Richardson et al., 2008; Sheets et al., 2007).

The purpose of this dissertation is to describe how the sheddase Bace2 coordinates with long range hormones to regulate melanophore cell behavior, and if these changes in melanophores have a consequence in malignancy. We first characterized all the cell behavior changes caused by Bace2 loss of function: *wanderlust* mutant melanophores acquire a dendritic cell morphology (a hallmark for differentiation) and actively divide, leading to ectopic migratory cells landing outside of the normal stripe. We next looked for the mechanism underlying this using a chemical suppressor screen, to look for drugs that can rescue this abnormality, ie. to convert a *wanderlust* phenotype into a WT.. It turned out that bace2 loss leads to hyperactivated PI3K/mTOR signaling, supported by the evidence that the abnormal melanophores can be rescued using PI3K/mTOR inhibitors. Finally, we examined the cause of this

hyperactivated PI3K/mTOR signaling and showed that Bace2 as a sheddase that cleaves the insulin receptor on melanophores and dampens melanophore sensitivity to the circulating ligand insulin b. When Bace2 is absent, the insulin receptor is intact and downstream PI3K/mTOR is activated in the presence of ligand.

We showed how a melanophore-specific sheddase can negatively regulate insulin receptor on melanophores by proteolytic cleavage, and that the extent of intact insulin receptor is vital for melanophore morphology, proliferation and migration through PI3K/mTOR signal transduction. Similar to the aberrant embryonic melanophores, melanoma cells are also dendritic, proliferative and invasive when BACE2 is lost, but whether BACE2 utilizes the same mechanism of cleaving the insulin receptor in melanoma cells remains to be tested.

4.2 Future directions

4.2.1 How Bace2 itself is regulated

We dissected the downstream effectors of Bace2 but a remaining question is how Bace2 itself is regulated. We examined *bace2* expression across developmental stages using the Sanger developmental RNA-seq analysis. This demonstrated that *bace2* is expressed at high levels at the zygote stage, consistent with maternal deposition. It then drops to low levels over the next 20 hours and begins to rise again around 25 somites and further increases up until 72hpf (Figure 36). This raised the hypothesis that *bace2* is regulated by melanophore-specific transcription factors. To assess this, we examined recently published data from Robert Cornell's group (Seberg et al., 2017),

where they used both ChIP-seq and transcriptomics to identify downstream targets of Mitf and Tfap2a. Although not specifically highlighted in their manuscript, in a personal communication to us, they indicated that their data is consistent with *bace2* being a likely direct transcriptional target of Tfap2a. Given our ongoing interest in *bace2* biology, we hope to perform future analysis of the *bace2* promoter to functionally dissect these regulatory elements.

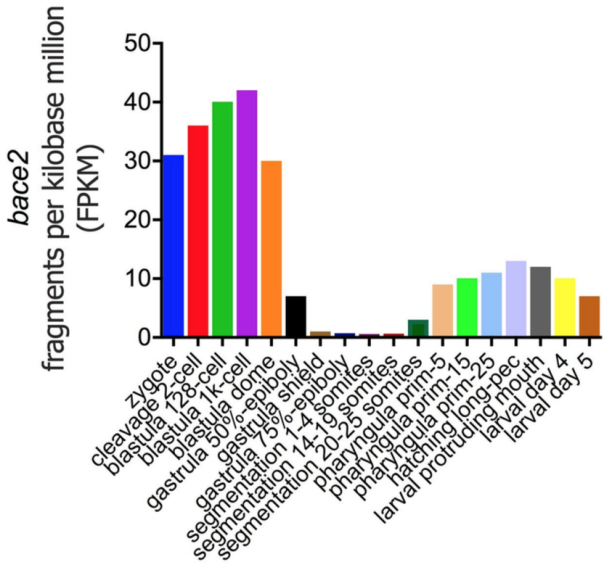

Figure 36. *bace2* expression in zebrafish embryos. *bace2* is maternally deposited at early development (from zygote to blastula dome) and then reactivated between prim-5 (24hpf) to 5dpf in WT embryos. Data is adapted from Sanger developmental RNA-seq analysis.

Insulin signaling has multiple negative feedback mechanism to titrate down excessive signaling. Insulin is known to induce insulin receptor internalization to decrease the number of insulin receptors on the plasma membrane (Di Guglielmo et al., 1998). Activated mTORC1/S6K signaling inhibits IRS-1 function (Rozengurt et al., 2014). We propose that Bace2 activity can also be regulated by a feedback loop within Insulin/PI3K/mTOR signaling. Excessive PI3K/mTOR caused by Bace2 low might trigger a transcriptional or post-translational activation of Bace2 to restore Bace2 activity.

4.2.2 How PI3K/mTOR regulates dendrite formation

We showed that activated PI3K/mTOR leads to dendritic melanophore morphology, but did not provide a mechanistic explanation. PI3K/mTOR signaling is well known to affect cytoskeleton arrangement and change neuron axon and dendrite patterning, in which PI3K signaling regulates downstream Rac/CDC42 signaling to drive dendrite neuronal morphology (Angliker and Rüegg, 2013; Jacinto et al., 2004; Liu et al., 2010; Sarbassov et al., 2004). We hypothesize that a similar mechanism is utilized in melanophore dendrites since they are also regulated by small GTP-binding proteins such as Rac and Rho, through a fine-tuned balance between Rho (which stimulates dendrite retraction) and Rac (which stimulates dendrite formation) (Scott, 2002). In the future, we would like to test if *wanderlust* mutants have excessive Rac GTPase activity because of hyperactivated PI3K/mTOR.

4.2.3 The source and other functions of insulin b ligand in zebrafish

Because of a genome duplication in zebrafish, zebrafish have two insulins. Insulin A is similar to pancreatic insulin in mammals and is responsible for

glucose homeostasis, but the source and function of insulin b is less understood (Papasani et al., 2006). Our work implies that insulin B is maternally deposited during early embryogenesis and then zygotically expressed in the head/brain region between 48hpf and 72hpf. CNS expressed insulin is seen in multiple organisms including not only zebrafish but also Drosophila (Gray et al., 2014; Luo et al., 2012), where they are believed to have functions in the CNS and so may have functions outside of glucose homeostasis (Deltour et al., 1993; Havrankova et al., 1978; Mehran et al., 2012; Molnár et al., 2014). In subsequent studies, we hope to delineate the types of cells producing insulin B and the exact differences between Insb and these other insulins.

4.2.4 How are other circulating factors regulated in a melanophore specific manner

Melanocytes are known to be regulated by multiple hormones, such as thyroid hormone, sex hormones and α-MSH (McMenamin et al., 2014; Natale et al., 2016; Spencer and Schallreuter, 2009). One remaining question is how are those general circulating hormones regulated in a cell-type specific manner and how do they coordinate with melanocyte differentiation states? Our work suggests a cleavage based mechanism where Bace2 cleaves and inactivates the insulin receptor to decrease sensitivity to circulating insulin. We hypothesize that cleavage based regulation is a generalized mechanism utilized by melanocytes to monitor their response to environmental factors. Sheddase availability could be regulated by a cell type specific transcription factor so that sheddases might act to connect cellular differentiation to the strength of ligand-induced signaling. Melanocytes are also expressing other

proteases such as ADAM-9 and ADAM-10 (Lee et al., 2010a; Zigrino et al., 2005). It is therefore intriguing to test if the network of sheddases within melanophores could cleave their own RTKs or GPCRs to fine-tune downstream signalings.

4.2.5 Mechanistic study of the roles of BACE2 in melanoma

We showed in Chapter 3 that melanoma cells respond to BACE2 loss in a similar manner to melanocytes, but failed to provide further mechanistic studies. In future, we would like to test if BACE2 cleaves the insulin receptor in human melanoma cells, and changes downstream PI3K/mTOR activity. We predict that Bace2 null melanoma cells would also have hyperactivated PI3K/mTOR in mammalian system and become addicted to this for survival. BACE2 is deleted in a small percentage of human melanoma patients and PI3K/mTOR inhibitors are likely to be very efficacious in this context.

Furthermore, humans only have pancreatic derived insulin. Our research showed that zebrafish insulin b alters melanocyte behavior. Accordingly, people with a rare disease of excess insulin secretion called acanthosis nigricans sometimes develop striking changes in skin pigmentation (Hermanns-Lê et al., 2004). We would like to investigate the roles of pancreatic insulin in promoting melanoma progression in the future.

CHAPTER 5: MATERIALS AND METHODS

5.1 Experimental model and subject details

Zebrafish

Fish Husbandry:

Fish stocks were reared under standard conditions at 28.5°C under 14:10 light:dark cycles. Healthy, immune-competent male and female adults of the AB strain were used for breeding (animals were typically ~8 months when bred). Animals were fed standard zebrafish diet consisting of brine shrimp followed by Zeigler pellets. For all mutant studies, we compared *bace2*$^{-/-}$ siblings to AB siblings derived from an initial incross of the AB and *bace2*$^{-/-}$ strain. Sex determination in embryos is not possible at the stages used in this study. Embryos were collected from natural mating and incubated in E3 buffer (5 mM NaCl, 0.17 mM KCl, 0.33 mM CaCl2, 0.33 mM MgSO4) at 28.5°C. The *bace2*$^{-/-}$ fish were obtained from the Wellcome Trust Sanger Institute.

Transgenic lines:

One-cell-stage *bace2*$^{-/-}$ embryos were injected with the given DNA construct *Tg(fugu dct: Z-bace2; cryaa: YFP)* at 25 ng/µl with Tol2 mRNA at 20 ng/µl. Embryos were screened at 3 days post fertilization for the presence of yellow fluorescent protein (YFP) in the eye lens. YFP positive embryos were grown to adulthood and outcrossed so as to identify founders that gave germline transmission. To quantify melanophores rescue, founders were outcrossed to *bace2*$^{-/-}$ and the F1 were screened for melanophores rescue and the presence of YFP positive lenses.

One-cell-stage *bace2*$^{-/-}$ embryos were injected with the given DNA construct *Tg(fugu tyrp1:dnIRS2-EGFP; cmlc2: mCherry)* at 25 ng/µl with Tol2 mRNA at

20 ng/µl. Embryos were screened at 30hpf for the presence of mCherry in the heart. dnIRS2(Ye et al., 2016) is a previously published dominant negative insulin receptor substrate 2 that non-productively binds to the insulin receptor to inhibit insulin signaling.

Tg(tyrp1b:membrane-mCherry) and *Tg(mitfa:EGFP)* fish strains were generous gifts from Dr. David Parichy and Dr. James Lister respectively. *bace2*$^{-/-}$ was crossed into these strains to generate *bace2*$^{-/-}$; *Tg(tyrp1b:membrane-mCherry)* and *bace2*$^{-/-}$; *Tg(mitfa:EGFP).*

Cell Lines

The ZMEL1 cell line(Heilmann et al., 2015), A375 cell line and HEK 293T cell line were maintained as previously described. All cells were cultured in DMEM with 10% FBS/penicillin/streptomycin/glutamine. The sex of the animal from which the ZMEL1 line was derived is unknown. HEK 293T cells are derived from a female fetus.

5.2 Method details

Genotyping of *bace2*$^{-/-}$ Fish

Tail clips from adult zebrafish were placed in microcentrifuge tubes or thermal cycler plates containing 50µl of 50 mM NaOH. Samples were boiled at 95℃for 30min, then cooled down with 5µl of 1M Tris-HCL (pH=8.0). A 1:10 dilution of the supernatant was used in PCR. Primer sequences for PCR are listed in Table S2. DNA was PCR amplified with Promega GoTag green mastermix and digested using Hpy188I enzyme (NEB catalog # R0617S). Limit Hpy188I digestion time to one hour to avoid non-specific digestion (star activity). *bace2*$^{-/-}$ confers a C to A mutation which abolishes the Hpy188I digestion site. WT

fish have two bands at 450bp and 240bp, *bace2*$^{-/-}$ fish have one band at 690bp, *bace2*$^{+/-}$ fish have three bands at 240bp, 450bp and 690bp.

Chemical Screen

The chemical screen was performed similar to prior publications (Kaufman et al., 2009). We aimed to identify suppressors of the *bace2*$^{-/-}$ melanophores phenotype by treating *bace2*$^{-/-}$ embryos from 24hpf to 72hpf with 30μM chemicals from Sigma LOPAC 1280 library. Chemicals were prepared from 10mM stock and diluted into 30μM in 300μl E3 with 0.3% (v/v) DMSO. Embryos were staged at both shield stage and 24hpf prior to drug treatment. Three embryos per well in 48-well-plates were scored. Eight DMSO-only wells were included in each plate as negative control. Plates were foil wrapped to protect from light and incubated at 28.5℃from 24hpf to 72hpf. At 72hpf, embryos were anaesthetized with tricaine and were subject to direct observation under light microscope. Melanophores rescue was scored from 0-5, with 0 to be mutant-like melanophores (i.e. no rescue) and 5 to be completely rescued into WT-like melanophores. Chemicals with scores >3 were subject to a second round of validation, with different aliquots of the library. Positive hits were ordered from Sigma and were tested for minimal concentration required to rescue *bace2*$^{-/-}$ phenotype.

Embryo Drug Treatment

Embryos were treated with the following chemicals (with working concentration, treatment time and catalog number). All chemicals are dissolved in DMSO.

PF-06663195 (Bace2 inhibitor): 100μM, various treating time (Sigma, catalog # PZ0262).

AS605240: 110nM, 24hpf-72hpf (Sigma, catalog # A0233)

Wortmannin: 230nM, 24hpf-72hpf (Sigma, catalog # W1628)

LY-294,002: 15μM, 24hpf-72hpf (Sigma, catalog # L9908)

Temsirolimus: 30μM, 24hpf-72hpf (Sigma, catalog # PZ0020)

PP242: 15μM, 24hpf-72hpf (Abcam, catalog # ab141405)

BMS-754807: 7.5μM, 24hpf-72hpf (Sigma, catalog # BM0003)

NVP-AEW541: 60μM, 24hpf-72hpf (Selleck Chemicals, catalog # S1034)

PTU: 300μM, 3dpF-5dpF (Sigma, catalog # P7629).

Morpholino Injections

All the morpholino oligonucleotides (MO) were synthesized by Gene ToolsTM LLC, resuspended in sterile water at a concentration of 1mM stock. MO stock was further diluted into working concentrations in sterile water and injected into zebrafish embryos at the one-cell stage by microinjection, at ~1.5nL/embryo. MO working concentration, sequence and reference information are listed in Table S1.

The efficacy of splicing morpholinos below have been confirmed using Reverse transcription PCR (RT-PCR), with primer information listed in Table S2.

The efficacy of mTOR splicing MO has been also confirmed using WB, with primary antibody: mTOR (7C10) Rabbit mAb (Cell Signaling Technology, catalog # 2983S). The efficacy of Insulin receptor ATG MO has been confirmed using WB, with primary antibody: insulin R β (C-19) (Santa Cruz Biotechnology, catalog # sc-711). The efficacy of Pdx1 and Hb9 ATG MO

have been confirmed indirectly using immunostaining against Insulin protein, with primary antibody: insulin (Genetex, catalog # GTX128490).

Measurement of Tailfin Melanophore Cell Area

The extent of melanophore dendricity in the tailfin was calculated as the area of melanophores covering the tailfin mesenchyme. This was quantified by thresholding the mCherry intensity or thresholding the bright field intensity to highlight the pixels that represent melanophores in each image, and measuring the area they cover with FIJI software.

ZMEL1 phospho-Histone H3 (pH3) Immunostaining

ZMEL1 were seeded at 6000 cells/well in white wall, clear bottom 96-well plates (Fisher Scientific, catalog # 07-200-566) in DMEM/10% FBS/ penicillin/streptomycin/glutamine. The cells were allowed to adhere overnight, and then media were changed to Bace2 inhibitor (PF-06663195) containing media at 12.5μM or 25μM with 0.025% (v/v) DMSO. Cells were grown for a total of 3 days after the addition of Bace2 inhibitor. At the end of the treatment, the cells were fixed with paraformaldehyde (4% in 1X PBS), permeabilized with 0.1% Triton-X-100 for 15 min at room temperature. Cells were rinsed with 1X PBS three times and then blocked with 1X PBS/5% goat serum/0.3% Triton X-100 for 1 hour at room temperature, and then stained with anti-pH3 primary antibody (1:1000, EMD Millipore, catalog # 05-806) diluted in antibody dilution buffer (1X PBS/1% BSA/0.3% Triton X-100) at 4℃overnight. Cells were rinsed with 1X PBS three times the next day and then stained with anti-mouse Alexa 647 (1:1000, CST, catalog # 4410) diluted in antibody dilution buffer for 1 hour at room temperature in the dark. Cells were rinsed three

times with 1X PBS and stained with Hoechst 33342 (4µg/ml, Thermo Fisher Scientific, catalog # H3570) for 30 min at room temperature in the dark. Cells were rinsed three times with 1X PBS and imaged using a GE INCell 6000. 6 fields were captured per well using a Nikon 10X Plan Apo objective, 0.45NA. Images of the Hoechst signal was captured via the DAPI channel in order to identify the nucleus. The pH3 was captured via the far-red channel to identify the mitotic cells. The image analysis script was performed within the Perkin Elmer Columbus software. Percentage of mitotic cells were quantified by calculating pH3 positive cells as a fraction of the total number of cells in each well.

RT-PCR

Zebrafish embryos were homogenized in 1ml of Trizol (Life Technologies, catalog #15596 - 018) on ice using Bel-Art micro-tube homogenizer (Fisher Scientific, catalog # 03-421-215) for one minute, with a pool of 5 to 50 embryos at 3dpF. Then total RNA from zebrafish embryos were extracted using Direct-zol RNA miniprep kit (Zymo Research, catalog # R2050). cDNA library was constructed using SuperScript III First-Strand kit (Thermo Fisher Scientific, catalog # 18080-400). cDNA from both the control embryos and the morpholino injected embryos were used in downstream PCR reaction to confirm the efficacy of morpholino knockdown.

Knockdown of *BACE2* in A375 Human Melanoma Cell Line

shRNAs were designed and constructed following(Fellmann et al., 2013). 97-mer oligonucleotides coding for six shRNAs against human *BACE2* (see sequence below) were PCR amplified using the primers miRE-Xho-fw (5'-

TGAACTCGAGAAGGTATAT TGCTGTTGACAGTGAGCG-3') and miRE-EcoOligo-rev (5'-TCTCGAATTCT AGCCCCTTGAAGTCCGAGGCAGTAGGC-3'), 0.05 ng oligonucleotide template, and the PfuUltra HF kit (Agilent), and cloned into miRE LT3GEP1R (pRRL) Tet-On all-in-one vector. Lentiviral particles were produced in HEK 293T cell transfected with miRE shRNA lentiviral vector, psPAX2 packaging plasmid and pMD2.G envelope plasmid. A375 was transduced with lentiviral particles under single-copy conditions, and then selected with puromycin (1µg/ml) for around one week, until GFP positive cells were enriched for 90%. Post puromycin selection, 1µg/ml doxycycline were included in culture media for 5 days and the protein lysates were collected to measure shRNA knockdown efficiency. Control shRNA targeting Renilla luciferase and two shRNAs (bace2.1690: shRNA#1, bace2.1742: shRNA#2) with the best knockdown efficiency were included for downstream functional assay. All shRNA sequence are listed in Table 4.

Cell Counting for Metamorphosis Zebrafish

24dpF age matched and size matched siblings were treated with epinephrine to contract pigment granules and also treated with 4mg/ml tricaine before imaging. Fish were tile scanned (22µm z step) using an upright Zeiss Discovery V16 equipped with a motorized stage in brightfield. Images were acquired with the Zeiss Zen software v1. Ten somites from dorsal and ventral sides of one fish (start the first somite in the beginning of dorsal fin, and count posteriorly) were defined as region of interest (ROI). Two artificial lines were drawn parallel to the vertebrate and aligned their one ends to the tail fin. Region inside of the two lines are defined as intra-stripe region, as WT zebrafish form melanophores mainly inside of this region; region outside of the

two lines are defined as inter-stripe region. Inter-stripe melanophores reside within ROI were counted manually.

in situ Hybridization (ISH)

ISH were performed as described in(Thisse and Thisse, 2008). Embryos were fixed at 24hpf, 48hpf and 72hpf. Probes were diluted to a working solution of 0.8 ng/μl. Staining time varied between probes from couple hours at room temperature, or overnight at 4℃. Fluorescent ISH (FISH) was performed as described in(Welten et al., 2006). In brief, post methanol fixation embryos are treated with 3% H_2O_2 in methanol for 20 min at room temperature to inhibit endogenous peroxidase activity. Then FISH follows the same procedure with regular ISH except those modifications: performing all hybridization and wash steps at 55℃instead of 70℃, with 0.25ng/μl for both *insb* antisense and sense probe. Dilute anti-DIG-POD antibody (1:2000, Sigma-Aldrich, catalog # 11207733910) for anti-DIG-HRP detection in antibody buffer and pre-adsorb for 2 h at room temperature with slow agitation. Incubate embryos overnight in anti-DIG-POD antibody and next day wash 6 times for 15 minutes in PBST at room temperature. Dilute TSA Plus Cyanine 3 reagent (1:50, PerkinElmer, catalog # NEL744001KT) in the amplification buffer supplied and incubate embryos with diluted TSA/Cyanine 3 reagent for 30min at room temperature in the dark. Wash 8 times for 15 minutes in PBST and then image embryos. double FISH (dFISH) follows the same procedure with single probe FISH except for the following modifications. Hybridization at 65℃with *bace2* riboprobe (3ng/μl) labelled with DIG (Sigma-Aldrich, catalog # 11277073910) and *crestin* riboprobe (2.92ng/μl) labelled with fluorescein (fluorescein-12-UTP, Sigma-Aldrich, catalog # 11685619910) in hybridization mix (HM+) with

5% dextran sulfate (Sigma-Aldrich, catalog # D8906-5G) to allow two targets to be visualized simultaneously. Embryos were then incubated overnight at 4°C with anti-DIG-AP antibody (1:5000, Sigma-Aldrich, catalog # 11093274910) and anti-fluorescein-HRP antibody (1:500, Sigma-Aldrich, catalog # 11426346910) followed by extensive washes in PBST. To detect HRP (*crestin*), embryos were incubated with TSA Plus fluorescein evaluation kit (1:50, PerkinElmer, catalog # NEL741E001KT) for 30 min in the dark in amplification buffer. Following the addition of 0.001% H_2O_2 signal was allowed to develop for 30 min. After two washes with PBST, Fast Red (Sigma, catalog # F4648) was used according to the manufacturer's instructions to detect the AP (*bace2*). The embryos were then extensively washed 4x15min in PBST, and DAPI was used as a nuclear counterstain. Mount embryos in low melting agarose for imaging acquisition. Tile scan images were collected with a Leica TCS SP5 II (DMI6000 CFS; acquisition software Leica Application Suite AF v. 2.6.3.8173). Confocal images were acquired at 1,024 × 1,024 pixels (20.0-µm z step) using a 10X and 40X objectives, with zoom-in factor of 3 for 120X defection. The 3D reconstructions of the *Insb, bace2* and *crestin* expression were performed using Imaris software.

Dct(Kelsh et al., 2000), *mitfa(Lister et al., 1999)*, *tyr(Mellgren and Johnson, 2004)*, *sox10(Dutton et al., 2001)*, *crestin(Luo et al., 2001)* and *c-kit(Parichy et al., 1999)* probes were generous gifts from Dr. David Parichy. *Pmela(Schonthaler et al., 2005)*, *ednrb1*a(Parichy et al., 2000) and *foxd3(Odenthal and Nüsslein-Volhard, 1998)* probes were generous gifts from Dr. James Lister. *Tyrp1b* probe DNA template was PCR amplified from MGC clone plasmid (Thermo Fisher Scientific, catalog # EDR1052-210947471), and *in vitro* transcribed using T3 RNA polymerase.

Bace2 probe DNA template was PCR amplified from plasmid pENTR-z-*bace2*, and *in vitro* transcribed using T3 RNA polymerase.

Insa probe was validated by (Thisse, B., Thisse, C. (2004) Fast Release Clones: A High Throughput Expression Analysis. ZFIN Direct Data Submission (http://zfin.org).). *Insa* probe DNA template was PCR amplified from MGC clone plasmid (Dharmacon, catalog # MDR1734-202792960), and *in vitro* transcribed using T3 RNA polymerase.

Insb probe was validated by(Junker et al., 2014). *Insb* probe DNA template was amplified from zebrafish cDNA library and then TOPO TA cloned into pCR™II-TOPO TA vector. The *insb* antisense probe was PCR amplified and then *in vitro* transcribed using T3 RNA polymerase. The *insb* sense probe (negative control) was digested with HindIII then *in vitro* transcribed using T7 RNA polymerase. Primer sequence is listed in Table S2. Probe sequence, source and reference information is listed in Table S3.

Embryos Protein Immunofluorescence

Embryos were kept in 300μM PTU to inhibit melanin synthesis. Embryos were fixed with 4% paraformaldehyde in PBS overnight at 4°C, then dehydrated in 100% methanol overnight at -20°C. Embryos were rehydrated with 50% methanol/PBS then into PBST (PBS with 0.1% Tween-20) for 5min each, then permeabilized with 100% acetone at -20°C for 12 min (for 24hpf embryos) or 20 min (for 2-3dpf embryos). Embryos were blocked with blocking buffer (PBST+1%DMSO+4%BSA) for 1 hour at room temperature. Antibodies were diluted in blocking buffer, applied to embryos and incubated overnight at 4°C. Embryos were then washed with washing buffer (PBST+1%DMSO) twice every 15 minutes for 2 hours at room temperature. Embryos were Incubate

with secondary antibody in blocking buffer for 2 hours at room temperature in dark. Embryos were then washed with washing buffer twice every 15 minutes for 1 hours at room temperature. For insulin staining: yolk was manually dissected off to visualize insulin staining in pancreas. For pS6 staining: pS6 signal co-localized with melanophores was measured to identify melanophore specific PI3K/mTOR activity. For 24hpf and 48hpf embryos, the transgenic *mitfa*: EGFP line was used to mark melanophores in EGFP. For 72hpf embryos, the transgenic *tyrp1b*: membrane-mCherry line was used to mark melanophores in mCherry. (This is because *tyrp1b* promoter is not on at 24hpf, and *mitfa* promoter is off at 72hpf). Embryos were mounted on agarose plate for imaging acquisition. Primary antibody: rabbit anti-zebrafish insulin (1:200, Genetex, catalog # GTX128490), rabbit anti-phospho-S6 Ribosomal Protein (Ser240/244) (D68F8) (1:800, CST, catalog # 5364), mouse anti-GFP (1:500, abcam, catalog # ab1218), chicken anti-mCherry (1:1000, abcam, catalog # ab205402). Secondary antibodies: Alexa-Fluor 488 anti-rabbit (1:200, CST, catalog # 4412), Alexa-Fluor 594 anti-rabbit (1:200, CST, catalog # 8889), Alexa-Fluor 594 anti-chicken (1:200, abcam, catalog # ab150176), Alexa-Fluor 488 anti-mouse (1:200, CST, catalog # 4408).

Creation of *pmela* CRISPR Mutant

Creation of *pmela* CRISPR knockout mutant was adapted from(Gagnon et al., 2014). Guide RNA (gRNA) was designed against the Pmela coding sequence, and synthesized via *in vitro* transcription. The gRNA was incubated with purified recombinant Cas9-3NLS protein (IDT, catalog # 1074181), and these were coinjected (300ng/µl gRNA+1µg/µl protein) into single cell zebrafish embryos, with 1.5nL injection volume per embryo. F0 embryos displayed

mosaic knockout phenotype similar to *fading vision* mutant(Schonthaler et al., 2005), and were raised into adulthood. F0 founders were incrossed to yield trans-heterozygous F1 fish. Pmela gRNA sequence is listed in the Key Resource Table.

Insa Positive Cell Area Measurement

Insa ISH pictures were used to measure the *insa* positive cell area. *Insa* positive cell area is quantified by thresholding the bright field intensity to highlight the pixels that represent *insa* in each image, and measuring the area they cover with FIJI software.

High Content Cell Morphology Analysis

High-content image analysis was used to measure the effects of pharmacological inhibition of Bace2 on ZMEL1 cell morphology. ZMEL1 were seeded at 4000 cells/well in black wall, clear bottom 96-well plates (PerkinElmer, catalog #6005182) in DMEM/10% FBS/ penicillin/streptomycin/glutamine. The cells were allowed to adhere overnight, and then media were changed to Bace2 inhibitor (PF-06663195) containing media at 12.5μM or 25μM with 0.025% (v/v) DMSO. Cells were grown for a total of 3 days after the addition of Bace2 inhibitor. At the end of the treatment, the cells were fixed with paraformaldehyde (4% in 1X PBS), permeabilized with 0.1% Triton-X-100 and stained using Hoechst 33342 (4μg/ml, Thermo Fisher Scientific, catalog # H3570) and HCS CellMask Deep Red Stain (1.7μg/ml, Thermo Fisher Scientific, catalog # H32721). Using a GE INCell 6000, 6 fields were captured per well using a Nikon 10X Plan Apo objective, 0.45NA. Images of the Hoechst signal was captured via the DAPI channel in

order to identify the nucleus. The HCS Cellmask Deep Red was captured via the far-red channel to identify the cell body.

The image analysis script was performed within the Perkin Elmer Columbus software. Briefly the Hoechst stained nuclei was used to initially segment objects and act as a seed region to segment the cells stained with HCS CellMask Deep Red. Cell morphology is the primary readout of this high-content assay and the primary cell morphology parameters used are length to width ratio. Cell length is defined as the maximum distance (in microns) between two points on the cell mask. Cell width is defined as the diameter of the largest circle that will fit within the cell or nuclear mask.

Knockout *insr* in ZMEL1

Alt-R CRISPR-Cas9 gRNAs against zebrafish *insra* and *insrb* were designed using CHOPCHOP website(Labun et al., 2016) and synthesized by IDT. The RNP complex containing gRNAs (11μM of each *insra* and *insrb* gRNA mixture), tracrRNA ATTO™ 550 (22μM, IDT, catalog # 1075928) guide complex and an S. pyogenes recombinant Cas9 endonuclease (18.3μM, IDT, catalog # 1074181) were prepared at room temperature following manufacturer's instruction. A non-target gRNA was included as negative control (22μM). The final complex (10μl RNP and 20μl of electroporation enhancer at 10.8μM) was nucleofected into 90μl cell suspension containing 8 million ZMEL1 cells using NEON transfection system (100μl kit, Thermo fisher Scientific, catalog # MPK10096, pulse voltage: 1400, pulse width: 20 and pulse number: 2) and plated back to fibronectin-coated flask. The tracrRNA ATTO™ 550 labelled ZMEL1 cells with RFP and was used to FACS sort RFP+ cells 3 days post nucleofection. Genomic DNA and protein lysates were

extracted from sorted cells to assay mutations using Surveyor assay and protein using Western Blot respectively. For surveyor assay, *insra* and *insrb* genomic sequence adjacent to gRNA PAM sites were PCR amplified and then digested with surveyor nuclease (IDT, catalog # 706020). gRNA sequences are listed in the Key Resource Table. Primers for Surveyor PCR are listed in Table S2.

Plasmid Construction and Cell Line Expression

The following plasmids were constructed using the Gateway Tol2kit.

Fugu dct: Z-bace2 (zebrafish bace2); cryaa: YFP

Fugu tyrp1:dnIRS2-EGFP; cmlc2: mCherry

CMV: Z-bace2-2a-GFP-394

CMV: Z-bace2 enzymatic dead-2a-GFP-394

CMV: Z-insra-Myc-394

CMV: Z-insrb-Myc-394

CMV: tdtomato-394 (used as vector control)

Zebrafish Bace2 (Z-bace2) cDNA was amplified from WT embryos' cDNA library and cloned into pENTR/D-TOPO vector.

Zebrafish Bace2 enzymatic dead cDNA was constructed by site-mutagenesis of two conserved protease sites (aspartic acids) into alanines (D98A and D292A) respectively.

Fugu *tyrp1* promoter was a generous gift from(Zou et al., 2006).

Zebrafish dnIRS2-GFP was a generous gift from(Ye et al., 2016) and then further cloned into pENTR/D-TOPO vector.

Zebrafish insra and insrb cDNA was amplified from WT embryos' cDNA library and cloned into pENTR/D-TOPO vector.

CMV: Z-pmela-FLAG was constructed by In-fusion cloning to clone Z-pmela cDNA into pCS2FLAG backbone (Addgene, catalog #16331). The FLAG tag was C-terminal fused to Z-pmela cDNA. Z-pmela cDNA was amplified from MGC clone plasmid (Open Biosystems, catalog # MDR1734-202779066). All primers are listed in Table S2.

Lipofectamine 2000 (Life Technologies, catalog # 11668019) was used to overexpress plasmids in HEK 293T cells.

Western Blot

Cell lysates were collected using RIPA buffer (Thermo Fisher Scientific, catalog # 89901), with addition of 1X protease inhibitor (Thermo Fisher Scientific, catalog # 78430), 1X phosphatase Inhibitor (Fisher Scientific, catalog #78441) and 5mM EDTA. Proteins concentrations were measured with Bradford (Sigma-Aldrich, catalog # B6916) according to kit direction. Protein were mixed with 6X SDS loading dye (Boston BioProducts, catalog # BP-111R) and boiled at 95℃for 10min. Proteins were run on pre-made mini protean TGX gels (Bio-Rad). Gels were transferred using Turbo™ Mini Nitrocellulose Transfer Pack (Bio-Rad, catalog # 1704158). Membranes were blocked in 5% milk for 1 hour at room temperature prior to addition of primary antibody overnight at 4℃. Membranes were washed with 1X TBST (0.1% Tween 20) for 3x10min, then incubated with secondary antibody for 1 hour at room temperature. Membranes were washed with 1X TBST for 3x10min. Signals were developed using ECL prime (GE Healthcare, catalog # RPN2236). Primary antibodies used for Western blot are: mTOR (7C10) mAb (1:1000, CST, catalog # 2983S), insulin R β (C-19) (1:200, Santa Cruz Biotechnology, catalog # sc-711), c-MYC (1:1000, Santa Cruz Biotechnology,

catalog # sc-40), BACE2 F-12 (1:100, Santa Cruz Biotechnology, catalog #sc-271286), FLAG (1:500, Sigma-Aldrich, catalog # F3165). Secondary antibodies were: rabbit anti-mouse IgG H&L (HRP) (1:10,000, Abcam, catalog # ab97046), goat anti-rabbit IgG H&L (HRP) (1:10,000, Abcam, catalog # ab97051).

Transwell Assay

$1X10^5$ ZMEL1 cells were seeded into 3.0μM transwell inserts (Corning catalog # 353492) in 500μl of culture media, in the presence or absence of 25μM Bace2 inhibitor PF-06663195 with 0.025% (v/v) DMSO. The receiving plates (Corning catalog # 353504) were filled with 500μl culture media, also in the presence or absence of 25μM Bace2 inhibitor. ZMEL1 were allowed to migrate for 48 hours, then sterile cotton swabs were used to gently clean the inside of each membrane 3 times. Hoechst 33342 were added to final concentration of 4μg/ml to facilitate cell counting. Image five different 20X fields per well and quantify cell numbers by image analysis software FIJI.

Gelatin Degradation Assays

Coverslips were prepared as in; briefly, autoclaved coverslips were coated with AlexaFluor 546-labeled gelatin (1 mg/ml) and crosslinked with 0.5% glutaraldehyde (Sigma) in 1X PBS. A layer of collagen I (Corning) in DPBS (Corning, with calcium and magnesium) at 0.5 mg/ml was subsequently polymerized on top of the gelatin-coated coverslip for 4 hrs at 37°C. 25,000 A375 melanoma cells were seeded directly onto the collagen I/gelatin mixed matrix-coated coverslips in DMEM supplemented with 10% FBS/penicillin/streptomycin/glutamine and 1μg/ml doxycycline overnight. Cells

were fixed with 4% paraformaldehyde (EMS) in 1X PBS, and stained with DAPI (Sigma) to localize cells. Images were acquired on a Leica DM5500B microscope with a 100X/1.4-0.7 NA HCX PL APO oil objective and a DFC345 FX camera. Matrix degradation was quantified using ImageJ, as described previously.

5.3 Quantification and statistical analysis

Statistical comparisons were performed with the aid of GraphPad PRISM 7 and the statistical details including sample size can be found in the figure legends. A p value of >0.05 is not considered statistically significant. * indicates $p<0.05$, ** indicates $p<0.01$, *** indicates $p<0.001$ and **** indicates $p<0.0001$.

Table 1. morpholinos working concentration, sequence and reference information.

MO Name	Working conc.	MO Sequence (5'-3')	Reference
Bace2 splicing MO	0.16mM	GTTACCACATAACATACCGTTTGTC	This paper
PI3K γ ATG MO	1mM	CATCATCACTGGCTTGCTGTTCCAT	(Li et al., 2015)
mTOR splicing MO	1mM	GGTTTGACACATTACCCTGAGCATG	(Makky et al., 2007)
Insra ATG MO	0.5mM	CAAAGTCCGCAGCCGCATTTTGACC	(Wan et al., 2014)
Insrb ATG MO	0.1mM	TGTGTCCAGCCGCATTCTGCCTCGC	(Wan et al., 2014)
Insa splicing MO	0.5mM	CCTCTACTTGACTTTCTTACCCAGA	(Ye et al., 2016)
Insb splicing MO	0.25mM	AAGTTGGAGACGTTGCTCACCCAGC	(Ye et al., 2016)
Pdx1 ATG MO	0.45mM	GATAGTAATGCTCTTCCCGATTCAT	(Kimmel et al., 2011)
Hb9 ATG MO	0.45mM	TTTTTAGATTTCTCCATCTGGCCCA	(Kimmel et al., 2011)

Table 1 (Continued)

PI3K α ATG MO	1mM	GTCTTGGAGGCATGATTTGTAATCC	(Li et al., 2015)
PI3K β ATG MO	1mM	GCATGGCAGAGAACACACTGAAGCC	(Li et al., 2015)
PI3K δ ATG MO	1mM	GGCATCGTGCAGGAAAACTCATCTAC	(Li et al., 2015)
Pmela ATG MO	0.1mM	GAGGAAGATGAGAGATGTCCACATG	(Schonthaler et al., 2005)
Pmelb ATG MO	0.2mM	GTAGAGAATAGCTTCATTGTGTCAC	(Burgoyne et al., 2015)

Table 2. primer sequence.

Primer	Sequence (5'-3')
bace2 genotype F1	TCCTTGTTGCAGTCTATCCCT
bace2 genotype R1	GCACTTGAACTCCTCAGTTACA
mTOR MO F1	GAGTTCATGTTCCTGCTG
mTOR MO R1	CCATCCAATGTAGCATTGG
Insa MO F1	CATTCCTCGCCTCTGCTTC
Insa MO R1	GGAGAGCATTAAGGCCTGTG
Insb MO F1	CAGACTCTGCTCACTCAGGAAA
Insb MO R1	GCGTGTAATGGTCATTTATTGC
Tyrp1b ISH F1	TGGATAACCGTATTACCGCC
Tyrp1b ISH R1	CGCGCAATTAACCCTCACTAAAGCACTAGTCATACCAGGATC
Bace2 ISH F2	CACCATGCGGCTCTACGGGCTACTG
Bace2 ISH R2	CGCGCAATTAACCCTCACTAAAGAGTCACTCACTTGATGCGATGGCGCA
Insa ISH F1	TGTACGGAAGTGTTACTTCTGCTC
Insa ISH R1	GGATCCATTAACCCTCACTAAAGGGAAGGCCGCGACCTGCAGCTC
Insb TOPO F3	AGGTGTGGCTGTTGGTGAAT

Table 2 (Continued)

Insb TOPO R3	CTGGCTGTTCAGCTGCAGTA
Insb ISH F1	AGGTGTGGCTGTTGGTGAAT
Insb ISH R1	GGATCCATTAACCCTCACTAAAGGGGAATTCGCCCTTCTGGCTG
Insra CRISPR F1	ATGTGACTCTGTGTTCTGTGCC
Insra CRISPR R1	TGCAGAATGCTGATTAACCAAT
Insrb CRISPR F1	GCCTATGCTCTCGTCTCACTCT
Insrb CRISPR R1	CCCATGTGTTTCATTCTAGCTG
bace2 pENTR/D-TOPO F1	CACCATGCGGCTCTACGGGCTACTG
bace2 pENTR/D-TOPO R1	CTTGATGCGATGGCGCACCAAAGA
insra pENTR/D-TOPO F1	CACCATGCGGCTGCGGACTTTGATT
insra-pENTR/D-TOPO-R1	AGAAGGGGTGGATCGGGGTAGAG
insrb pENTR/D-TOPO F1	CACCATGCGGCTGGACACATCTGTGG
insr pENTR/D-TOPO R1	GGACGGACTAGATCTGGGTAAAGACAG
pmela cDNA F1	CGATTTAAAGCTATGCACCATGTGGACATCTCTCATCTTCCT
pmela cDNA R1	ATCATCCTTGTAATCCACCACGCGTCCCAGCAGAAGT

Table 3. *in situ* hybridization (ISH) probes, source and reference.

ISH probe	Source	Reference
Dct	Gift from David Parichy (University of Virginia)	Kelsh et al., 2000
Mitfa	Gift from David Parichy (University of Virginia)	Lister et al., 1999
Tyr	Gift from David Parichy (University of Virginia)	Mellgren and Johnson, 2004
Sox10	Gift from David Parichy (University of Virginia)	Dutton et al., 2001
Crestin	Gift from David Parichy (University of Virginia)	Luo et al., 2001
c-kit	Gift from David Parichy (University of Virginia)	Parichy et al., 1999
Pmela	Gift from James Lister (Virginia Commonwealth University)	Schonthaler et al., 2005
ednrb1a	Gift from James Lister (Virginia Commonwealth University)	Parichy et al., 2000
Tyrp1b	Thermo Fisher Scientific	cat # EDR1052-210947471
Bace2	This thesis	
Foxd3	Gift from James Lister (Virginia Commonwealth University)	Odenthal and Nüsslein-Volhard 1998
Insa	Dharmacon	cat # MDR1734-202792960
Insb	This thesis	(Junker et al., 2014)

Table 4. shRNA sequence to knockdown BACE2 in human melanoma cell A375.

shRNA	Sequence (5'-3')
Renilla Luciferase (shRNA control)	TGCTGTTGACAGTGAGCGCAGGAATTATAATGCTTATCTATAGTGAAGCCACAGATGTATAGATAAGCATTATAATTCCTATGCCTACTGCCTCGGA
bace2.1690 (shRNA #1)	TGCTGTTGACAGTGAGCGATCAGACATCGCTGGAAATGAATAGTGAAGCCACAGATGTATTCATTTCCAGCGATGTCTGACTGCCTACTGCCTCGGA
bace2.1742 (shRNA #2)	TGCTGTTGACAGTGAGCGATCAGCTATTAAGAAAATCACATAGTGAAGCCACAGATGTATGTGATTTTCTTAATAGCTGAGTGCCTACTGCCTCGGA
bace2.1462	TGCTGTTGACAGTGAGCGACAGGTGCTGCAGTGTCTGAAATAGTGAAGCCACAGATGTATTTCAGACACTGCAGCACCTGCTGCCTACTGCCTCGGA
bace2.2002	TGCTGTTGACAGTGAGCGATGCCACCAACATAAAACAAAATAGTGAAGCCACAGATGTATTTTGTTTTATGTTGGTGGCACTGCCTACTGCCTCGGA
bace2.1891	TGCTGTTGACAGTGAGCGCTCCTCCCTACTTCCAAGAAAATAGTGAAGCCACAGATGTATTTTCTTGGAAGTAGGGAGGATTGCCTACTGCCTCGGA
bace2.2006	TGCTGTTGACAGTGAGCGAACCAACATAAAACAAAACCAATAGTGAAGCCACAGATGTATTGGTTTTGTTTTATGTTGGTGTGCCTACTGCCTCGGA

CHAPTER 6: REFERENCES

Abdel-Malek, Z., Swope, V.B., Suzuki, I., Akcali, C., Harriger, M.D., Boyce, S.T., Urabe, K., and Hearing, V.J. (1995). Mitogenic and melanogenic stimulation of normal human melanocytes by melanotropic peptides. Proc Natl Acad Sci USA *92*, 1789–1793.

Abdi, E.A., Tan, Y.H., and McPherson, T.A. (1988). Natural human interferon-beta in metastatic malignant melanoma. A phase II study. Acta Oncol. *27*, 815–817.

Abdul-Hay, S.O., Sahara, T., McBride, M., Kang, D., and Leissring, M.A. (2012). Identification of BACE2 as an avid ß-amyloid-degrading protease. Mol. Neurodegener. *7*, 46.

Acquati, F., Accarino, M., Nucci, C., Fumagalli, P., Jovine, L., Ottolenghi, S., and Taramelli, R. (2000). The gene encoding DRAP (BACE2), a glycosylated transmembrane protein of the aspartic protease family, maps to the down critical region. FEBS Lett. *468*, 59–64.

Aguirre, V., Werner, E.D., Giraud, J., Lee, Y.H., Shoelson, S.E., and White, M.F. (2002). Phosphorylation of Ser307 in insulin receptor substrate-1 blocks interactions with the insulin receptor and inhibits insulin action. J. Biol. Chem. *277*, 1531–1537.

Ahmad, F., and Goldstein, B.J. (1995). Purification, identification and subcellular distribution of three predominant protein-tyrosine phosphatase enzymes in skeletal muscle tissue. Biochim. Biophys. Acta *1248*, 57–69.

Ahmed, R.R., Holler, C.J., Webb, R.L., Li, F., Beckett, T.L., and Murphy, M.P. (2010). BACE1 and BACE2 enzymatic activities in Alzheimer's disease. J. Neurochem. *112*, 1045–1053.

Albino, A.P., Lloyd, K.O., Houghton, A.N., Oettgen, H.F., and Old, L.J. (1981). Heterogeneity in surface antigen and glycoprotein expression of cell lines derived from different melanoma metastases of the same patient. Implications for the study of tumor antigens. J. Exp. Med. *154*, 1764–1778.

Ando, H., Watabe, H., Valencia, J.C., Yasumoto, K., Furumura, M., Funasaka, Y., Oka, M., Ichihashi, M., and Hearing, V.J. (2004). Fatty acids regulate pigmentation via proteasomal degradation of tyrosinase: a new aspect of ubiquitin-proteasome function. J. Biol. Chem. *279*, 15427–15433.

Angliker, N., and Rüegg, M.A. (2013). In vivo evidence for mTORC2-mediated actin cytoskeleton rearrangement in neurons. Bioarchitecture *3*, 113–118.

Ankeny, R.A. (2001). The natural history of Caenorhabditis elegans research. Nat. Rev. Genet. *2*, 474–479.

Ascierto, P.A., Kirkwood, J.M., Grob, J.-J., Simeone, E., Grimaldi, A.M., Maio,

M., Palmieri, G., Testori, A., Marincola, F.M., and Mozzillo, N. (2012). The role of BRAF V600 mutation in melanoma. J. Transl. Med. *10*, 85.

Bandarchi, B., Ma, L., Navab, R., Seth, A., and Rasty, G. (2010). From melanocyte to metastatic malignant melanoma. Dermatol. Res. Pract. *2010*.

Barbet, N.C., Schneider, U., Helliwell, S.B., Stansfield, I., Tuite, M.F., and Hall, M.N. (1996). TOR controls translation initiation and early G1 progression in yeast. Mol. Biol. Cell *7*, 25–42.

Barretina, J., Caponigro, G., Stransky, N., Venkatesan, K., Margolin, A.A., Kim, S., Wilson, C.J., Lehár, J., Kryukov, G.V., Sonkin, D., et al. (2012). The Cancer Cell Line Encyclopedia enables predictive modelling of anticancer drug sensitivity. Nature *483*, 603–607.

Baynash, A.G., Hosoda, K., Giaid, A., Richardson, J.A., Emoto, N., Hammer, R.E., and Yanagisawa, M. (1994). Interaction of endothelin-3 with endothelin-B receptor is essential for development of epidermal melanocytes and enteric neurons. Cell *79*, 1277–1285.

van Bebber, F., Hruscha, A., Willem, M., Schmid, B., and Haass, C. (2013). Loss of Bace2 in zebrafish affects melanocyte migration and is distinct from Bace1 knock out phenotypes. J. Neurochem. *127*, 471–481.

Belfiore, A., Frasca, F., Pandini, G., Sciacca, L., and Vigneri, R. (2009). Insulin receptor isoforms and insulin receptor/insulin-like growth factor receptor hybrids in physiology and disease. Endocr. Rev. *30*, 586–623.

Belleudi, F., Cardinali, G., Kovacs, D., Picardo, M., and Torrisi, M.R. (2010). KGF Promotes Paracrine Activation of the SCF/c-KIT Axis from Human Keratinocytes to Melanoma Cells. Transl. Oncol. *3*, 80–90.

Bennett, B.D., Babu-Khan, S., Loeloff, R., Louis, J.C., Curran, E., Citron, M., and Vassar, R. (2000). Expression analysis of BACE2 in brain and peripheral tissues. J. Biol. Chem. *275*, 20647–20651.

Béréziat, V., Kasus-Jacobi, A., Perdereau, D., Cariou, B., Girard, J., and Burnol, A.-F. (2002). Inhibition of insulin receptor catalytic activity by the molecular adapter Grb14. J. Biol. Chem. *277*, 4845–4852.

Boissy, R.E. (2003). Melanosome transfer to and translocation in the keratinocyte. Exp. Dermatol. *12 Suppl 2*, 5–12.

Bondurand, N., Pingault, V., Goerich, D.E., Lemort, N., Sock, E., Le Caignec, C., Wegner, M., and Goossens, M. (2000). Interaction among SOX10, PAX3 and MITF, three genes altered in Waardenburg syndrome. Hum. Mol. Genet. *9*, 1907–1917.

Bravo, D.A., Gleason, J.B., Sanchez, R.I., Roth, R.A., and Fuller, R.S. (1994). Accurate and efficient cleavage of the human insulin proreceptor by the human proprotein-processing protease furin. Characterization and kinetic parameters using the purified, secreted soluble protease expressed by a

recombinant baculovirus. J. Biol. Chem. *269*, 25830–25837.

Brenner, S. (1974). The genetics of Caenorhabditis elegans. Genetics *77*, 71–94.

Brenner, M., and Hearing, V.J. (2008). Modifying skin pigmentation - approaches through intrinsic biochemistry and exogenous agents. Drug Discov. Today Dis. Mech. *5*, e189–e199.

Britsch, S., Goerich, D.E., Riethmacher, D., Peirano, R.I., Rossner, M., Nave, K.A., Birchmeier, C., and Wegner, M. (2001). The transcription factor Sox10 is a key regulator of peripheral glial development. Genes Dev. *15*, 66–78.

Brou, C., Logeat, F., Gupta, N., Bessia, C., LeBail, O., Doedens, J.R., Cumano, A., Roux, P., Black, R.A., and Israël, A. (2000). A novel proteolytic cleavage involved in Notch signaling: the role of the disintegrin-metalloprotease TACE. Mol. Cell *5*, 207–216.

de Bruijn, E., Cuppen, E., and Feitsma, H. (2009). Highly efficient ENU mutagenesis in zebrafish. Methods Mol. Biol. *546*, 3–12.

Brüning, J.C., Winnay, J., Bonner-Weir, S., Taylor, S.I., Accili, D., and Kahn, C.R. (1997). Development of a novel polygenic model of NIDDM in mice heterozygous for IR and IRS-1 null alleles. Cell *88*, 561–572.

Budi, E.H., Patterson, L.B., and Parichy, D.M. (2011). Post-embryonic nerve-associated precursors to adult pigment cells: genetic requirements and dynamics of morphogenesis and differentiation. PLoS Genet. *7*, e1002044.

Buffey, J.A., Messenger, A.G., Taylor, M., Ashcroft, A.T., Westgate, G.E., and MacNeil, S. (1994). Extracellular matrix derived from hair and skin fibroblasts stimulates human skin melanocyte tyrosinase activity. Br. J. Dermatol. *131*, 836–842.

Burgoyne, T., O'Connor, M.N., Seabra, M.C., Cutler, D.F., and Futter, C.E. (2015). Regulation of melanosome number, shape and movement in the zebrafish retinal pigment epithelium by OA1 and PMEL. J. Cell Sci. *128*, 1400–1407.

Cable, J., Jackson, I.J., and Steel, K.P. (1995). Mutations at the W locus affect survival of neural crest-derived melanocytes in the mouse. Mech. Dev. *50*, 139–150.

Cai, B., Thorp, E.B., Doran, A.C., Subramanian, M., Sansbury, B.E., Lin, C.-S., Spite, M., Fredman, G., and Tabas, I. (2016). MerTK cleavage limits proresolving mediator biosynthesis and exacerbates tissue inflammation. Proc Natl Acad Sci USA *113*, 6526–6531.

Cao, P.D., Cheung, W.K.C., and Nguyen, D.X. (2011). Cell lineage specification in tumor progression and metastasis. Discov. Med. *12*, 329–340.

Carreira, S., Goodall, J., Denat, L., Rodriguez, M., Nuciforo, P., Hoek, K.S., Testori, A., Larue, L., and Goding, C.R. (2006). Mitf regulation of Dia1 controls

melanoma proliferation and invasiveness. Genes Dev. *20*, 3426–3439.

Casas, S., Casini, P., Piquer, S., Altirriba, J., Soty, M., Cadavez, L., Gomis, R., and Novials, A. (2010). BACE2 plays a role in the insulin receptor trafficking in pancreatic ß-cells. Am. J. Physiol. Endocrinol. Metab. *299*, E1087-95.

Ceol, C.J., Houvras, Y., Jane-Valbuena, J., Bilodeau, S., Orlando, D.A., Battisti, V., Fritsch, L., Lin, W.M., Hollmann, T.J., Ferré, F., et al. (2011). The histone methyltransferase SETDB1 is recurrently amplified in melanoma and accelerates its onset. Nature *471*, 513–517.

Chakraborty, A.K., Orlow, S.J., Bolognia, J.L., and Pawelek, J.M. (1991). Structural/functional relationships between internal and external MSH receptors: modulation of expression in Cloudman melanoma cells by UVB radiation. J. Cell. Physiol. *147*, 1–6.

Cheung, W.K.C., and Nguyen, D.X. (2015). Lineage factors and differentiation states in lung cancer progression. Oncogene *34*, 5771–5780.

Chien, A.J., Moore, E.C., Lonsdorf, A.S., Kulikauskas, R.M., Rothberg, B.G., Berger, A.J., Major, M.B., Hwang, S.T., Rimm, D.L., and Moon, R.T. (2009). Activated Wnt/beta-catenin signaling in melanoma is associated with decreased proliferation in patient tumors and a murine melanoma model. Proc Natl Acad Sci USA *106*, 1193–1198.

Cooper, C.D., and Raible, D.W. (2009). Mechanisms for reaching the differentiated state: Insights from neural crest-derived melanocytes. Semin. Cell Dev. Biol. *20*, 105–110.

Costin, G.-E., and Hearing, V.J. (2007). Human skin pigmentation: melanocytes modulate skin color in response to stress. FASEB J. *21*, 976–994.

Cui, R., Widlund, H.R., Feige, E., Lin, J.Y., Wilensky, D.L., Igras, V.E., D'Orazio, J., Fung, C.Y., Schanbacher, C.F., Granter, S.R., et al. (2007). Central role of p53 in the suntan response and pathologic hyperpigmentation. Cell *128*, 853–864.

Curran, K., Raible, D.W., and Lister, J.A. (2009). Foxd3 controls melanophore specification in the zebrafish neural crest by regulation of Mitf. Dev. Biol. *332*, 408–417.

Dahlem, T.J., Hoshijima, K., Jurynec, M.J., Gunther, D., Starker, C.G., Locke, A.S., Weis, A.M., Voytas, D.F., and Grunwald, D.J. (2012). Simple methods for generating and detecting locus-specific mutations induced with TALENs in the zebrafish genome. PLoS Genet. *8*, e1002861.

Dankort, D., Curley, D.P., Cartlidge, R.A., Nelson, B., Karnezis, A.N., Damsky, W.E., You, M.J., DePinho, R.A., McMahon, M., and Bosenberg, M. (2009). Braf(V600E) cooperates with Pten loss to induce metastatic melanoma. Nat. Genet. *41*, 544–552.

Davis, R.H. (2004). The age of model organisms. Nat. Rev. Genet. *5*, 69–76.

De Mazière, A.M., Muehlethaler, K., van Donselaar, E., Salvi, S., Davoust, J., Cerottini, J.-C., Lévy, F., Slot, J.W., and Rimoldi, D. (2002). The melanocytic protein Melan-A/MART-1 has a subcellular localization distinct from typical melanosomal proteins. Traffic *3*, 678–693.

Deltour, L., Leduque, P., Blume, N., Madsen, O., Dubois, P., Jami, J., and Bucchini, D. (1993). Differential expression of the two nonallelic proinsulin genes in the developing mouse embryo. Proc Natl Acad Sci USA *90*, 527–531.

Di Como, C.J., and Arndt, K.T. (1996). Nutrients, via the Tor proteins, stimulate the association of Tap42 with type 2A phosphatases. Genes Dev. *10*, 1904–1916.

Di Guglielmo, G.M., Drake, P.G., Baass, P.C., Authier, F., Posner, B.I., and Bergeron, J.J. (1998). Insulin receptor internalization and signalling. Mol. Cell. Biochem. *182*, 59–63.

Diven, D.G., Gwinup, G., and Newton, R.C. (1989). The thyroid. Dermatol. Clin. *7*, 547–558.

Dooley, C.M., Schwarz, H., Mueller, K.P., Mongera, A., Konantz, M., Neuhauss, S.C.F., Nüsslein-Volhard, C., and Geisler, R. (2013). Slc45a2 and V-ATPase are regulators of melanosomal pH homeostasis in zebrafish, providing a mechanism for human pigment evolution and disease. Pigment Cell Melanoma Res. *26*, 205–217.

Driever, W., Solnica-Krezel, L., Schier, A.F., Neuhauss, S.C., Malicki, J., Stemple, D.L., Stainier, D.Y., Zwartkruis, F., Abdelilah, S., Rangini, Z., et al. (1996). A genetic screen for mutations affecting embryogenesis in zebrafish. Development *123*, 37–46.

Du, J., Miller, A.J., Widlund, H.R., Horstmann, M.A., Ramaswamy, S., and Fisher, D.E. (2003). MLANA/MART1 and SILV/PMEL17/GP100 are transcriptionally regulated by MITF in melanocytes and melanoma. Am. J. Pathol. *163*, 333–343.

Dutton, K.A., Pauliny, A., Lopes, S.S., Elworthy, S., Carney, T.J., Rauch, J., Geisler, R., Haffter, P., and Kelsh, R.N. (2001). Zebrafish colourless encodes sox10 and specifies non-ectomesenchymal neural crest fates. Development *128*, 4113–4125.

Duval, C., Cohen, C., Chagnoleau, C., Flouret, V., Bourreau, E., and Bernerd, F. (2014). Key regulatory role of dermal fibroblasts in pigmentation as demonstrated using a reconstructed skin model: impact of photo-aging. PLoS ONE *9*, e114182.

D'Alessandris, C., Andreozzi, F., Federici, M., Cardellini, M., Brunetti, A., Ranalli, M., Del Guerra, S., Lauro, D., Del Prato, S., Marchetti, P., et al. (2004). Increased O-glycosylation of insulin signaling proteins results in their impaired activation and enhanced susceptibility to apoptosis in pancreatic

beta-cells. FASEB J. *18*, 959–961.

Ebanks, J.P., Wickett, R.R., and Boissy, R.E. (2009). Mechanisms regulating skin pigmentation: the rise and fall of complexion coloration. Int. J. Mol. Sci. *10*, 4066–4087.

Edery, P., Attié, T., Amiel, J., Pelet, A., Eng, C., Hofstra, R.M., Martelli, H., Bidaud, C., Munnich, A., and Lyonnet, S. (1996). Mutation of the endothelin-3 gene in the Waardenburg-Hirschsprung disease (Shah-Waardenburg syndrome). Nat. Genet. *12*, 442–444.

Edmondson, S.R., Russo, V.C., McFarlane, A.C., Wraight, C.J., and Werther, G.A. (1999). Interactions between growth hormone, insulin-like growth factor I, and basic fibroblast growth factor in melanocyte growth. J. Clin. Endocrinol. Metab. *84*, 1638–1644.

Egger, M.E., Callender, G.G., McMasters, K.M., Ross, M.I., Martin, R.C.G., Edwards, M.J., Urist, M.M., Noyes, R.D., Sussman, J.J., Reintgen, D.S., et al. (2013). Diversity of stage III melanoma in the era of sentinel lymph node biopsy. Ann. Surg. Oncol. *20*, 956–963.

Eichhoff, O.M., Zipser, M.C., Xu, M., Weeraratna, A.T., Mihic, D., Dummer, R., and Hoek, K.S. (2010). The immunohistochemistry of invasive and proliferative phenotype switching in melanoma: a case report. Melanoma Res. *20*, 349–355.

Elworthy, S., Lister, J.A., Carney, T.J., Raible, D.W., and Kelsh, R.N. (2003). Transcriptional regulation of mitfa accounts for the sox10 requirement in zebrafish melanophore development. Development *130*, 2809–2818.

Engelman, J.A. (2009). Targeting PI3K signalling in cancer: opportunities, challenges and limitations. Nat. Rev. Cancer *9*, 550–562.

Eom, D.S., and Parichy, D.M. (2017). A macrophage relay for long-distance signaling during postembryonic tissue remodeling. Science *355*, 1317–1320.

Eom, D.S., Inoue, S., Patterson, L.B., Gordon, T.N., Slingwine, R., Kondo, S., Watanabe, M., and Parichy, D.M. (2012). Melanophore migration and survival during zebrafish adult pigment stripe development require the immunoglobulin superfamily adhesion molecule Igsf11. PLoS Genet. *8*, e1002899.

Eom, D.S., Bain, E.J., Patterson, L.B., Grout, M.E., and Parichy, D.M. (2015). Long-distance communication by specialized cellular projections during pigment pattern development and evolution. Elife *4*.

Ernfors, P. (2010). Cellular origin and developmental mechanisms during the formation of skin melanocytes. Exp. Cell Res. *316*, 1397–1407.

Eskova, A., Chauvigné, F., Maischein, H.-M., Ammelburg, M., Cerdà, J., Nüsslein-Volhard, C., and Irion, U. (2017). Gain-of-function mutations in Aqp3a influence zebrafish pigment pattern formation through the tissue environment. Development *144*, 2059–2069.

Esterházy, D., Stützer, I., Wang, H., Rechsteiner, M.P., Beauchamp, J., Döbeli, H., Hilpert, H., Matile, H., Prummer, M., Schmidt, A., et al. (2011). Bace2 is a β cell-enriched protease that regulates pancreatic β cell function and mass. Cell Metab. *14*, 365–377.

Fellmann, C., Hoffmann, T., Sridhar, V., Hopfgartner, B., Muhar, M., Roth, M., Lai, D.Y., Barbosa, I.A.M., Kwon, J.S., Guan, Y., et al. (2013). An optimized microRNA backbone for effective single-copy RNAi. Cell Rep. *5*, 1704–1713.

Fluhrer, R., Capell, A., Westmeyer, G., Willem, M., Hartung, B., Condron, M.M., Teplow, D.B., Haass, C., and Walter, J. (2002). A non-amyloidogenic function of BACE-2 in the secretory pathway. J. Neurochem. *81*, 1011–1020.

Foley, J.E., Maeder, M.L., Pearlberg, J., Joung, J.K., Peterson, R.T., and Yeh, J.-R.J. (2009). Targeted mutagenesis in zebrafish using customized zinc-finger nucleases. Nat. Protoc. *4*, 1855–1867.

Friedman, R.M. (2008). Clinical uses of interferons. Br. J. Clin. Pharmacol. *65*, 158–162.

Frohnhöfer, H.G., Krauss, J., Maischein, H.-M., and Nüsslein-Volhard, C. (2013). Iridophores and their interactions with other chromatophores are required for stripe formation in zebrafish. Development *140*, 2997–3007.

Fu, Z., Gilbert, E.R., and Liu, D. (2013). Regulation of insulin synthesis and secretion and pancreatic Beta-cell dysfunction in diabetes. Curr. Diabetes Rev. *9*, 25–53.

Furuya, R., Akiu, S., Ideta, R., Naganuma, M., Fukuda, M., and Hirobe, T. (2002). Changes in the proliferative activity of epidermal melanocytes in serum-free primary culture during the development of ultraviolet radiation B-induced pigmented spots in hairless mice. Pigment Cell Res. *15*, 348–356.

Gagnon, J.A., Valen, E., Thyme, S.B., Huang, P., Akhmetova, L., Pauli, A., Montague, T.G., Zimmerman, S., Richter, C., and Schier, A.F. (2014). Efficient mutagenesis by Cas9 protein-mediated oligonucleotide insertion and large-scale assessment of single-guide RNAs. PLoS ONE *9*, e98186.

Gao, J., Aksoy, B.A., Dogrusoz, U., Dresdner, G., Gross, B., Sumer, S.O., Sun, Y., Jacobsen, A., Sinha, R., Larsson, E., et al. (2013). Integrative analysis of complex cancer genomics and clinical profiles using the cBioPortal. Sci. Signal. *6*, pl1.

Garcia, R.J., Ittah, A., Mirabal, S., Figueroa, J., Lopez, L., Glick, A.B., and Kos, L. (2008). Endothelin 3 induces skin pigmentation in a keratin-driven inducible mouse model. J. Invest. Dermatol. *128*, 131–142.

Garofalo, R.S., and Rosen, O.M. (1988). Tissue localization of Drosophila melanogaster insulin receptor transcripts during development. Mol. Cell. Biol. *8*, 1638–1647.

Garraway, L.A., and Sellers, W.R. (2006). Lineage dependency and lineage-

survival oncogenes in human cancer. Nat. Rev. Cancer *6*, 593–602.

Garraway, L.A., Widlund, H.R., Rubin, M.A., Getz, G., Berger, A.J., Ramaswamy, S., Beroukhim, R., Milner, D.A., Granter, S.R., Du, J., et al. (2005). Integrative genomic analyses identify MITF as a lineage survival oncogene amplified in malignant melanoma. Nature *436*, 117–122.

Geissler, E.N., Ryan, M.A., and Housman, D.E. (1988). The dominant-white spotting (W) locus of the mouse encodes the c-kit proto-oncogene. Cell *55*, 185–192.

Goding, C.R. (2007). Melanocytes: the new black. Int. J. Biochem. Cell Biol. *39*, 275–279.

Goding, C.R. (2011). Commentary. A picture of Mitf in melanoma immortality. Oncogene *30*, 2304–2306.

Gray, S.M., Meijer, R.I., and Barrett, E.J. (2014). Insulin regulates brain function, but how does it get there? Diabetes *63*, 3992–3997.

Gray-Schopfer, V., Wellbrock, C., and Marais, R. (2007). Melanoma biology and new targeted therapy. Nature *445*, 851–857.

Grichnik, J.M., Burch, J.A., Burchette, J., and Shea, C.R. (1998). The SCF/KIT pathway plays a critical role in the control of normal human melanocyte homeostasis. J. Invest. Dermatol. *111*, 233–238.

Grunwald, D.J., and Eisen, J.S. (2002). Headwaters of the zebrafish -- emergence of a new model vertebrate. Nat. Rev. Genet. *3*, 717–724.

Guillot, R., Muriach, B., Rocha, A., Rotllant, J., Kelsh, R.N., and Cerdá-Reverter, J.M. (2016). Thyroid Hormones Regulate Zebrafish Melanogenesis in a Gender-Specific Manner. PLoS ONE *11*, e0166152.

Haeusler, R.A., McGraw, T.E., and Accili, D. (2018). Biochemical and cellular properties of insulin receptor signalling. Nat. Rev. Mol. Cell Biol. *19*, 31–44.

Haffter, P., Granato, M., Brand, M., Mullins, M.C., Hammerschmidt, M., Kane, D.A., Odenthal, J., van Eeden, F.J., Jiang, Y.J., Heisenberg, C.P., et al. (1996). The identification of genes with unique and essential functions in the development of the zebrafish, Danio rerio. Development *123*, 1–36.

Hamada, H., Watanabe, M., Lau, H.E., Nishida, T., Hasegawa, T., Parichy, D.M., and Kondo, S. (2014). Involvement of Delta/Notch signaling in zebrafish adult pigment stripe patterning. Development *141*, 318–324.

Hara, M., Yaar, M., and Gilchrest, B.A. (1995). Endothelin-1 of keratinocyte origin is a mediator of melanocyte dendricity. J. Invest. Dermatol. *105*, 744–748.

Harris, M.L., Baxter, L.L., Loftus, S.K., and Pavan, W.J. (2010). Sox proteins in melanocyte development and melanoma. Pigment Cell Melanoma Res. *23*, 496–513.

Harrison, K.A., Thaler, J., Pfaff, S.L., Gu, H., and Kehrl, J.H. (1999). Pancreas dorsal lobe agenesis and abnormal islets of Langerhans in Hlxb9-deficient mice. Nat. Genet. *23*, 71–75.

Havrankova, J., Schmechel, D., Roth, J., and Brownstein, M. (1978). Identification of insulin in rat brain. Proc Natl Acad Sci USA *75*, 5737–5741.

Havrankova, J., Roth, J., and Brownstein, M.J. (1979). Concentrations of insulin and insulin receptors in the brain are independent of peripheral insulin levels. Studies of obese and streptozotocin-treated rodents. J. Clin. Invest. *64*, 636–642.

Heilmann, S., Ratnakumar, K., Langdon, E., Kansler, E., Kim, I., Campbell, N.R., Perry, E., McMahon, A., Kaufman, C., van Rooijen, E., et al. (2015). A quantitative system for studying metastasis using transparent zebrafish. Cancer Res. *75*, 4272–4282.

Hellström, A.R., Watt, B., Fard, S.S., Tenza, D., Mannström, P., Narfström, K., Ekesten, B., Ito, S., Wakamatsu, K., Larsson, J., et al. (2011). Inactivation of Pmel alters melanosome shape but has only a subtle effect on visible pigmentation. PLoS Genet. *7*, e1002285.

Hemming, R., Agatep, R., Badiani, K., Wyant, K., Arthur, G., Gietz, R.D., and Triggs-Raine, B. (2001). Human growth factor receptor bound 14 binds the activated insulin receptor and alters the insulin-stimulated tyrosine phosphorylation levels of multiple proteins. Biochem. Cell Biol. *79*, 21–32.

Hentges, K., Thompson, K., and Peterson, A. (1999). The flat-top gene is required for the expansion and regionalization of the telencephalic primordium. Development *126*, 1601–1609.

Hentges, K.E., Sirry, B., Gingeras, A.C., Sarbassov, D., Sonenberg, N., Sabatini, D., and Peterson, A.S. (2001). FRAP/mTOR is required for proliferation and patterning during embryonic development in the mouse. Proc Natl Acad Sci USA *98*, 13796–13801.

Hermanns-Lê, T., Scheen, A., and Piérard, G.E. (2004). Acanthosis nigricans associated with insulin resistance : pathophysiology and management. Am. J. Clin. Dermatol. *5*, 199–203.

Hirai, Y., Nose, A., Kobayashi, S., and Takeichi, M. (1989). Expression and role of E- and P-cadherin adhesion molecules in embryonic histogenesis. I. Lung epithelial morphogenesis. Development *105*, 263–270.

Hirobe, T. (1978). Stimulation of dendritogenesis in the epidermal melanocytes of newborn mice by melanocyte-stimulating hormone. J. Cell Sci. *33*, 371–383.

Hirobe, T. (2011). How are proliferation and differentiation of melanocytes regulated? Pigment Cell Melanoma Res. *24*, 462–478.

Hoashi, T., Watabe, H., Muller, J., Yamaguchi, Y., Vieira, W.D., and Hearing, V.J. (2005). MART-1 is required for the function of the melanosomal matrix

protein PMEL17/GP100 and the maturation of melanosomes. J. Biol. Chem. *280*, 14006–14016.

Hoek, K.S., and Goding, C.R. (2010). Cancer stem cells versus phenotype-switching in melanoma. Pigment Cell Melanoma Res. *23*, 746–759.

Hoek, K.S., Eichhoff, O.M., Schlegel, N.C., Döbbeling, U., Kobert, N., Schaerer, L., Hemmi, S., and Dummer, R. (2008). In vivo switching of human melanoma cells between proliferative and invasive states. Cancer Res. *68*, 650–656.

Hornyak, T.J., Hayes, D.J., Chiu, L.Y., and Ziff, E.B. (2001). Transcription factors in melanocyte development: distinct roles for Pax-3 and Mitf. Mech. Dev. *101*, 47–59.

Hosoda, K., Hammer, R.E., Richardson, J.A., Baynash, A.G., Cheung, J.C., Giaid, A., and Yanagisawa, M. (1994). Targeted and natural (piebald-lethal) mutations of endothelin-B receptor gene produce megacolon associated with spotted coat color in mice. Cell *79*, 1267–1276.

Hou, L., and Pavan, W.J. (2008). Transcriptional and signaling regulation in neural crest stem cell-derived melanocyte development: do all roads lead to Mitf? Cell Res. *18*, 1163–1176.

Hou, J.C., Min, L., and Pessin, J.E. (2009). Insulin granule biogenesis, trafficking and exocytosis. Vitam. Horm. *80*, 473–506.

Houghton, A.N., Eisinger, M., Albino, A.P., Cairncross, J.G., and Old, L.J. (1982). Surface antigens of melanocytes and melanomas. Markers of melanocyte differentiation and melanoma subsets. J. Exp. Med. *156*, 1755–1766.

Houghton, A.N., Real, F.X., Davis, L.J., Cordon-Cardo, C., and Old, L.J. (1987). Phenotypic heterogeneity of melanoma. Relation to the differentiation program of melanoma cells. J. Exp. Med. *165*, 812–829.

Hsiao, J.J., and Fisher, D.E. (2014). The roles of microphthalmia-associated transcription factor and pigmentation in melanoma. Arch. Biochem. Biophys. *563*, 28–34.

Hultman, K.A., and Johnson, S.L. (2010). Differential contribution of direct-developing and stem cell-derived melanocytes to the zebrafish larval pigment pattern. Dev. Biol. *337*, 425–431.

Hultman, K.A., Budi, E.H., Teasley, D.C., Gottlieb, A.Y., Parichy, D.M., and Johnson, S.L. (2009). Defects in ErbB-dependent establishment of adult melanocyte stem cells reveal independent origins for embryonic and regeneration melanocytes. PLoS Genet. *5*, e1000544.

Hussain, I., Powell, D.J., Howlett, D.R., Chapman, G.A., Gilmour, L., Murdock, P.R., Tew, D.G., Meek, T.D., Chapman, C., Schneider, K., et al. (2000). ASP1 (BACE2) cleaves the amyloid precursor protein at the beta-secretase site. Mol.

Cell. Neurosci. *16*, 609–619.

Hussain, I., Christie, G., Schneider, K., Moore, S., and Dingwall, C. (2001). Prodomain processing of Asp1 (BACE2) is autocatalytic. J. Biol. Chem. *276*, 23322–23328.

Ignatius, M.S., Moose, H.E., El-Hodiri, H.M., and Henion, P.D. (2008). colgate/hdac1 Repression of foxd3 expression is required to permit mitfa-dependent melanogenesis. Dev. Biol. *313*, 568–583.

Imokawa, G. (2004). Autocrine and paracrine regulation of melanocytes in human skin and in pigmentary disorders. Pigment Cell Res. *17*, 96–110.

Imokawa, G., Yada, Y., and Miyagishi, M. (1992). Endothelins secreted from human keratinocytes are intrinsic mitogens for human melanocytes. J. Biol. Chem. *267*, 24675–24680.

Irion, U., Krauss, J., and Nüsslein-Volhard, C. (2014). Precise and efficient genome editing in zebrafish using the CRISPR/Cas9 system. Development *141*, 4827–4830.

Iyengar, S., Kasheta, M., and Ceol, C.J. (2015). Poised Regeneration of Zebrafish Melanocytes Involves Direct Differentiation and Concurrent Replenishment of Tissue-Resident Progenitor Cells. Dev. Cell *33*, 631–643.

Jacinto, E., Loewith, R., Schmidt, A., Lin, S., Rüegg, M.A., Hall, A., and Hall, M.N. (2004). Mammalian TOR complex 2 controls the actin cytoskeleton and is rapamycin insensitive. Nat. Cell Biol. *6*, 1122–1128.

Jaworski, J., Spangler, S., Seeburg, D.P., Hoogenraad, C.C., and Sheng, M. (2005). Control of dendritic arborization by the phosphoinositide-3'-kinase-Akt-mammalian target of rapamycin pathway. J. Neurosci. *25*, 11300–11312.

Jian, Q., An, Q., Zhu, D., Hui, K., Liu, Y., Chi, S., and Li, C. (2014). MicroRNA 340 is involved in UVB-induced dendrite formation through the regulation of RhoA expression in melanocytes. Mol. Cell. Biol. *34*, 3407–3420.

Jiang, H., Guo, W., Liang, X., and Rao, Y. (2005). Both the establishment and the maintenance of neuronal polarity require active mechanisms: critical roles of GSK-3beta and its upstream regulators. Cell *120*, 123–135.

Jordan, S.A., and Jackson, I.J. (2000). A late wave of melanoblast differentiation and rostrocaudal migration revealed in patch and rump-white embryos. Mech. Dev. *92*, 135–143.

Junker, J.P., Noël, E.S., Guryev, V., Peterson, K.A., Shah, G., Huisken, J., McMahon, A.P., Berezikov, E., Bakkers, J., and van Oudenaarden, A. (2014). Genome-wide RNA Tomography in the zebrafish embryo. Cell *159*, 662–675.

Kadekaro, A.L., Kavanagh, R.J., Wakamatsu, K., Ito, S., Pipitone, M.A., and Abdel-Malek, Z.A. (2003). Cutaneous photobiology. The melanocyte vs. the sun: who will win the final round? Pigment Cell Res. *16*, 434–447.

Kasuga, K., Kaneko, H., Nishizawa, M., Onodera, O., and Ikeuchi, T. (2007). Generation of intracellular domain of insulin receptor tyrosine kinase by gamma-secretase. Biochem. Biophys. Res. Commun. *360*, 90–96.

Kasus-Jacobi, A., Perdereau, D., Auzan, C., Clauser, E., Van Obberghen, E., Mauvais-Jarvis, F., Girard, J., and Burnol, A.F. (1998). Identification of the rat adapter Grb14 as an inhibitor of insulin actions. J. Biol. Chem. *273*, 26026–26035.

Kaufman, C.K., White, R.M., and Zon, L. (2009). Chemical genetic screening in the zebrafish embryo. Nat. Protoc. *4*, 1422–1432.

Kaufman, C.K., Mosimann, C., Fan, Z.P., Yang, S., Thomas, A.J., Ablain, J., Tan, J.L., Fogley, R.D., van Rooijen, E., Hagedorn, E.J., et al. (2016). A zebrafish melanoma model reveals emergence of neural crest identity during melanoma initiation. Science *351*, aad2197.

Kawaguchi, M., Hozumi, Y., and Suzuki, T. (2015). ADAM protease inhibitors reduce melanogenesis by regulating PMEL17 processing in human melanocytes. J. Dermatol. Sci. *78*, 133–142.

Kelsh, R.N., Brand, M., Jiang, Y.J., Heisenberg, C.P., Lin, S., Haffter, P., Odenthal, J., Mullins, M.C., van Eeden, F.J., Furutani-Seiki, M., et al. (1996). Zebrafish pigmentation mutations and the processes of neural crest development. Development *123*, 369–389.

Kelsh, R.N., Schmid, B., and Eisen, J.S. (2000). Genetic analysis of melanophore development in zebrafish embryos. Dev. Biol. *225*, 277–293.

Kelsh, R.N., Harris, M.L., Colanesi, S., and Erickson, C.A. (2009). Stripes and belly-spots -- a review of pigment cell morphogenesis in vertebrates. Semin. Cell Dev. Biol. *20*, 90–104.

Kettleborough, R.N.W., Busch-Nentwich, E.M., Harvey, S.A., Dooley, C.M., de Bruijn, E., van Eeden, F., Sealy, I., White, R.J., Herd, C., Nijman, I.J., et al. (2013). A systematic genome-wide analysis of zebrafish protein-coding gene function. Nature *496*, 494–497.

Kim, I.S., Heilmann, S., Kansler, E.R., Zhang, Y., Zimmer, M., Ratnakumar, K., Bowman, R.L., Simon-Vermot, T., Fennell, M., Garippa, R., et al. (2017). Microenvironment-derived factors driving metastatic plasticity in melanoma. Nat. Commun. *8*, 14343.

Kim, Y.-T., Downs, D., Wu, S., Dashti, A., Pan, Y., Zhai, P., Wang, X., Zhang, X.C., and Lin, X. (2002). Enzymic properties of recombinant BACE2. Eur. J. Biochem. *269*, 5668–5677.

Kimmel, R.A., Onder, L., Wilfinger, A., Ellertsdottir, E., and Meyer, D. (2011). Requirement for Pdx1 in specification of latent endocrine progenitors in zebrafish. BMC Biol. *9*, 75.

Kimmel, R.A., Dobler, S., Schmitner, N., Walsen, T., Freudenblum, J., and

Meyer, D. (2015). Diabetic pdx1-mutant zebrafish show conserved responses to nutrient overload and anti-glycemic treatment. Sci. Rep. *5*, 14241.

Kippenberger, S., Bernd, A., Bereiter-Hahn, J., Ramirez-Bosca, A., and Kaufmann, R. (1998). The mechanism of melanocyte dendrite formation: the impact of differentiating keratinocytes. Pigment Cell Res. *11*, 34–37.

Knutson, V.P. (1991). Proteolytic processing of the insulin receptor beta subunit is associated with insulin-induced receptor down-regulation. J. Biol. Chem. *266*, 15656–15662.

Konieczkowski, D.J., Johannessen, C.M., Abudayyeh, O., Kim, J.W., Cooper, Z.A., Piris, A., Frederick, D.T., Barzily-Rokni, M., Straussman, R., Haq, R., et al. (2014). A melanoma cell state distinction influences sensitivity to MAPK pathway inhibitors. Cancer Discov. *4*, 816–827.

Kopitz, C., Gerg, M., Bandapalli, O.R., Ister, D., Pennington, C.J., Hauser, S., Flechsig, C., Krell, H.-W., Antolovic, D., Brew, K., et al. (2007). Tissue inhibitor of metalloproteinases-1 promotes liver metastasis by induction of hepatocyte growth factor signaling. Cancer Res. *67*, 8615–8623.

Kos, R., Reedy, M.V., Johnson, R.L., and Erickson, C.A. (2001). The winged-helix transcription factor FoxD3 is important for establishing the neural crest lineage and repressing melanogenesis in avian embryos. Development *128*, 1467–1479.

Koster, M.I., and Roop, D.R. (2007). Mechanisms regulating epithelial stratification. Annu. Rev. Cell Dev. Biol. *23*, 93–113.

Krauss, J., Frohnhöfer, H.G., Walderich, B., Maischein, H.-M., Weiler, C., Irion, U., and Nüsslein-Volhard, C. (2014). Endothelin signalling in iridophore development and stripe pattern formation of zebrafish. Biol. Open *3*, 503–509.

Kumar, V., Zhang, M.-X., Swank, M.W., Kunz, J., and Wu, G.-Y. (2005). Regulation of dendritic morphogenesis by Ras-PI3K-Akt-mTOR and Ras-MAPK signaling pathways. J. Neurosci. *25*, 11288–11299.

Labun, K., Montague, T.G., Gagnon, J.A., Thyme, S.B., and Valen, E. (2016). CHOPCHOP v2: a web tool for the next generation of CRISPR genome engineering. Nucleic Acids Res. *44*, W272-6.

Lamason, R.L., Mohideen, M.-A.P.K., Mest, J.R., Wong, A.C., Norton, H.L., Aros, M.C., Jurynec, M.J., Mao, X., Humphreville, V.R., Humbert, J.E., et al. (2005). SLC24A5, a putative cation exchanger, affects pigmentation in zebrafish and humans. Science *310*, 1782–1786.

Laplante, M., and Sabatini, D.M. (2009). mTOR signaling at a glance. J. Cell Sci. *122*, 3589–3594.

Laplante, M., and Sabatini, D.M. (2012). mTOR signaling in growth control and disease. Cell *149*, 274–293.

Lee, M., Goodall, J., Verastegui, C., Ballotti, R., and Goding, C.R. (2000).

Direct regulation of the Microphthalmia promoter by Sox10 links Waardenburg-Shah syndrome (WS4)-associated hypopigmentation and deafness to WS2. J. Biol. Chem. *275*, 37978–37983.

Lee, S.B., Schramme, A., Doberstein, K., Dummer, R., Abdel-Bakky, M.S., Keller, S., Altevogt, P., Oh, S.T., Reichrath, J., Oxmann, D., et al. (2010a). ADAM10 is upregulated in melanoma metastasis compared with primary melanoma. J. Invest. Dermatol. *130*, 763–773.

Lee, Y., Nachtrab, G., Klinsawat, P.W., Hami, D., and Poss, K.D. (2010b). Ras controls melanocyte expansion during zebrafish fin stripe regeneration. Dis. Model. Mech. *3*, 496–503.

Leemhuis, J., Boutillier, S., Barth, H., Feuerstein, T.J., Brock, C., Nürnberg, B., Aktories, K., and Meyer, D.K. (2004). Rho GTPases and phosphoinositide 3-kinase organize formation of branched dendrites. J. Biol. Chem. *279*, 585–596.

Lévesque, M., Feng, Y., Jones, R.A., and Martin, P. (2013). Inflammation drives wound hyperpigmentation in zebrafish by recruiting pigment cells to sites of tissue damage. Dis. Model. Mech. *6*, 508–515.

Levy, C., Khaled, M., and Fisher, D.E. (2006). MITF: master regulator of melanocyte development and melanoma oncogene. Trends Mol. Med. *12*, 406–414.

Li, P., Lahvic, J.L., Binder, V., Pugach, E.K., Riley, E.B., Tamplin, O.J., Panigrahy, D., Bowman, T.V., Barrett, F.G., Heffner, G.C., et al. (2015). Epoxyeicosatrienoic acids enhance embryonic haematopoiesis and adult marrow engraftment. Nature *523*, 468–471.

Lin, J.Y., and Fisher, D.E. (2007). Melanocyte biology and skin pigmentation. Nature *445*, 843–850.

Lister, J.A., Robertson, C.P., Lepage, T., Johnson, S.L., and Raible, D.W. (1999). nacre encodes a zebrafish microphthalmia-related protein that regulates neural-crest-derived pigment cell fate. Development *126*, 3757–3767.

Liu, L., Luo, Y., Chen, L., Shen, T., Xu, B., Chen, W., Zhou, H., Han, X., and Huang, S. (2010). Rapamycin inhibits cytoskeleton reorganization and cell motility by suppressing RhoA expression and activity. J. Biol. Chem. *285*, 38362–38373.

Lizcano, J.M., and Alessi, D.R. (2002). The insulin signalling pathway. Curr. Biol. *12*, R236-8.

Logan, D.W., Burn, S.F., and Jackson, I.J. (2006). Regulation of pigmentation in zebrafish melanophores. Pigment Cell Res. *19*, 206–213.

Lopez Lopez, C., Caputo, A., Liu, F., Riviere, M.E., Rouzade-Dominguez, M.L., Thomas, R.G., Langbaum, J.B., Lenz, R., Reiman, E.M., Graf, A., et al.

(2017). The alzheimer's prevention initiative generation program: evaluating CNP520 efficacy in the prevention of alzheimer's disease. J Prev Alzheimers Dis *4*, 242–246.

Lowings, P., Yavuzer, U., and Goding, C.R. (1992). Positive and negative elements regulate a melanocyte-specific promoter. Mol. Cell. Biol. *12*, 3653–3662.

Luetteke, N.C., Qiu, T.H., Peiffer, R.L., Oliver, P., Smithies, O., and Lee, D.C. (1993). TGF alpha deficiency results in hair follicle and eye abnormalities in targeted and waved-1 mice. Cell *73*, 263–278.

Luo, J., Becnel, J., Nichols, C.D., and Nässel, D.R. (2012). Insulin-producing cells in the brain of adult Drosophila are regulated by the serotonin 5-HT1A receptor. Cell. Mol. Life Sci. *69*, 471–484.

Luo, R., An, M., Arduini, B.L., and Henion, P.D. (2001). Specific pan-neural crest expression of zebrafish Crestin throughout embryonic development. Dev. Dyn. *220*, 169–174.

MacDonald, P.E., Joseph, J.W., and Rorsman, P. (2005). Glucose-sensing mechanisms in pancreatic beta-cells. Philos Trans R Soc Lond, B, Biol Sci *360*, 2211–2225.

Mackenzie, M.A., Jordan, S.A., Budd, P.S., and Jackson, I.J. (1997). Activation of the receptor tyrosine kinase Kit is required for the proliferation of melanoblasts in the mouse embryo. Dev. Biol. *192*, 99–107.

Maddux, B.A., and Goldfine, I.D. (2000). Membrane glycoprotein PC-1 inhibition of insulin receptor function occurs via direct interaction with the receptor alpha-subunit. Diabetes *49*, 13–19.

Mahalwar, P., Singh, A.P., Fadeev, A., Nüsslein-Volhard, C., and Irion, U. (2016). Heterotypic interactions regulate cell shape and density during color pattern formation in zebrafish. Biol. Open *5*, 1680–1690.

Makky, K., Tekiela, J., and Mayer, A.N. (2007). Target of rapamycin (TOR) signaling controls epithelial morphogenesis in the vertebrate intestine. Dev. Biol. *303*, 501–513.

Mandal, M., Wu, Y., Misiaszek, J., Li, G., Buevich, A., Caldwell, J.P., Liu, X., Mazzola, R.D., Orth, P., Strickland, C., et al. (2016). Structure-Based Design of an Iminoheterocyclic β-Site Amyloid Precursor Protein Cleaving Enzyme (BACE) Inhibitor that Lowers Central Aβ in Nonhuman Primates. J. Med. Chem. *59*, 3231–3248.

Markus, A., Zhong, J., and Snider, W.D. (2002). Raf and akt mediate distinct aspects of sensory axon growth. Neuron *35*, 65–76.

Massague, J., Pilch, P.F., and Czech, M.P. (1981). A unique proteolytic cleavage site on the beta subunit of the insulin receptor. J. Biol. Chem. *256*, 3182–3190.

McArthur, G.A. (2014). Adjuvant interferon in melanoma: is duration of therapy important? J. Clin. Oncol. *32*, 171–173.

McGlinchey, R.P., Shewmaker, F., McPhie, P., Monterroso, B., Thurber, K., and Wickner, R.B. (2009). The repeat domain of the melanosome fibril protein Pmel17 forms the amyloid core promoting melanin synthesis. Proc Natl Acad Sci USA *106*, 13731–13736.

McMenamin, S.K., Bain, E.J., McCann, A.E., Patterson, L.B., Eom, D.S., Waller, Z.P., Hamill, J.C., Kuhlman, J.A., Eisen, J.S., and Parichy, D.M. (2014). Thyroid hormone-dependent adult pigment cell lineage and pattern in zebrafish. Science *345*, 1358–1361.

Mehran, A.E., Templeman, N.M., Brigidi, G.S., Lim, G.E., Chu, K.-Y., Hu, X., Botezelli, J.D., Asadi, A., Hoffman, B.G., Kieffer, T.J., et al. (2012). Hyperinsulinemia drives diet-induced obesity independently of brain insulin production. Cell Metab. *16*, 723–737.

Mellgren, E.M., and Johnson, S.L. (2004). A requirement for kit in embryonic zebrafish melanocyte differentiation is revealed by melanoblast delay. Dev. Genes Evol. *214*, 493–502.

Miller, M.A., Meyer, A.S., Beste, M.T., Lasisi, Z., Reddy, S., Jeng, K.W., Chen, C.-H., Han, J., Isaacson, K., Griffith, L.G., et al. (2013). ADAM-10 and -17 regulate endometriotic cell migration via concerted ligand and receptor shedding feedback on kinase signaling. Proc Natl Acad Sci USA *110*, E2074-83.

Miller, M.A., Oudin, M.J., Sullivan, R.J., Wang, S.J., Meyer, A.S., Im, H., Frederick, D.T., Tadros, J., Griffith, L.G., Lee, H., et al. (2016). Reduced Proteolytic Shedding of Receptor Tyrosine Kinases Is a Post-Translational Mechanism of Kinase Inhibitor Resistance. Cancer Discov. *6*, 382–399.

Mohamed, A., Gonzalez, R.S., Lawson, D., Wang, J., and Cohen, C. (2013). SOX10 expression in malignant melanoma, carcinoma, and normal tissues. Appl. Immunohistochem. Mol. Morphol. *21*, 506–510.

Molnár, G., Faragó, N., Kocsis, Á.K., Rózsa, M., Lovas, S., Boldog, E., Báldi, R., Csajbók, É., Gardi, J., Puskás, L.G., et al. (2014). GABAergic neurogliaform cells represent local sources of insulin in the cerebral cortex. J. Neurosci. *34*, 1133–1137.

Montagne, J., Stewart, M.J., Stocker, H., Hafen, E., Kozma, S.C., and Thomas, G. (1999). Drosophila S6 kinase: a regulator of cell size. Science *285*, 2126–2129.

Mort, R.L., Jackson, I.J., and Patton, E.E. (2015). The melanocyte lineage in development and disease. Development *142*, 1387.

Morvan, D., Steyaert, J.M., Schwartz, L., Israel, M., and Demidem, A. (2012). Normal human melanocytes exposed to chronic insulin and glucose supplementation undergo oncogenic changes and methyl group metabolism

cellular redistribution. Am. J. Physiol. Endocrinol. Metab. *302*, E1407-18.

Mountjoy, K.G., Robbins, L.S., Mortrud, M.T., and Cone, R.D. (1992). The cloning of a family of genes that encode the melanocortin receptors. Science *257*, 1248–1251.

Müller, E.J., Galichet, A., Wiener, D., Marti, E., Drögemüller, C., Welle, M., Roosje, P., Leeb, T., and Suter, M.M. (2014). Keratinocyte biology and pathology. Vet. Dermatol. *25*, 236–238.

Nagarajan, A., Petersen, M.C., Nasiri, A.R., Butrico, G., Fung, A., Ruan, H.-B., Kursawe, R., Caprio, S., Thibodeau, J., Bourgeois-Daigneault, M.-C., et al. (2016). MARCH1 regulates insulin sensitivity by controlling cell surface insulin receptor levels. Nat. Commun. *7*, 12639.

Nakamasu, A., Takahashi, G., Kanbe, A., and Kondo, S. (2009). Interactions between zebrafish pigment cells responsible for the generation of Turing patterns. Proc Natl Acad Sci USA *106*, 8429–8434.

Nakayama, A., Nguyen, M.T., Chen, C.C., Opdecamp, K., Hodgkinson, C.A., and Arnheiter, H. (1998). Mutations in microphthalmia, the mouse homolog of the human deafness gene MITF, affect neuroepithelial and neural crest-derived melanocytes differently. Mech. Dev. *70*, 155–166.

Napolitano, G., and Ballabio, A. (2016). TFEB at a glance. J. Cell Sci. *129*, 2475–2481.

Natale, C.A., Duperret, E.K., Zhang, J., Sadeghi, R., Dahal, A., O'Brien, K.T., Cookson, R., Winkler, J.D., and Ridky, T.W. (2016). Sex steroids regulate skin pigmentation through nonclassical membrane-bound receptors. Elife *5*.

Newton, J.M., Cohen-Barak, O., Hagiwara, N., Gardner, J.M., Davisson, M.T., King, R.A., and Brilliant, M.H. (2001). Mutations in the human orthologue of the mouse underwhite gene (uw) underlie a new form of oculocutaneous albinism, OCA4. Am. J. Hum. Genet. *69*, 981–988.

Nishikawa, S., Kusakabe, M., Yoshinaga, K., Ogawa, M., Hayashi, S., Kunisada, T., Era, T., Sakakura, T., and Nishikawa, S. (1991). In utero manipulation of coat color formation by a monoclonal anti-c-kit antibody: two distinct waves of c-kit-dependency during melanocyte development. EMBO J. *10*, 2111–2118.

Nishimura, E.K., Jordan, S.A., Oshima, H., Yoshida, H., Osawa, M., Moriyama, M., Jackson, I.J., Barrandon, Y., Miyachi, Y., and Nishikawa, S.-I. (2002). Dominant role of the niche in melanocyte stem-cell fate determination. Nature *416*, 854–860.

Nishimura, E.K., Granter, S.R., and Fisher, D.E. (2005). Mechanisms of hair graying: incomplete melanocyte stem cell maintenance in the niche. Science *307*, 720–724.

Nüsslein-Volhard, C., and Wieschaus, E. (1980). Mutations affecting segment

number and polarity in Drosophila. Nature *287*, 795–801.

Odenthal, J., and Nüsslein-Volhard, C. (1998). fork head domain genes in zebrafish. Dev. Genes Evol. *208*, 245–258.

Oetting, W.S., and King, R.A. (1999). Molecular basis of albinism: mutations and polymorphisms of pigmentation genes associated with albinism. Hum. Mutat. *13*, 99–115.

Okabayashi, Y., Maddux, B.A., McDonald, A.R., Logsdon, C.D., Williams, J.A., and Goldfine, I.D. (1989). Mechanisms of insulin-induced insulin-receptor downregulation. Decrease of receptor biosynthesis and mRNA levels. Diabetes *38*, 182–187.

Oldham, S., Montagne, J., Radimerski, T., Thomas, G., and Hafen, E. (2000). Genetic and biochemical characterization of dTOR, the Drosophila homolog of the target of rapamycin. Genes Dev. *14*, 2689–2694.

Orme, J.J., Du, Y., Vanarsa, K., Mayeux, J., Li, L., Mutwally, A., Arriens, C., Min, S., Hutcheson, J., Davis, L.S., et al. (2016). Heightened cleavage of Axl receptor tyrosine kinase by ADAM metalloproteases may contribute to disease pathogenesis in SLE. Clin. Immunol. *169*, 58–68.

Paigen, K. (2003). One hundred years of mouse genetics: an intellectual history. II. The molecular revolution (1981-2002). Genetics *163*, 1227–1235.

Papasani, M.R., Robison, B.D., Hardy, R.W., and Hill, R.A. (2006). Early developmental expression of two insulins in zebrafish (Danio rerio). Physiol. Genomics *27*, 79–85.

Parichy, D.M. (2003). Pigment patterns: fish in stripes and spots. Curr. Biol. *13*, R947-50.

Parichy, D.M., Rawls, J.F., Pratt, S.J., Whitfield, T.T., and Johnson, S.L. (1999). Zebrafish sparse corresponds to an orthologue of c-kit and is required for the morphogenesis of a subpopulation of melanocytes, but is not essential for hematopoiesis or primordial germ cell development. Development *126*, 3425–3436.

Parichy, D.M., Mellgren, E.M., Rawls, J.F., Lopes, S.S., Kelsh, R.N., and Johnson, S.L. (2000). Mutational analysis of endothelin receptor b1 (rose) during neural crest and pigment pattern development in the zebrafish Danio rerio. Dev. Biol. *227*, 294–306.

Patterson, L.B., and Parichy, D.M. (2013). Interactions with iridophores and the tissue environment required for patterning melanophores and xanthophores during zebrafish adult pigment stripe formation. PLoS Genet. *9*, e1003561.

Patton, E.E., and Zon, L.I. (2001). The art and design of genetic screens: zebrafish. Nat. Rev. Genet. *2*, 956–966.

Patton, E.E., Widlund, H.R., Kutok, J.L., Kopani, K.R., Amatruda, J.F.,

Murphey, R.D., Berghmans, S., Mayhall, E.A., Traver, D., Fletcher, C.D.M., et al. (2005). BRAF mutations are sufficient to promote nevi formation and cooperate with p53 in the genesis of melanoma. Curr. Biol. *15*, 249–254.

Paus, R., Botchkarev, V.A., Botchkareva, N.V., Mecklenburg, L., Luger, T., and Slominski, A. (1999). The skin POMC system (SPS). Leads and lessons from the hair follicle. Ann. N. Y. Acad. Sci. *885*, 350–363.

Peschon, J.J., Slack, J.L., Reddy, P., Stocking, K.L., Sunnarborg, S.W., Lee, D.C., Russell, W.E., Castner, B.J., Johnson, R.S., Fitzner, J.N., et al. (1998). An essential role for ectodomain shedding in mammalian development. Science *282*, 1281–1284.

Peterson, R.T., Link, B.A., Dowling, J.E., and Schreiber, S.L. (2000). Small molecule developmental screens reveal the logic and timing of vertebrate development. Proc Natl Acad Sci USA *97*, 12965–12969.

Peterson, R.T., Shaw, S.Y., Peterson, T.A., Milan, D.J., Zhong, T.P., Schreiber, S.L., MacRae, C.A., and Fishman, M.C. (2004). Chemical suppression of a genetic mutation in a zebrafish model of aortic coarctation. Nat. Biotechnol. *22*, 595–599.

Picardo, M., Dell'Anna, M.L., Ezzedine, K., Hamzavi, I., Harris, J.E., Parsad, D., and Taieb, A. (2015). Vitiligo. Nat. Rev. Dis. Primers *1*, 15011.

Pinner, S., Jordan, P., Sharrock, K., Bazley, L., Collinson, L., Marais, R., Bonvin, E., Goding, C., and Sahai, E. (2009). Intravital imaging reveals transient changes in pigment production and Brn2 expression during metastatic melanoma dissemination. Cancer Res. *69*, 7969–7977.

Porta, C., Paglino, C., and Mosca, A. (2014). Targeting PI3K/Akt/mTOR Signaling in Cancer. Front. Oncol. *4*, 64.

Price, A.C., Weadick, C.J., Shim, J., and Rodd, F.H. (2008). Pigments, patterns, and fish behavior. Zebrafish *5*, 297–307.

Puig, O., and Tjian, R. (2005). Transcriptional feedback control of insulin receptor by dFOXO/FOXO1. Genes Dev. *19*, 2435–2446.

Quintana, E., Shackleton, M., Sabel, M.S., Fullen, D.R., Johnson, T.M., and Morrison, S.J. (2008). Efficient tumour formation by single human melanoma cells. Nature *456*, 593–598.

Quintana, E., Shackleton, M., Foster, H.R., Fullen, D.R., Sabel, M.S., Johnson, T.M., and Morrison, S.J. (2010). Phenotypic heterogeneity among tumorigenic melanoma cells from patients that is reversible and not hierarchically organized. Cancer Cell *18*, 510–523.

Rashidi, B., Gamagami, R., Sasson, A., Sun, F.X., Geller, J., Moossa, A.R., and Hoffman, R.M. (2000). An orthotopic mouse model of remetastasis of human colon cancer liver metastasis. Clin. Cancer Res. *6*, 2556–2561.

Ravandi, F., Estrov, Z., Kurzrock, R., Breitmeyer, J.B., Maschek, B.J., and

Talpaz, M. (1999). A phase I study of recombinant interferon-beta in patients with advanced malignant disease. Clin. Cancer Res. *5*, 3990–3998.

Richardson, J., Lundegaard, P.R., Reynolds, N.L., Dorin, J.R., Porteous, D.J., Jackson, I.J., and Patton, E.E. (2008). mc1r Pathway regulation of zebrafish melanosome dispersion. Zebrafish *5*, 289–295.

Rochin, L., Hurbain, I., Serneels, L., Fort, C., Watt, B., Leblanc, P., Marks, M.S., De Strooper, B., Raposo, G., and van Niel, G. (2013). BACE2 processes PMEL to form the melanosome amyloid matrix in pigment cells. Proc Natl Acad Sci USA *110*, 10658–10663.

Rozengurt, E., Soares, H.P., and Sinnet-Smith, J. (2014). Suppression of feedback loops mediated by PI3K/mTOR induces multiple overactivation of compensatory pathways: an unintended consequence leading to drug resistance. Mol. Cancer Ther. *13*, 2477–2488.

Rubinstein, A.L., Lee, D., Luo, R., Henion, P.D., and Halpern, M.E. (2000). Genes dependent on zebrafish cyclops function identified by AFLP differential gene expression screen. Genesis *26*, 86–97.

Sáez-Ayala, M., Montenegro, M.F., Sánchez-Del-Campo, L., Fernández-Pérez, M.P., Chazarra, S., Freter, R., Middleton, M., Piñero-Madrona, A., Cabezas-Herrera, J., Goding, C.R., et al. (2013). Directed phenotype switching as an effective antimelanoma strategy. Cancer Cell *24*, 105–119.

Safer, J.D. (2011). Thyroid hormone action on skin. Dermatoendocrinol *3*, 211–215.

Saldana-Caboverde, A., and Kos, L. (2010). Roles of endothelin signaling in melanocyte development and melanoma. Pigment Cell Melanoma Res. *23*, 160–170.

Sarbassov, D.D., Ali, S.M., Kim, D.-H., Guertin, D.A., Latek, R.R., Erdjument-Bromage, H., Tempst, P., and Sabatini, D.M. (2004). Rictor, a novel binding partner of mTOR, defines a rapamycin-insensitive and raptor-independent pathway that regulates the cytoskeleton. Curr. Biol. *14*, 1296–1302.

Sather, S., Kenyon, K.D., Lefkowitz, J.B., Liang, X., Varnum, B.C., Henson, P.M., and Graham, D.K. (2007). A soluble form of the Mer receptor tyrosine kinase inhibits macrophage clearance of apoptotic cells and platelet aggregation. Blood *109*, 1026–1033.

Saxton, R.A., and Sabatini, D.M. (2017). mTOR Signaling in Growth, Metabolism, and Disease. Cell *169*, 361–371.

Schauer, E., Trautinger, F., Köck, A., Schwarz, A., Bhardwaj, R., Simon, M., Ansel, J.C., Schwarz, T., and Luger, T.A. (1994). Proopiomelanocortin-derived peptides are synthesized and released by human keratinocytes. J. Clin. Invest. *93*, 2258–2262.

Schelter, F., Grandl, M., Seubert, B., Schaten, S., Hauser, S., Gerg, M.,

Boccaccio, C., Comoglio, P., and Krüger, A. (2011). Tumor cell-derived Timp-1 is necessary for maintaining metastasis-promoting Met-signaling via inhibition of Adam-10. Clin. Exp. Metastasis *28*, 793–802.

Schiaffino, M.V. (2010). Signaling pathways in melanosome biogenesis and pathology. Int. J. Biochem. Cell Biol. *42*, 1094–1104.

Schonthaler, H.B., Lampert, J.M., von Lintig, J., Schwarz, H., Geisler, R., and Neuhauss, S.C.F. (2005). A mutation in the silver gene leads to defects in melanosome biogenesis and alterations in the visual system in the zebrafish mutant fading vision. Dev. Biol. *284*, 421–436.

Schwahn, D.J., Timchenko, N.A., Shibahara, S., and Medrano, E.E. (2005). Dynamic regulation of the human dopachrome tautomerase promoter by MITF, ER-alpha and chromatin remodelers during proliferation and senescence of human melanocytes. Pigment Cell Res. *18*, 203–213.

Schwartz, M.W., Figlewicz, D.P., Baskin, D.G., Woods, S.C., and Porte, D. (1992). Insulin in the brain: a hormonal regulator of energy balance. Endocr. Rev. *13*, 387–414.

Scott, G. (2002). Rac and rho: the story behind melanocyte dendrite formation. Pigment Cell Res. *15*, 322–330.

Seberg, H.E., Van Otterloo, E., Loftus, S.K., Liu, H., Bonde, G., Sompallae, R., Gildea, D.E., Santana, J.F., Manak, J.R., Pavan, W.J., et al. (2017). TFAP2 paralogs regulate melanocyte differentiation in parallel with MITF. PLoS Genet. *13*, e1006636.

Shakhova, O., Zingg, D., Schaefer, S.M., Hari, L., Civenni, G., Blunschi, J., Claudinot, S., Okoniewski, M., Beermann, F., Mihic-Probst, D., et al. (2012). Sox10 promotes the formation and maintenance of giant congenital naevi and melanoma. Nat. Cell Biol. *14*, 882–890.

Sheets, L., Ransom, D.G., Mellgren, E.M., Johnson, S.L., and Schnapp, B.J. (2007). Zebrafish melanophilin facilitates melanosome dispersion by regulating dynein. Curr. Biol. *17*, 1721–1734.

Shi, S.-H., Jan, L.Y., and Jan, Y.-N. (2003). Hippocampal neuronal polarity specified by spatially localized mPar3/mPar6 and PI 3-kinase activity. Cell *112*, 63–75.

Shimshek, D.R., Jacobson, L.H., Kolly, C., Zamurovic, N., Balavenkatraman, K.K., Morawiec, L., Kreutzer, R., Schelle, J., Jucker, M., Bertschi, B., et al. (2016). Pharmacological BACE1 and BACE2 inhibition induces hair depigmentation by inhibiting PMEL17 processing in mice. Sci. Rep. *6*, 21917.

Shymanets, A., Prajwal, Bucher, K., Beer-Hammer, S., Harteneck, C., and Nürnberg, B. (2013). p87 and p101 subunits are distinct regulators determining class IB phosphoinositide 3-kinase (PI3K) specificity. J. Biol. Chem. *288*, 31059–31068.

Smith, B.J., Huang, K., Kong, G., Chan, S.J., Nakagawa, S., Menting, J.G., Hu, S.-Q., Whittaker, J., Steiner, D.F., Katsoyannis, P.G., et al. (2010). Structural resolution of a tandem hormone-binding element in the insulin receptor and its implications for design of peptide agonists. Proc Natl Acad Sci USA *107*, 6771–6776.

Somerville, C., and Koornneef, M. (2002). A fortunate choice: the history of Arabidopsis as a model plant. Nat. Rev. Genet. *3*, 883–889.

Sommer, L. (2011). Generation of melanocytes from neural crest cells. Pigment Cell Melanoma Res. *24*, 411–421.

Spencer, J.D., and Schallreuter, K.U. (2009). Regulation of pigmentation in human epidermal melanocytes by functional high-affinity beta-melanocyte-stimulating hormone/melanocortin-4 receptor signaling. Endocrinology *150*, 1250–1258.

Stern, H.M., Murphey, R.D., Shepard, J.L., Amatruda, J.F., Straub, C.T., Pfaff, K.L., Weber, G., Tallarico, J.A., King, R.W., and Zon, L.I. (2005). Small molecules that delay S phase suppress a zebrafish bmyb mutant. Nat. Chem. Biol. *1*, 366–370.

Streisinger, G., Singer, F., Walker, C., Knauber, D., and Dower, N. (1986). Segregation analyses and gene-centromere distances in zebrafish. Genetics *112*, 311–319.

Stützer, I., Selevsek, N., Esterházy, D., Schmidt, A., Aebersold, R., and Stoffel, M. (2013). Systematic proteomic analysis identifies β-site amyloid precursor protein cleaving enzyme 2 and 1 (BACE2 and BACE1) substrates in pancreatic β-cells. J. Biol. Chem. *288*, 10536–10547.

Sulaimon, S.S., and Kitchell, B.E. (2003). The biology of melanocytes. Vet. Dermatol. *14*, 57–65.

Sun, J., Hao, Z., Luo, H., He, C., Mei, L., Liu, Y., Wang, X., Niu, Z., Chen, H., Li, J.-D., et al. (2017). Functional analysis of a nonstop mutation in MITF gene identified in a patient with Waardenburg syndrome type 2. J. Hum. Genet. *62*, 703–709.

Tadokoro, T., Itami, S., Hosokawa, K., Terashi, H., and Takayasu, S. (1997). Human genital melanocytes as androgen target cells. J. Invest. Dermatol. *109*, 513–517.

Tadokoro, T., Yamaguchi, Y., Batzer, J., Coelho, S.G., Zmudzka, B.Z., Miller, S.A., Wolber, R., Beer, J.Z., and Hearing, V.J. (2005). Mechanisms of skin tanning in different racial/ethnic groups in response to ultraviolet radiation. J. Invest. Dermatol. *124*, 1326–1332.

Tamplin, O.J., White, R.M., Jing, L., Kaufman, C.K., Lacadie, S.A., Li, P., Taylor, A.M., and Zon, L.I. (2012). Small molecule screening in zebrafish: swimming in potential drug therapies. Wiley Interdiscip. Rev. Dev. Biol. *1*, 459–468.

Tap, W.D., Gong, K.-W., Dering, J., Tseng, Y., Ginther, C., Pauletti, G., Glaspy, J.A., Essner, R., Bollag, G., Hirth, P., et al. (2010). Pharmacodynamic characterization of the efficacy signals due to selective BRAF inhibition with PLX4032 in malignant melanoma. Neoplasia *12*, 637–649.

Tapon, N., and Hall, A. (1997). Rho, Rac and Cdc42 GTPases regulate the organization of the actin cytoskeleton. Curr. Opin. Cell Biol. *9*, 86–92.

Tassabehji, M., Newton, V.E., and Read, A.P. (1994). Waardenburg syndrome type 2 caused by mutations in the human microphthalmia (MITF) gene. Nat. Genet. *8*, 251–255.

Tavakkol, A., Elder, J.T., Griffiths, C.E., Cooper, K.D., Talwar, H., Fisher, G.J., Keane, K.M., Foltin, S.K., and Voorhees, J.J. (1992). Expression of growth hormone receptor, insulin-like growth factor 1 (IGF-1) and IGF-1 receptor mRNA and proteins in human skin. J. Invest. Dermatol. *99*, 343–349.

Taylor, K.L., Lister, J.A., Zeng, Z., Ishizaki, H., Anderson, C., Kelsh, R.N., Jackson, I.J., and Patton, E.E. (2011). Differentiated melanocyte cell division occurs in vivo and is promoted by mutations in Mitf. Development *138*, 3579–3589.

van Tetering, G., van Diest, P., Verlaan, I., van der Wall, E., Kopan, R., and Vooijs, M. (2009). Metalloprotease ADAM10 is required for Notch1 site 2 cleavage. J. Biol. Chem. *284*, 31018–31027.

Thisse, C., and Thisse, B. (2008). High-resolution in situ hybridization to whole-mount zebrafish embryos. Nat. Protoc. *3*, 59–69.

Thody, A.J., and Graham, A. (1998). Does alpha-MSH have a role in regulating skin pigmentation in humans? Pigment Cell Res. *11*, 265–274.

Thomanetz, V., Angliker, N., Cloëtta, D., Lustenberger, R.M., Schweighauser, M., Oliveri, F., Suzuki, N., and Rüegg, M.A. (2013). Ablation of the mTORC2 component rictor in brain or Purkinje cells affects size and neuron morphology. J. Cell Biol. *201*, 293–308.

Thomas, A.J., and Erickson, C.A. (2008). The making of a melanocyte: the specification of melanoblasts from the neural crest. Pigment Cell Melanoma Res. *21*, 598–610.

Thomas, A.J., and Erickson, C.A. (2009). FOXD3 regulates the lineage switch between neural crest-derived glial cells and pigment cells by repressing MITF through a non-canonical mechanism. Development *136*, 1849–1858.

Thorpe, L.M., Yuzugullu, H., and Zhao, J.J. (2015). PI3K in cancer: divergent roles of isoforms, modes of activation and therapeutic targeting. Nat. Rev. Cancer *15*, 7–24.

Toyoshima, Y., Monson, C., Duan, C., Wu, Y., Gao, C., Yakar, S., Sadler, K.C., and LeRoith, D. (2008). The role of insulin receptor signaling in zebrafish embryogenesis. Endocrinology *149*, 5996–6005.

Tryon, R.C., and Johnson, S.L. (2012). Clonal and lineage analysis of melanocyte stem cells and their progeny in the zebrafish. Methods Mol. Biol. *916*, 181–195.

Tsatmali, M., Ancans, J., Yukitake, J., and Thody, A.J. (2000). Skin POMC peptides: their actions at the human MC-1 receptor and roles in the tanning response. Pigment Cell Res. *13 Suppl 8*, 125–129.

Uhlén, M., Fagerberg, L., Hallström, B.M., Lindskog, C., Oksvold, P., Mardinoglu, A., Sivertsson, Å., Kampf, C., Sjöstedt, E., Asplund, A., et al. (2015). Proteomics. Tissue-based map of the human proteome. Science *347*, 1260419.

Uong, A., and Zon, L.I. (2010). Melanocytes in development and cancer. J. Cell. Physiol. *222*, 38–41.

Vandamme, N., and Berx, G. (2014). Melanoma cells revive an embryonic transcriptional network to dictate phenotypic heterogeneity. Front. Oncol. *4*, 352.

Vassar, R. (2014). BACE1 inhibitor drugs in clinical trials for Alzheimer's disease. Alzheimers Res Ther *6*, 89.

Venugopal, C., Demos, C.M., Rao, K.S.J., Pappolla, M.A., and Sambamurti, K. (2008). Beta-secretase: structure, function, and evolution. CNS Neurol. Disord. Drug Targets *7*, 278–294.

Vetrini, F., Auricchio, A., Du, J., Angeletti, B., Fisher, D.E., Ballabio, A., and Marigo, V. (2004). The microphthalmia transcription factor (Mitf) controls expression of the ocular albinism type 1 gene: link between melanin synthesis and melanosome biogenesis. Mol. Cell. Biol. *24*, 6550–6559.

Videira, I.F. dos S., Moura, D.F.L., and Magina, S. (2013). Mechanisms regulating melanogenesis. An. Bras. Dermatol. *88*, 76–83.

Walderich, B., Singh, A.P., Mahalwar, P., and Nüsslein-Volhard, C. (2016). Homotypic cell competition regulates proliferation and tiling of zebrafish pigment cells during colour pattern formation. Nat. Commun. *7*, 11462.

Walter, J. (2013). Fishing for function--distinct roles of Bace1 and Bace2 in Zebrafish development. J. Neurochem. *127*, 435–437.

Wan, J., Zhao, X.-F., Vojtek, A., and Goldman, D. (2014). Retinal injury, growth factors, and cytokines converge on β-catenin and pStat3 signaling to stimulate retina regeneration. Cell Rep. *9*, 285–297.

Ward, C.W., and Lawrence, M.C. (2009). Ligand-induced activation of the insulin receptor: a multi-step process involving structural changes in both the ligand and the receptor. Bioessays *31*, 422–434.

Watanabe, M., Iwashita, M., Ishii, M., Kurachi, Y., Kawakami, A., Kondo, S., and Okada, N. (2006). Spot pattern of leopard Danio is caused by mutation in the zebrafish connexin41.8 gene. EMBO Rep. *7*, 893–897.

Wehrle-Haller, B. (2003). The role of Kit-ligand in melanocyte development and epidermal homeostasis. Pigment Cell Res. *16*, 287–296.

Weiss, M., Steiner, D.F., and Philipson, L.H. (2000). Insulin Biosynthesis, Secretion, Structure, and Structure-Activity Relationships. In Endotext, L.J. De Groot, G. Chrousos, K. Dungan, K.R. Feingold, A. Grossman, J.M. Hershman, C. Koch, M. Korbonits, R. McLachlan, M. New, et al., eds. (South Dartmouth (MA): MDText.com, Inc.), p.

Welten, M.C.M., de Haan, S.B., van den Boogert, N., Noordermeer, J.N., Lamers, G.E.M., Spaink, H.P., Meijer, A.H., and Verbeek, F.J. (2006). ZebraFISH: fluorescent in situ hybridization protocol and three-dimensional imaging of gene expression patterns. Zebrafish *3*, 465–476.

White, J.G. (2013). Getting into the mind of a worm--a personal view. WormBook 1–10.

White, J.G., Southgate, E., Thomson, J.N., and Brenner, S. (1986). The structure of the nervous system of the nematode Caenorhabditis elegans. Philos Trans R Soc Lond, B, Biol Sci *314*, 1–340.

White, R., Rose, K., and Zon, L. (2013). Zebrafish cancer: the state of the art and the path forward. Nat. Rev. Cancer *13*, 624–636.

White, R.M., Sessa, A., Burke, C., Bowman, T., LeBlanc, J., Ceol, C., Bourque, C., Dovey, M., Goessling, W., Burns, C.E., et al. (2008). Transparent adult zebrafish as a tool for in vivo transplantation analysis. Cell Stem Cell *2*, 183–189.

White, R.M., Cech, J., Ratanasirintrawoot, S., Lin, C.Y., Rahl, P.B., Burke, C.J., Langdon, E., Tomlinson, M.L., Mosher, J., Kaufman, C., et al. (2011). DHODH modulates transcriptional elongation in the neural crest and melanoma. Nature *471*, 518–522.

Wilcox, G. (2005). Insulin and insulin resistance. Clin. Biochem. Rev. *26*, 19–39.

Williams, J.S., Hsu, J.Y., Rossi, C.C., and Artinger, K.B. (2018). Requirement of zebrafish pcdh10a and pcdh10b in melanocyte precursor migration. Dev. Biol.

Yamaguchi, Y., Flier, J.S., Yokota, A., Benecke, H., Backer, J.M., and Moller, D.E. (1991). Functional properties of two naturally occurring isoforms of the human insulin receptor in Chinese hamster ovary cells. Endocrinology *129*, 2058–2066.

Yamaguchi, Y., Brenner, M., and Hearing, V.J. (2007). The regulation of skin pigmentation. J. Biol. Chem. *282*, 27557–27561.

Yamaguchi, Y., Passeron, T., Hoashi, T., Watabe, H., Rouzaud, F., Yasumoto, K., Hara, T., Tohyama, C., Katayama, I., Miki, T., et al. (2008). Dickkopf 1 (DKK1) regulates skin pigmentation and thickness by affecting Wnt/beta-

catenin signaling in keratinocytes. FASEB J. *22*, 1009–1020.

Yamaguchi, Y., Morita, A., Maeda, A., and Hearing, V.J. (2009). Regulation of skin pigmentation and thickness by Dickkopf 1 (DKK1). J. Investig. Dermatol. Symp. Proc. *14*, 73–75.

Yan, R., Munzner, J.B., Shuck, M.E., and Bienkowski, M.J. (2001). BACE2 functions as an alternative alpha-secretase in cells. J. Biol. Chem. *276*, 34019–34027.

Ye, L., Robertson, M.A., Mastracci, T.L., and Anderson, R.M. (2016). An insulin signaling feedback loop regulates pancreas progenitor cell differentiation during islet development and regeneration. Dev. Biol. *409*, 354–369.

Yoo, S.K., Deng, Q., Cavnar, P.J., Wu, Y.I., Hahn, K.M., and Huttenlocher, A. (2010). Differential regulation of protrusion and polarity by PI3K during neutrophil motility in live zebrafish. Dev. Cell *18*, 226–236.

Youngren, J.F. (2007). Regulation of insulin receptor function. Cell. Mol. Life Sci. *64*, 873–891.

Zarogoulidis, P., Lampaki, S., Turner, J.F., Huang, H., Kakolyris, S., Syrigos, K., and Zarogoulidis, K. (2014). mTOR pathway: A current, up-to-date mini-review (Review). Oncol. Lett. *8*, 2367–2370.

Zhang, H., Stallock, J.P., Ng, J.C., Reinhard, C., and Neufeld, T.P. (2000). Regulation of cellular growth by the Drosophila target of rapamycin dTOR. Genes Dev. *14*, 2712–2724.

Zigrino, P., Mauch, C., Fox, J.W., and Nischt, R. (2005). Adam-9 expression and regulation in human skin melanoma and melanoma cell lines. Int. J. Cancer *116*, 853–859.

Zou, J., Beermann, F., Wang, J., Kawakami, K., and Wei, X. (2006). The Fugu tyrp1 promoter directs specific GFP expression in zebrafish: tools to study the RPE and the neural crest-derived melanophores. Pigment Cell Res. *19*, 615–627.